EFFECTS OF CATIONIC POLYMER COLLOIDAL PARTICLE SIZE ON THE REACTIVITY OF ORGANIC ANIONS

By

GUANG LIU

Bachelor of Science

Tsinghua University

Beijing, P.R.China

1990

Submitted to the Faculty of the
Graduate College of the
Oklahoma State University
in partial fulfillment of
the requirements for
the Degree of
MASTER OF SCIENCE
May, 2000

EFFECTS OF CATIONIC POLYMER COLLOIDAL

PARTICLE SIZE ON THE REACTIVITY

OF ORGANIC ANIONS

Thesis Approved:

Warren T. Ford

Thesis Advisor

Wayne B. Powell

Dean of the Graduate College

PREFACE

The diameters of small spherical polymeric particles on the order of 2×10^{-7} m, known as polymer latexes, are 1000-10000 times smaller than polymer resins. Their internal structures are entangled polymer coils with ionic functional groups so that they can be used as highly efficient catalytic media to promote various types of reactions such as decontamination of chemical warfare agents and insecticides in the field.

Since the rates of reactions catalyzed by polymer beads are limited by slow transfer of one or both reactants to the active sites inside particles, these smaller colloidal polymer particles used as catalytic media have advantages due to their high surface areas and the short paths to the active sites.

This research investigated the effects of particle size on the catalytic activity by using cationic polystyrene particles having average diameter of 20 nm, 135 nm, and 1 μm as catalytic media. These three different size particles showed different reaction rates. The kinetics with particles 1 μm in diameter had a retardation period at the beginning of the reaction process. This work verified that polymer latex particles < 1 μm never suffered diffusional limitations to reaction rates.

ACKNOWLEDGMENTS

First, I would like to express deep appreciation to my research advisor, Dr.Warren T. Ford, for his instruction, inspiration and support during my research period. Also my appreciation is extended to my senior colleagues who worked at the same group and same lab with me for their tolerance and guidance. I am willing to thank Paul Miller, Ken Hampton, Yijun Pan, Spence Pilcher and Jason Kreider. Especial thanks go to Paul Miller for his kindly providing me emulsion latex samples.

Second, I am very grateful to Dr. John I. Gelder and Dr. Satomi Niwayama for serving on my advisory committee. I wish to thank Dr. Feng Qiu and Dr. Margaret Eastman for their mentoring on NMR experiments and Ms. Phoebe Doss for her help on EM experiments. In addition, I must acknowledge the Department of Chemistry and U.S. Army Research Office for their financial support in the form of teaching and research assistantships during my graduate study at Oklahoma State University.

Finally, I want to give my heartfelt love and gratitude to my parents for their understanding and sacrifices during the course of my graduate study. No words can suffice to express my affection to my wife, Zhimin Ma, for her timeless love and spiritual encouragement, and to my lovely daughter, Elizabeth Fangxi Liu, for her enticing smile. I owe them a lot. I wish I could dedicate this work to them.

TABLE OF CONTENTS

Chapter Page

LIST OF TABLES

LIST OF FIGURES

Figure Page

LIST OF SCHEMES

CHAPTER I

INTRODUCTION

Phase Transfer Catalysis

Because most organic compounds are insoluble in water, and many inorganic reagents are insoluble in nonpolar organic solvents, numerous organic synthetic methods have been devised to get organic and inorganic reactants into the same phase so that the required reaction can take place. One of them is phase transfer catalysis (PTC), which is a powerful tool currently used in many areas of chemistry. Phase transfer catalysis can be characterized as a technique for conducting reactions between two or more reagents in two or more phases, when a reaction is inhibited because the reactants cannot easily come together. A simple example of PTC is the reaction of 1-chlorooctane and aqueous sodium cyanide.[1] Without catalyst, heating of this two-phase mixture under reflux and with vigorous stirring for 1 or 2 days gives no apparent reaction. However, if 1 wt % of the quaternary ammonium salt, $(C_6H_{13})_4N^+Cl^-$, is added, then displacement reaction occurs rapidly producing 1-cyanooctane in near 100% conversion in 2-3 h (eq 1).

$$n\text{-}C_8H_{17}Cl + NaCN\ (aq) \rightarrow n\text{-}C_8H_{17}CN + NaCl \qquad (1)$$

In this reaction, the phase transfer catalyst promotes the solubility of the anion, CN^-, in organic solvent by providing a lipophilic counterion, $(C_6H_{13})_4N^+$, to partially extract the reactive anion into the organic phase so that the reaction proceeds rapidly. Phase transfer catalysis has been widely studied and there are a few excellent sources for this subject.[1-3]

Besides the soluble low molar mass catalysts such as a tetraalkylammonium ion or the crown ether complex of a sodium or potassium ion,[4,5] some insoluble systems also are needed as effective catalytic systems with the aim of recovery and reuse due to environmental requirements. In reality many reactions do proceed under heterogeneous conditions, such as at the phase interface, or more commonly in the phase in which one reactant is highly soluble and the other slightly soluble. To overcome such a problem by providing a means for combination of substrates and reagents, molecular aggregates, also referred to as association colloids, have been used as heterogeneous media to facilitate the rates of chemical reactions in aqueous solution for many years. Among them the most widely studied are surfactant micelles,[6] bilayer vesicles,[7] ion exchange resins,[8] polyelectrolytes,[9] and polymer colloids.[10-15] In this research project the phase transfer catalysts are polymer colloids.

Polymer Colloids

A polymer colloid, i.e. a latex, is a heterogeneous mixture which consists of dispersed polymer particles in a continuous liquid phase such as water. Typically water-based polymer latexes are produced by emulsion polymerization, which has been widely exploited for producing adhesives, paints, coatings and rubbers in industry. In such a kind of colloid system, the solid particles are small, usually within 50-500 nm in diameter, and consist of a lipophilic core of organic polymer and a surface with surfactant ions or polymer end group ions that provide electrostatic interaction between charged sites, so these particles are colloidally stable. Polymer colloids generally have a milky

appearance, but can have a bluish, translucent appearance when the latex particles are small enough. Also they have a low viscosity, almost like that of water.

Polymer colloids substituted with quaternary ammonium ions can be used as phase transfer catalysts. Due to lipophilicity of the organic polymer core, the particle can extract organic substrates from the aqueous environment into the particle phase so that the particle becomes a second phase of the reaction mixture. Inside the particle phase the concentration of substrate is much higher than in the aqueous phase. On the other hand, those charged sites inside and on the particle surface, which are introduced by chemical modification at the particle-fluid interface, serve as ion exchange sites for ions such as hydroxide or other nucleophiles. By the intimate combination of organic substrates and reagents the overall reaction can be accelerated by several orders of magnitude larger than that in the aqueous phase.

Cationic polymer latexes are made by a so-called shot growth emulsion polymerization process.[16] The general structure of a cationic latex is shown in Scheme 1. The crosslinking agent divinylbenzene allows the polymer chains only to swell in water. The N^+ monomer (styrylmethyl)trimethylammonium chloride provides the surface active sites for latex particle formation. These monodisperse polymer colloids are free of surfactant and polyelectrolytes so that they can provide a uniform catalytic environment. By incorporating positively charged quaternary ammonium ions into the polymer structure these cationic polymer latexes can serve as highly efficient catalytic media for reactions of anions and organic substrates due to large numbers of binding sites distributed throughout the particle as well as on the surface. This catalysis research can be potentially applied in the reactions such as hydrolysis and neutralization of toxic

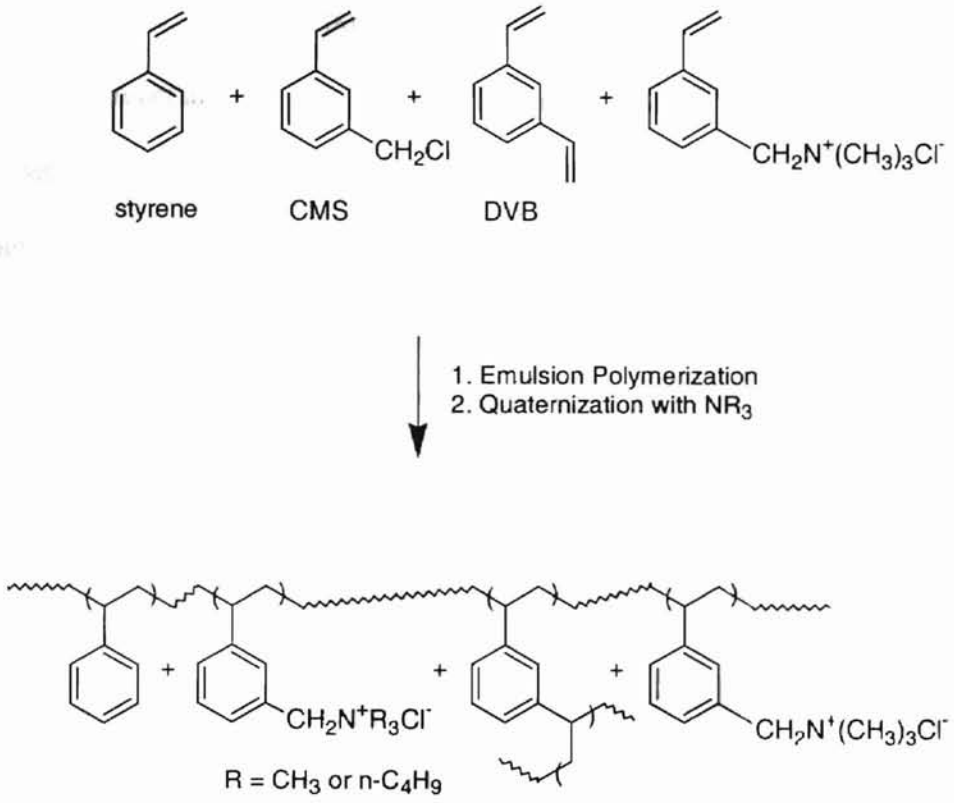

Scheme 1. General structure of cationic polymer latex

organophosphorous warfare agents and insecticides in the field.

The most active cationic polystyrene latex containing quaternary ammonium sites catalyzes the decarboxylation of 6-nitrobenzisoxazole-3-carboxylate in aqueous solution with an enhancement in the observed rate constant in excess of 10,000 times over the rate constant in water alone.[14]

Moreover, these cationic polymer colloids can be used as anion-exchange latexes when one of the reactants or a catalyst is an anion that binds strongly to the particles. This has been accomplished using cross-linked polystyrene latexes containing (styrylmethyl)tributylammonium chloride repeat units which increase the *o*-iodosobenzoate (IBA) anion-catalyzed reaction rate of hydrolysis of *p*-nitrophenyl diphenyl phosphate (PNPDPP) up to 6,300 times higher than that in the absence of latexes.[13]

Recently many new systems studied as catalysts in aqueous solutions have been introduced. They include dendrimers,[17-19] polyampholyte microgels,[20] alkyl methacrylate latexes,[21] and metal complexes of crown ethers.[22] By comparison among these systems named above the polymer latexes have some interesting advantages:[23] 1) Polymer latexes can be used in dilute concentration so that their uses as heterogeneous catalysts are not limited to a critical concentration such as the critical micelle concentration (CMC) of low molar mass surfactants. 2) Polymer latex particles can be recycled by ultrafiltration and hence reused. Of course, the polymer latexes have their shortcomings. One of them is that polymer latexes are colloidally unstable at high electrolyte concentrations so that they may coagulate.[24]

Research Objectives

Insoluble polymeric catalysts usually employ crosslinked polystyrene beads that were intended for use as Merrifield resins (40-80 μm in diameter) for solid-phase peptide synthesis[25] or as ion-exchange resins[26] (400-600 μm in diameter) for water treatment. However, the bead catalysts often are less active than their solution counterparts because rates of reactions are limited by mass transfer of reactants from solution to the bead surface and intraparticle diffusion of reactants from the surface to the active sites within the bead, which can be evidenced by the fact that the observed reaction rates depend on particle size and the speed of mixing.[27] For instance, when the reaction of 1-bromooctane in toluene with concentrated aqueous NaCN (eq 2)

$$H(CH_2)_8Br(org) + NaCN(aq) \rightarrow H(CH_2)_8CN(org) + NaBr(aq) \qquad (2)$$

was catalyzed by crosslinked polystyrene beads with the range from 40 to 600 μm in diameter, having (styrylmethyl)tributylphosphonium ion exchange sites, the observed rate increased with decreasing bead size and faster stirring, which indicated the slow mass transfer of reactants to the bead surface. However, in the above experiments even using the smallest beads the reaction rates never much reached the asymptotic limit at which rate does not depend on particle size. Recently, Ford, Lee and Yu examined the hydrolysis of organophosphates with cationic polymer latexes and found remarkably high catalytic activity.[13-15] Nevertheless, those cationic polymer latexes were produced by emulsion polymerization and their typical particle sizes in diameters were 200-300 nm. When these colloidal polymer particles are used as catalytic media, their high surface areas and the short diffusion paths to the particle interiors have been assumed to create no

mass transfer or intraparticle diffusional limitation to reaction rates, but this assumption has never been tested so far.

In order to investigate the effect of particle size on the catalytic activity, this research tested the above prediction using small amounts of anion exchange polystyrene particles with diameters of about 20 nm, 200 nm and 1 μm respectively to catalyze decarboxylation of 6-nitrobenzisoxazole-3-carboxylate in aqueous media.

The preparation of polymer colloidal particles around 20 nm, 200 nm and 1 μm in diameter is not routine. For this purpose, different polymerization techniques such as microemulsion, emulsion and dispersion polymerization are applied in order of increasing particle size. All quaternary ammonium groups in these latex particles were formed by the substitution reaction of trimethylamine or tributylamine with the vinylbenzyl chloride (VBC) units built into the latex particles. Because the study of catalysis by polymer colloids requires that all dispersions contain negligibly small amounts of impurities that might also catalyze the reactions, such as soluble cationic polyelectrolytes and other additives needed in various polymerization processes, these latexes after copolymerization and quaternization were purified by ultrafiltration or dialysis. The kinetic analysis of decarboxylation of 6-nitrobenzisoxazole-3-carboxylate in aqueous media used as a model reaction was tracked by UV spectroscopy.

Polymerization Methods

Although microemulsion polymerization, emulsion polymerization and dispersion polymerization are all particle forming polymerization processes, they have properties that make them unique from each other. These differences are:

1) Initial state of the polymerization mixture;

2) Kinetics of polymerization;

3) Mechanism of particle formation;

4) Sizes of the final polymer particles.

The goal of this part is to provide a concise methodological description of these three polymerization methods used in my research.

(1) Emulsion Polymerization

Emulsion polymerization is a classic method to form polymer particles with 50-500 nm diameters. It has been extensively studied[28] and successfully used in various industrial fields including coatings, paints, inks, adhesives, and rubbers. So at first we would like to briefly introduce the features of emulsion polymerization, then compare it with microemulsion polymerization and dispersion polymerization.

An emulsion before polymerization consists of kinetically stable monomer droplets (1-10 μm), monomer swollen micelles (3-10 nm), and a water-rich continuum saturated with molecularly dispersed monomer and surfactant that is present at the critical micelle concentration (CMC).[29] In emulsion polymerization it has long been accepted that the principal locus for initiation is the aqueous phase. In this case radicals generated in the aqueous phase either enter the monomer-swollen micelles and rapidly polymerize the solubilized monomer, or they capture monomer molecules dissolved in the aqueous phase to form oligomeric radicals which then precipitate from solution to form stable primary latex particles. In either case, the polymeric particles become the loci of propagation and grow by recruiting monomer that diffuses from the emulsified monomer

droplets through the aqueous phase. Particle stabilization during the reaction is achieved by adsorption of emulsifier molecules from non-initiated micelles and emulsified droplets. In this process the emulsified monomer droplets are considered not to play a significant role in initiation loci other than as a source of monomer, for their overall surface area is so small compared to that of the swollen micelles or primary latex particles that monomer droplets are inefficient free radical capturers.

Three intervals can be identified during emulsion polymerization, which are depicted in Figure 1.[30] Particle nucleation takes place in interval I, and the polymerization rate increases with time as the number of particles increases. The end of this interval is signaled by the disappearance of micelles and the adsorption of most surfactants at the surface of the growing polymer particles. This interval usually ends at conversions of ≤ 10 %. In the propagation interval (Interval II), the nucleation of particles is complete and the polymerization proceeds in the polymer particles. The monomer concentration in the particles is maintained at equilibrium (saturation) level by diffusion of monomer from droplets through the aqueous phase. This interval also features a constant number of monomer-swollen latex particles and an increase in particle size. Interval II ends when all the monomer droplets are consumed and corresponds to a conversion range of 10-40 %. Interval III, the completion stage, is characterized by a decreasing polymerization rate. Here, almost all of the remaining monomer is now confined to the latex particles and continues to react until it is all consumed.

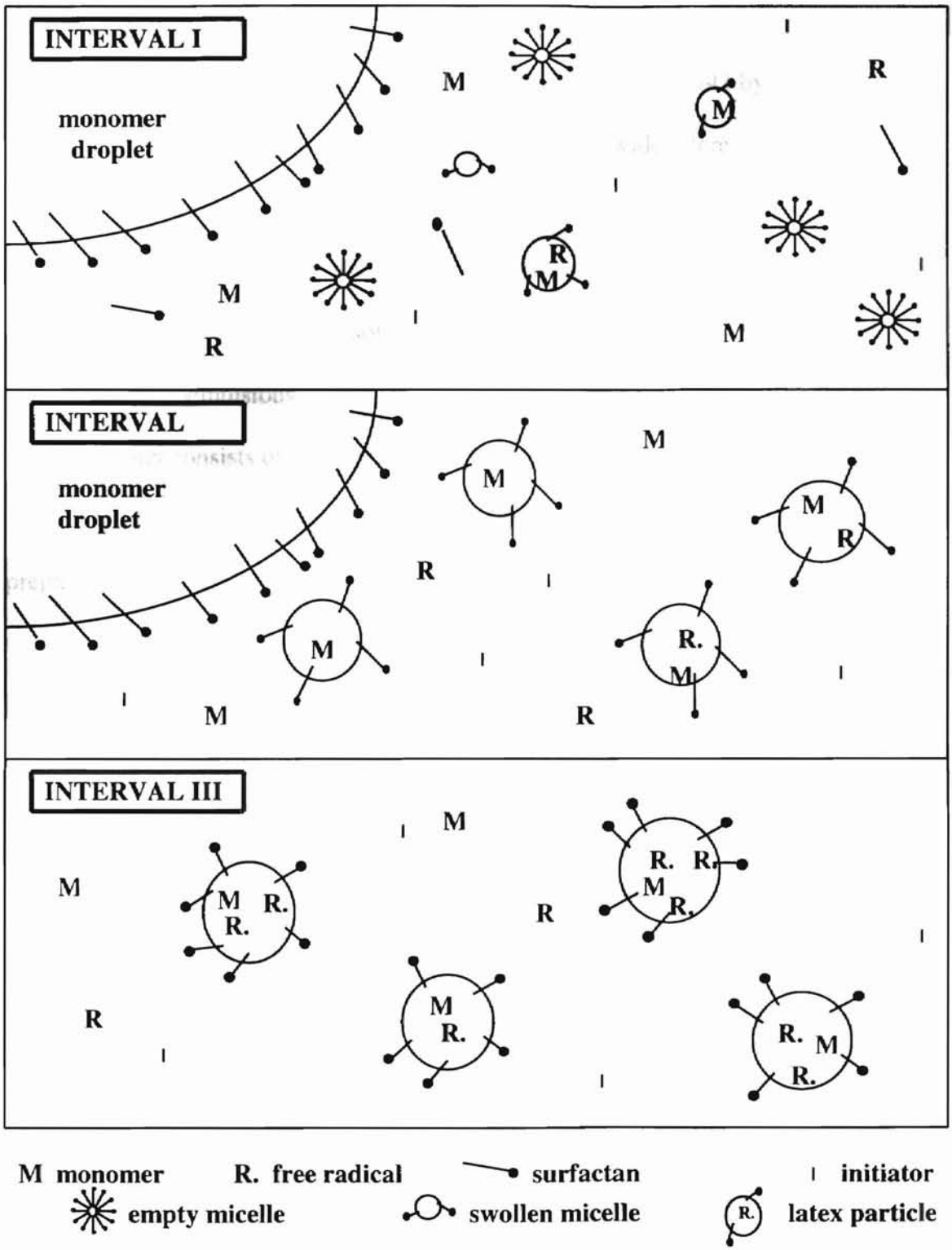

Figure 1. The three intervals of a conventional emulsion polymerization

(2) Microemulsion Polymerization

The concept of a microemulsion was first introduced in 1943 by Hoar and Schulman.[31] Since then this subject has been attracting a wide interest not only in academic circles but also from industrial research and development. Generally microemulsions are defined as the clear thermodynamically stable dispersions of two immiscible liquids or liquid and solid. In contrast to the opaque, milky conventional emulsions, microemulsions are transparent or translucent. The dispersed phase in a microemulsion consists of very small droplets with diameter in the range of 5-50 nm.

Polymerization in microemulsions is a relatively new technique for the preparation of ultrafine latex particles ("nanolatex particles") with an average diameter in the range 5-50 nm. Polymerization of water-soluble monomers (e.g., acrylic acid or acrylamide) in water-in oil (w/o) microemulsions, as well as hydrophobic monomers (e.g., styrene or methyl methacrylate) in oil-in-water (o/w) microemulsions, has been extensively reviewed by Candau[32] and Antonietti et al.[33] Moreover, a great deal of research in polymerization in microemulsions has been devoted to the kinetics, particle creation rates, molecular weight averages, and particle size distributions of the specific systems.[34-40] Recently, the microstructure of PMMA latex particles in terms of tacticity formed in microemulsions was also investigated.[41]

Typically, microemulsion formulations contain oil, water, surfactants and sometimes cosurfactants or other additives. Thus, to produce a microlatex, one prepares a microemulsion of monomer and then this undergoes a polymerization initiated by thermal decomposition of an initiator or by UV radiation. A kinetic scenario which was

developed to describe a mechanism of microemulsion polymerization in o/w system is the so-called Candau-Leong-Fitch model (CLF-model)[42] which is sketched in Figure 2.

Before polymerization, due to the high concentration of surfactants in the system and extremely large surface of micelles formed by surfactants, almost all monomers are solubilized in these swollen micelles and these parental microemulsion droplets are still very small and almost equal size.

At the beginning of the polymerization (a), the radicals generated in the aqueous phase enter some of the microemulsion droplets and start the polymerization. Once polymer is formed inside the particles, the system components will redistribute to maintain equilibrium. It was believed that the oil core of microemulsion droplets will disappear at very low conversion. These nucleated particles grow by transport of monomers from outside unpolymerized microemulsion droplets and the inactive polymer particles. This transport process can be performed either by diffusion or by collision (b). But the collision mechanism may not be expected for ionic surfactant microemulsion because of electrostatic repulsion. The free initiator radicals are preferentially captured by the monomer-swollen micelles, which might be simply due to their number, or can be caused by a different permeability through the surfactant layers.

Transport of monomer into the growing latex particles occurs from all monomer-swollen micelles simultaneously. This transport process is fast with respect to polymer chain growth so that there is plenty of time for the system to rearrange to maintain the monomer distribution close to equilibrium as polymerization progresses.

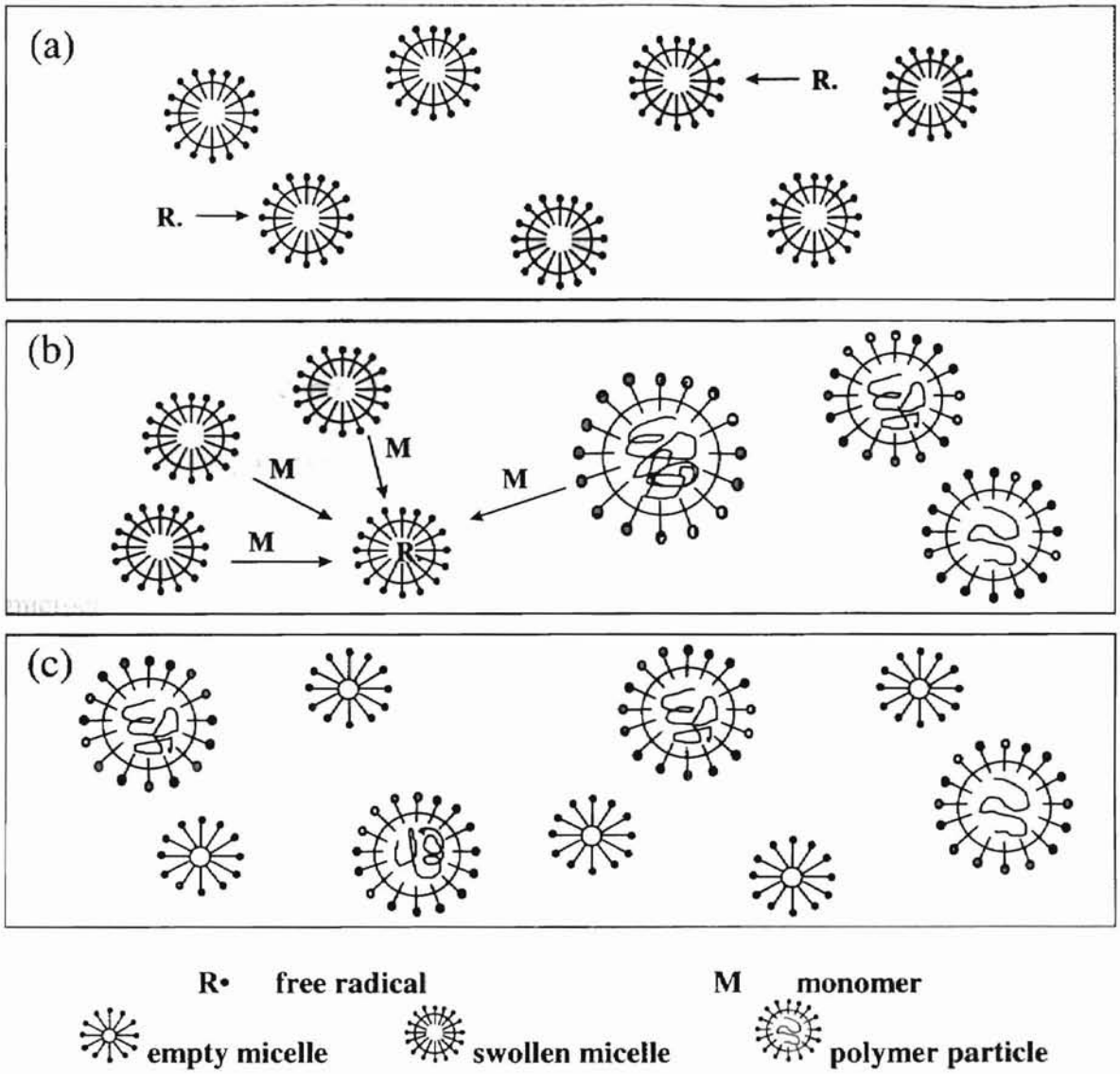

(a) **Nucleation in Microemulsion Droplets**

(b) **Monomer Transport**

(c) **Polymer particles and large surplus of empty micelles**

Figure 2. Microemulsion polymerization mechanism of the CLF-model

At the end of the polymerization (c), latex particles larger than the primary microemulsion droplets coexist with a large excess of empty micelles which have had their contents of monomer depleted.

The peculiar aspect of this model is that the probability of particle nucleation for every new radical generated is unity, even at the end of the reaction. This means that particle nucleation occurs continuously throughout the polymerization, which can be proved by the independence of the particle size on the conversion of polymerization and the number of the polymer chains per particle.[36]

Based on the above description there are a few different characteristics of o/w microemulsion polymerization in comparison with conventional emulsion polymerization: (1) No monomer droplets exist in microemulsions. (2) Polymerization occurs only in the monomer reservoir encapsulated in the particle. (3) The system is optically transparent throughout the polymerization process.

Polymerization in microemulsion offers great opportunities to synthesize special polymer materials or polymer colloids with high functionality on the particle surface. This can be achieved either by ternary copolymerization of monomer, functional comonomer and cross-linker in sturdy microemulsions[43,44] or by surface modification of functionalized nanoparticles in microemulsion.[45,46] However these two convenient ways of surface functionalization of microlatexes are all based upon the fact that more polar functional monomers get remarkably enriched at the oil/water interface and are fixed by the copolymerization procedure.[33] Because of such high degree of functionalization on the particle surface, nanolatexes have numerous promising applications for example in drug delivery,[47] microencapsulation,[48] and biomedical diagnosis,[49] provided that suitable

ligands or binding groups are linked to the surface to ensure recognition. Moreover, the very large specific area of particles in the 20-30 nm diameter range may offer new opportunities in other areas such as catalysis and chromatography.[33]

(3) Dispersion Polymerization

Dispersion polymerization is another heterogeneous polymerization process, which leads to the formation of spherical particles in the region of about 0.5-10 μm in diameter ("microspheres"). The basics of this method of preparation of monodisperse micron-sized polymer colloids have been reviewed by Barrett.[50]

Among the main uses for dispersion polymers are surface coating for metal panels, particularly in the automotive industry and food canning. Dispersion polymerization products are also exploited for chromatographic media, pressure-sensitive adhesives, printing inks and electroreprographics as developers and toners.

A dispersion polymerization process starts as a homogeneous mixture of monomer and comonomer, organic solvent, soluble polymer that functions as a steric stabilizer, and initiator. The solvent can dissolve monomer and stabilizer but is a poor solvent for the resulting polymer. Figure 3 shows a scheme for the nucleation and growth of sterically stabilized particles in nonaqueous dispersion polymerization.[51]

The striking feature of dispersion polymerization is that initially there is only one phase and therefore all monomer, stabilizer and initiator are distributed throughout the reaction medium (a). Upon heating, the initiator decomposes and the free radicals react with solute monomer to form oligomeric radicals (b). Depending on the solvency of the organic medium for the resulting oligomeric radicals, at a critical chain length, the

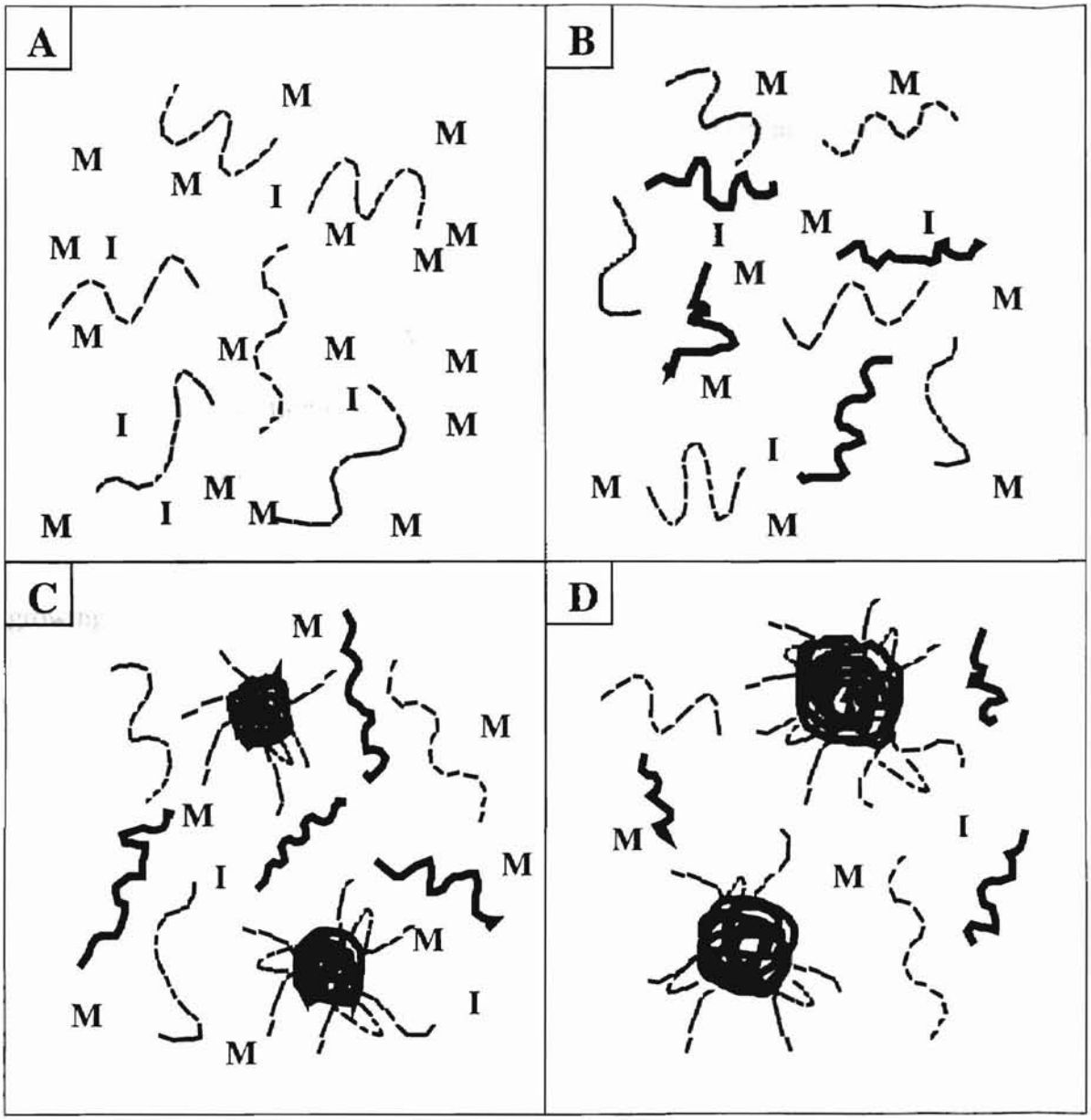

Figure 3. Schematic presentation of dispersion polymerization process

oligomers precipitate and adsorb stabilizer to form stable particle nuclei (c). Once the primary particles have been formed, they absorb monomer from the continuous phase and are swollen by the polymerization medium. As result, polymerization proceeds largely within the individual particles until all of the monomer is consumed (d).

Typical examples of dispersion polymerization are those of styrene and methyl methacrylate systems studied by Almog et al.[52] and Ottewill et al.[53] Particle size in dispersion polymerization is governed by the temperature of polymerization, concentrations of monomer and initiator, and the type and concentration of stabilizer which determine the ability of the stabilizer to maintain the colloidal stability of the growing particles. In addition, the solvency and polarity of the polymerization medium strongly influences particle size. The effect of medium solvency on particle size in dispersion polymerization of styrene in C_1-C_5 alcohols and various alcohol-ether or alcohol-water mixtures was extensively investigated by Ober et al.[54]

Specific functional groups can also be built into microspheres by means of copolymerization of styrene and functional comonomers. For example, functional microspheres have been made with chloromethyl groups,[55,56] formyl groups and sulfonyl chloride groups.[57] Chemical modification of these functional microspheres can further be carried out, such as introducing cationic groups[58] and binding amino ligands.[56]

In the next chapter we report how these three polymerization methods were applied to make three different sizes of particles and we used them to catalyze the decarboxylation reaction.

REFERENCES

1. Starks, C. M.; Liotta, C. L.; Halpern, M. *Phase-Transfer Catalysis*; Chapman and Hall: New York, 1994.
2. Nakamura, A.; Tsutsui, M. *Principles and Applications of Homogeneous Catalysis*; John Wiley and Sons: New York, 1980.
3. Thomas, J. M.; Thomas, W. J. *Principles and Practice of Heterogeneous Catalysis*; VCH: Weinheim, 1997.
4. Starks, C. M. *J. Am. Chem. Soc.* **1971**, 93, 195.
5. Sam, D.; Simmons, H. E. *J. Am. Chem. Soc.* **1972**, 94, 4024.
6. Fendler, J. H.; Fendler, E. J. *Catalysis in Micellar and Macromolecular Systems*; Academic Press: New York, 1975.
7. Grätzel, M.; Kalyanasundaram, K. *Kinetics and Catalysis in Microheterogeneous Systems*; Marcel Dekker, Inc.: New York, 1991.
8. Tomoi, M.; Ford, W. T. *Synthesis and Separations Using Functional Polymers*; Sherrington, D. C.; Hodge, P., Eds.; Wiley: Chichester, 1988.
9. Fife, W. K. *Trends Polym. Sci.* **1995**, 3, 214.
10. Ford, W. T. *React. Funct. Polym.* **1997**, 33, 47.
11. Miller, P. D.; Ford, W. T. *Polym. Mater. Sci. Eng.* **1997**, 76, 318.
12. Ford, W. T.; Lee, J.-J.; Yu, H. *Supramol. Chem.* **1995**, 5, 21.
13. Lee, J.-J.; Ford, W. T. *J. Am. Chem. Soc.* **1994**, 116, 3753.
14. Lee, J.-J.; Ford, W. T. *J. Org. Chem.* **1993**, 58, 4070.
15. Ford, W. T.; Yu, H. *Langmuir* **1993**, 9, 1999.

16. Ford, W. T.; Yu, H.; Lee, J.-J.; El-Hamshary, H. *Langmuir* **1993**, 9, 1698.

17. Lee, J.-J.; Ford, W. T.; Moore, J. A.; Li, Y. *Macromolecules* **1994**, 27, 4632.

18. Vassilev, K.; Kreider, J.; Miller, P. D.; Ford, W. T. ***React. Funct. Polym.*** **1999**, 41, 205.

19. Vassilev, K.; Ford, W. T. *J. Polym. Sci., Part A: Polym. Chem.* **1999**, 37, 2727.

20. Hampton, K. W.; Ph.D. Dissertation, Oklahoma State University, 1999.

21. Miller, P. D.; Ford, W. T. *Chem. Commun.* **1998**, 1151.

22. Cacciapaglia, R.; Mandolini, L.; Arnecke, R.; Bohmer, V.; Vogt, W. *J. Chem. Soc., Perkin Trans. 2* **1998**, 2, 419.

23. Miller, P. D.; Ford, W. T. *Langmuir*, in press.

24. Fitch, R. M. *Polymer Colloids: A Comprehensive Introduction*; Academic Press: San Diego, 1997; p202.

25. Fields, G. B. In *Molecular Biomethods Handbook*; Rapley, R.; Walker, J. M., Eds.; Humana Press: Totowa, 1998; p527.

26. Moss, R. A.; Chung, Y.-C. *Langmuir* **1990**, 6, 1614.

27. Ford, W. T.; Tomoi, M. *Adv.Polym.Sci.* **1984**, 55, 49.

28. Lovell, P. A.; El-Aasser, M. S., Eds.; *Emulsion Polymerization and Emulsion Polymers*; Wiley: Chichester, 1997.

29. Odian, G. G. *Principles of Polymerization*, 3rd ed.; John Wiley and Sons: New York, 1991; p335.

30. Gilbert, R. G. *Emulsion Polymerization*; Academic Press: London, 1995; p51.

31. Hoar, J. P.; Schulman, J. H. *Nature* **1943**, 152,102.

32. Candau, F. In *Polymerization in Organized Media*; Paleos, C. M., Ed.; Gordon Science Publications: Philadelphia, PA, 1992; p215.

33. Antonietti, M.; Basten, R.; Lohmann, S. *Macromol. Chem. Phys.***1995**, 196, 441.

34. Guo, J. S.; El-Aasser, M. S.; Vanderhoff, J. W. *J. Polym. Sci., Polym. Chem. Ed.* **1989**, 27,691.

35. Guo, J. S.; Sudol, E. D.; Vanderhoff, J. W.; El-Aasser, M. S. *J. Polym. Sci., Polym. Chem. Ed.* **1992**, 30, 703.

36. Guo, J. S.; Sudol, E. D.; Vanderhoff, J. W.; El-Aasser, M. S. *J. Polym. Sci., Polym. Chem. Ed.* **1992**, 30, 691.

37. Gan, L. M.; Lee, K. C.; Ng, S. C. *Langmuir* **1995**, 11, 449.

38. Larpent, C.; Tadros, T. F. *Colloid Polym. Sci.* **1991**, 269, 1171.

39. Morgan, J. D.; Lusvardi, K. M.; Kaler, E. W. *Macromolecules* **1997**, 30, 1897.

40. Puig, J. E.; Perez-Luna, V. H.; Perez-Gonzalez, M.; Macias, E. R.; Rodriguez, B. E.; Kaler, E. W. *Colloid Polym. Sci.* **1993**, 271, 114.

41. Pilcher, S. C.; Ford, W. T. *Macromolecules* **1998**, 21, 3454.

42. Candau, F.; Leong, Y. S.; Fitch, R. M. *J. Polym. Sci., Polym. Chem. Ed.* **1985**, 23, 193.

43. Antonietti, M.; Lohmann, S.; Cornelius, V. N. *Macromolecules* **1992**, 25, 1139.

44. Antonietti, M.; Bremser, W.; Lohmann, S. *Prog. Colloid Polym. Sci.* **1992**, 89, 62.

45. Larpent, C.; Bernard, E.; Richard, J.; Vaslin, S. *React. Funct. Polym.* **1997**, 33, 49.

46. Li, P.; Xu, J.; Wu, C.; *J. Polym. Sci., Part A: Polym. Chem.* **1998**, 36, 2103.

47. Fritz, H.; Maier, M.; Bayer, E. *J. Colloid Interface Sci.* **1997**, 195, 272.

48. Dupuy, B.; Cadic, C.; Gin, H.; Baquey, C.; Dufy, B.; Ducassou, D. *Biomaterials* **1991**, 12, 493.

49. Gasco, M. R.; Trotta, M. *Int. J. Pharm.* **1986**, 29, 267.

50. Barrett, K. E. J. Ed., *Dispersion Polymerization in Organic Media*; Wiley: London, 1975.

51. Tseng, C. M.; Lu, Y. Y.; El-Aasser, M. S.; Vanderhoff, J. W. *J. Polym. Sci., Polym. Chem. Ed.* **1986**, 24, 2995.

52. Almog, Y.; Levy, M. *J. Polym. Sci., Polym. Chem. Ed.* **1982**, 20, 417.

53. Antl, L.; Goodwin, J. W.; Hill, R. D.; Ottewill, R. H.; Owens, S. M.; Papworth, S. *Colloids and Surfaces*, **1986**, 17, 67.

54. Lok, K. P.; Ober, C. K. *Can. J. Chem.* **1985**, 63, 209.

55. Okubo, M.; Ikegami, K.; Yamamoto, Y. *Colloid. Polym. Sci.* **1989**, 267, 193.

56. Margel, S.; Nov, E.; Fisher, I. *J. Polym. Sci., Part A: Polym. Chem.* **1991**, 29, 347.

57. Shahar, M.; Meshulam, H.; Margel, S. *J. Polym. Sci., Polym. Chem. Ed.* **1986**, 24, 203.

58. Okubo, M.; Iwasaki, Y.; Yamamoto, Y. *Colloid. Polym. Sci.* **1992**, 270, 733.

CHAPTER II

Catalysis of Decarboxylation of 6-Nitrobenzisoxazole-3-carboxylate by Cationic Polymer Particles with Different Sizes

ABSTRACT

Polystyrene latexes with quaternary ammonium ion-exchange sites were used as catalyst for the decarboxylation of 6-nitrobenzisoxazole-3-carboxylate in aqueous media. The latex particles respectively with 20 nm, 135 nm and 1.05 μm or so in diameter were prepared by microemulsion, emulsion and dispersion copolymerization of styrene and vinylbenzyl chloride using divinylbenzene as cross-linker and AIBN as initiator. Treatment of these latexes with tributylamine or trimethylamine produced colloidal particles containing quaternary ammonium chloride repeat units which can function as anion-exchange sites. A decarboxylation rate constant (k_{obsd}) of 9000 times the rate constant in water alone was achieved in emulsion particles containing 36 mol % of (styrylmethyl)tributylammonium chloride repeat units at pH 11.2 and 25.0°C. The value of the intraparticle rate constant (k_L) of the decarboxylation reaction in the emulsion latex is larger than those in the microemulsion latex and the dispersion latex, which means there is no diffusion limitation in emulsion-based particles. A detailed comparison of these kinetic investigations with microemulsion, emulsion and dispersion latex particles is presented.

INTRODUCTION

Polymer latexes have diameters 10-100 times larger than micelles and 1000-10000 times smaller than ion exchange resins. By incorporating positively charged sites throughout the particles, polymer latexes can function as highly efficient catalysts. However, unlike polymer latexes the polymer bead catalysts often are less active because rates of reactions are limited by mass transfer of reactants from solution to the bead surface and intraparticle diffusion of reactants from the surface to the active sites within the bead.[1] Equation 1[2] gives us the diffusion time of a molecule or ion from the surface of a particle to 50% of the active sites,

$$t_{1/2} = 0.030\ r_0^2/D \qquad (1)$$

where r_0 represents the spherical particle radius and D represents the diffusion coefficient of the molecule or ion.

Smaller particles reduce the diffusion length and hence the diffusion time. When polymer colloidal particles are used as phase transfer catalysts the much smaller sizes and greater surface areas per unit mass of polymer latexes than of polymer beads should overcome such diffusional limitations. In this case we can imagine that the observed rate depends only on the intraparticle and solution phase rate constants and on concentrations in the two phases.

Polystyrene latexes have been investigated as phase transfer catalysts for a number of years.[3] The kinetics of reactions within these latexes have been analyzed using both

enzyme and ion exchange models. These reactions have shown that polymer colloids used as highly efficient catalytic media promote the reaction rates several orders of magnitude higher than that observed in the absence of latex particles.

The most active cationic polystyrene latex containing quaternary ammonium sites catalyzes the decarboxylation of 6-nitrobenzisoxazole-3-carboxylate (**1**) in aqueous solution with an enhancement in the observed rate constant in excess of 10,000 times over the rate constant in water alone.[4] The decarboxylation mechanism is shown in Scheme 1.

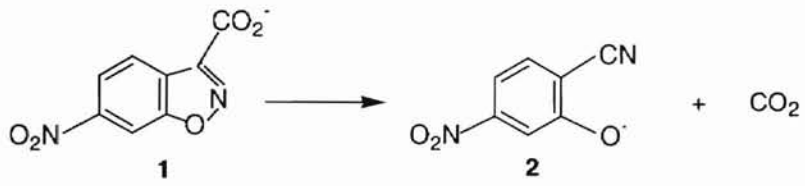

Scheme 1. Decarboxylation of 6-nitrobenzisoxazole-3-carboxylate

Moreover, these cationic polymer colloids can be used as anion-exchange latexes when one of the reactants or a catalyst is an anion that binds strongly to the particles. This has been accomplished using cross-linked polystyrene latexes containing (styrylmethyl)tributylammonium chloride repeat units which increase the *o*-iodosobenzoate (IBA) anion-catalyzed reaction rate of hydrolysis of *p*-nitrophenyl diphenyl phosphate (PNPDPP) up to 6,300 times higher than that in the absence of latexes.[5] Scheme 2 shows the hydrolysis reaction mechanism.

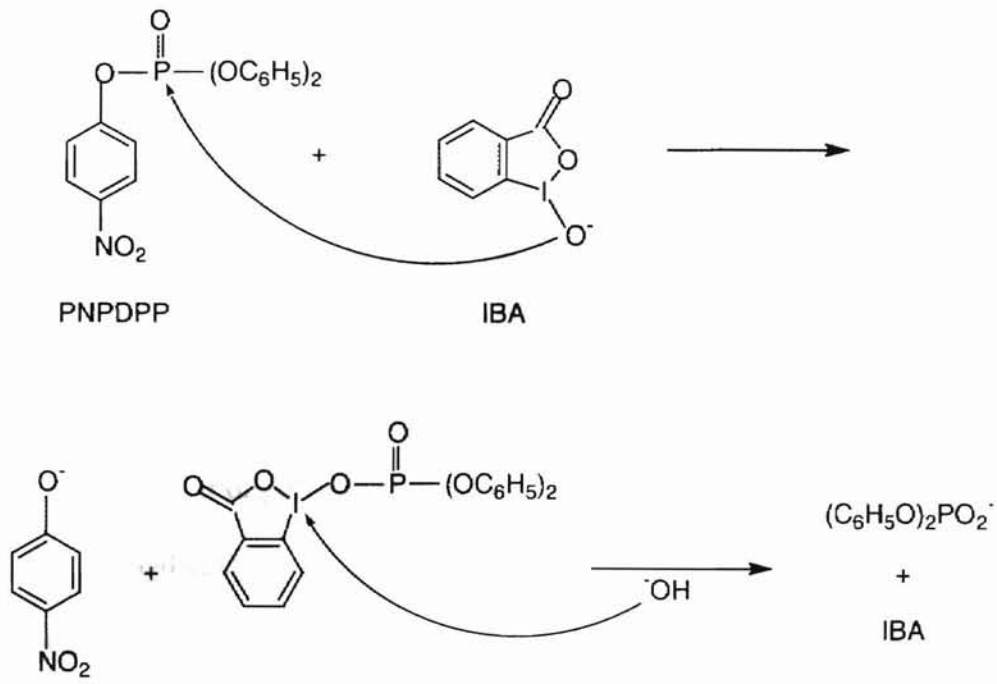

Scheme 2. IBA-catalyzed reaction of PNPDPP

The above catalytic activity observed in the latexes is due to both higher local concentrations of reactants and faster rates of reaction in the polymer phase than in the aqueous phase. Although these latex particles result in rates of reactions similar to those observed in cationic micellar catalysis,[6,7] they were produced by emulsion polymerization and their typical diameters are 200-300 nm.[8] Thus, it has been assumed that when the cationic colloidal polymer particles < 1 μm in diameter are used as catalytic media, their high surface areas and the short diffusion paths to the particle interiors give rise to little or no diffusional limitation to reaction rates.[9] However, since microlatexes combine the advantages of homogeneous and heterogeneous systems, Antonietti et al. planned to examine the catalytic activity of nanoparticles to see if there is a further increase of the catalytic potential for the microemulsion-based systems.[10] But we haven't found their

report about this issue up to date. Also, for catalysis using the dispersion latex particles around 1 μm, we did not find any related literatures.

In order to investigate the effect of particle size on the catalytic activity, once we thought about the hydrolysis of PNPDPP. But due to the insolubility of PNPDPP in water the substrate partitions completely into the latex phase. Hence, the kinetic results from hydrolysis of PNPDPP will not really indicate the rate of diffusion of PNPDPP into particles and the effect of polymer particle size on the rate of reactions. For this reason we have used small amounts of cationic polystyrene particles, which are about 20 nm, 200 nm and 1 μm in diameter respectively, to catalyze decarboxylation of 6-nitrobenzisoxazole-3-carboxylate in aqueous media.

The decarboxylation of **1** provides a simple chemical model for the biologically important decarboxylation[11], since it is unimolecular and is not catalyzed by acids or bases. However, this reaction is a very solvent dependent reaction. For example, the rate of decarboxylation of 6-nitrobenzisoxazole-3-carboxylate is 10^8 times faster in hexamethylphosphoramide than in aqueous solution.[12]

Because of the solvent-sensitive nature of this reaction, it has been used to probe the reactive microenvironment in a great number of colloidal media. Table 1 presents the comparison of results of first-order rate constants of decarboxylation of **1** at appropriate latex concentrations under which light scattering doesn't matter to measurement of the kinetics by tracking the UV-visible absorbance of the product **2**, 2-cyano-5-nitrophenoxide ion.

Table 1. First-order Rate Constants of Decarboxylation of 1 Catalyzed by Latexes at 25.0 °C Using 2 mM NaOH[a]

	Substrate(1) (10^{-5} M)	Latex (mg/mL)	$[N^+]$[b] (10^{-4} M)	k_{obsd}/k_w[c]
TMAQ60×1[d]	13.04	0.559	19.06	220
TMAQ39×1[d]	13.04	0.500	13.16	250
TEAQ32×1[d]	6.58	0.619	13.20	800
TBAQ24×1[d]	6.58	0.463	7.42	10500

[a] Ref. 4. [b] Concentration of quaternary ammonium unit. [c] The first-order rate constant in water was $k_w = 3.1 \times 10^{-6}$ s^{-1}. [d] TMA = trimethylammonium, TEA = triethylammonium, TBA = tri-n-butyl ammonium. The numbers refer to mol % quaternary ammonium units in latexes.

Table 1 shows that less quaternary ammonium units in the latex lead to faster rate of the reaction. In addition, the larger the ionic radius of the quaternary ammonium group, the higher the catalytic activity of the latex. Hence, these indicate that the more lipophilic the environment inside the latex particle, the more active the latex as a phase transfer catalyst. In general, there are two facts that affect the rate of decarboxylation. One is that the lipophilic property of internal structure of the latex particle determines the extent of extraction of the hydrophobic substrate. Another fact is that the anionic reagents in such an environment are less solvated by water and are more reactive.

EXPERIMENTAL

Materials

Styrene (Aldrich) and vinylbenzyl chloride (VBC, Aldrich) were distilled under vacuum in order to remove the inhibitor and oligomeric impurities, and stored at 5°C. Before use the distilled styrene, VBC and divinylbenzene (DVB, 80%) were filtered through an activated aluminum oxide column. Tributylamine (99%, Aldrich) and 25-27 wt % aqueous trimethylamine (Aldrich) as quaternization agent, poly (N-vinylpyrrolidone) with a nominal molecular weight of 40,000 (PVP, Polysciences) as stabilizer, Triton N-57 (Sigma) as costabilizer, and stearyltrimethylammonium chloride (STAC, TCI) as surfactant were used as received. 2,2'-Azobisisobutyronitrile (AIBN, Aldrich) was used after recrystallization from methanol. Methyl 6-nitrobenzisoxazole-3-carboxylate (Pfaltz & Bauer) was recrystallized from methanol to produce yellowish needles that were characterized by ^{1}H NMR and had mp 131-132 °C (lit.[13] mp = 131-132°C). Deionized water with a resistivity of 1.9×10^6 Ω cm was used in all experiments.

Synthesis of Microlatexes

Into a 50 mL Erlenmeyer flask were added 3.0 g of STAC and 20.5 mL of water. The mixture was heated and stirred by a magnetic stirrer until the mixture became homogeneous and transparent. On the other hand, into a 50 mL three-necked round bottom flask were added 0.825 mL (0.750 g) of styrene, 0.70 mL (0.750 g) of VBC, 0.021 mL (0.0188 g) of DVB and 0.0075 g of AIBN. The flask was slightly shaken to form the oil phase. The flask was equipped with a condenser, an overhead stirrer and a nitrogen

inlet. After that, the water phase was added to the oil phase, and the mixture was stirred for 0.5 h at room temperature. Then the reaction mixture was heated for 4 h in a 60°C oil bath and nitrogen blanketing was maintained through the reaction. Polymerization produced a stable, translucent microlatex with a bluish tint.

Synthesis of Microspheres

Into a 125 Erlenmeyer flask were placed 0.375 g of PVP, 0.125 g of Triton N-57 and 21.5 g (27.4 mL) ethanol. The mixture was stirred by a magnetic stirrer until the mixture became homogeneous. On the other hand, into a 100 mL three-necked round bottom flask were placed 0.825 mL (0.750 g) of styrene, 2.10 mL (2.25 g) of VBC, 0.012 mL (0.0113 g) of DVB and 0.015 g of AIBN. The flask was slightly shaken to form the oil phase. The flask was equipped with a condenser, an overhead stirrer and a nitrogen inlet. After that, the ethanol phase was added to the monomer phase, and the mixture became homogeneous and transparent under stirring. Then the reaction was carried out for 24 h in a 70°C oil bath. Nitrogen blanketing and stirring were maintained through the reaction. After polymerization a milky dispersion was produced, and some particles sedimented after several days.

TBA Quaternization

A mixture of 12 mL of latex (0.731 g solid, 2.36 mmol of VBC groups), 5 mL of DI water, 1.2 mL of 99 % tributylamine (4.72 mmol) was added into a 50 mL one-necked round bottom flask and heated to reflux for 48 h.

TMA Quaternization

A mixture of 10 mL of latex (1.30 g solid, 5.11 mmol of VBC groups), 10 mL of DI water and 3.89 mL of 25-27 wt % aqueous trimethylamine solution (15.33 mmol) was added into a glass beaker within a stainless steel reactor having a magnetic stirrer. The reactor was sealed and at least 2/3 immersed in a 65°C oil bath for 72 h.

Latex Purification

After quaternization the transparent microlatex was dialyzed in 50,000 MW cut-off tubing membrane (Spectra/Por® 7 Molecular Porous Regenerated Cellulose) first by methanol for 3 days, then by DI water for 1 day. The dialysate of methanol was changed twice per day, and the dialysate of DI water was changed every 2-3 hours.

After quaternization the dispersion latexes were dialyzed in 50,000 MW cut-off tubing membrane (Spectra/Por® 7 Molecular Porous Regenerated Cellulose) by methanol for 1 day to remove the low molecular weight organic compounds, then ultrafiltered with methanol using PTFE membrane (0.45 μm, Gelman) for 2 days to remove the stabilizer of PVP. Finally the dispersion latexes were ultrafiltered with DI water for 1 day to remove methanol.

IR and NMR Spectra of the Latexes

After replacing water by methanol through dialysis for 2 days a sample of latex (30 mg solid) was taken into a wide mouth jar. The latex was first evaporated in air until most of methanol was removed, then transferred into a vacuum desiccator and dried for 6 h at room temperature. The IR sample was made in a KBr pellet. The NMR sample was made in a NMR tube containing 0.5 mL of DMSO-d_6 to swell 10 mg of dried smashed

latex particle. Standard ^{1}H NMR acquisition and processing conditions for low molar mass compounds in solutions were used here.

Microemulsion latex (unquaternized): IR (cm^{-1}): 1270~1265 (strong, $PhCH_2Cl$).

Microemulsion TBA latex: IR (cm^{-1}): the peak at 1270-1265 disappeared.

Microemulsion TMA latex: IR (cm^{-1}): the peak at 1270-1265 disappeared.

Since the pure particles of microemulsion, emulsion and dispersion latex have the same chemical structures, the IR spectra of emulsion and dispersion latexes are as almost the same as those of microemulsion latexes.

Dispersion TBA latex: ^{1}H NMR (300 MHz, DMSO-d_6, δ ppm): 0.90 (broad, $-CH_3$); 1.31 (broad, CH_2 next to CH_3); 1.53 (broad, middle-CH_2-); 2.97 (broad, NCH_2-); 3.20 (sharp, CH_3 of impurity methanol); 3.37 (sharp and high, impurity H_2O); 4.41 (broad, $ArCH_2N$); 6.48 and 7.08 (broad, ArH).

Dispersion TMA latex: ^{1}H NMR (300 MHz, DMSO-d_6, δ ppm): 1.43 (broad, backbone CH_2 of polymer); 2.98 (broad, quaternized $N(CH_3)_3$); 3.37 (sharp and high, impurity H_2O); 4.45 (broad, $ArCH_2N$); 6.48 and 7.08 (broad, ArH).

Solid Contents of the Latexes

The solid contents of all latex samples after purification were determined by accurately measuring 2.0 mL of each latex into a small vial and drying to constant weight in a 120°C oven. The results were the average of three measurements that varied within a range of 2 %.

Determination of Chloride Ion Contents

To determine the chloride ion contents, 10.00 mL of purified latex was pipetted volumetrically into a 30 mL beaker, and 5 mL of deionized water and 1.2 mL of 5 M $NaNO_3$ were added for adjusting solution ionic strength. Some drops of 1 N HNO_3 were added to adjust the solution pH near to 2 using Fisher Scientific pH meter (Model 25). The mixture was titrated with standard 0.0494 M $AgNO_3$ solution using an ORION chloride-selective electrode (Model 9617BN). The titration curve of milliliters of titrant vs. millivolts was constructed. The end point was determined by the normal midpoint method for potentiometric titration. The measurements of $[Cl^-]$ performed in triplicate were reproducible to within 3% of the mean.

Particle Size Measurement

The particle sizes of microlatexes and dispersion latexes were measured respectively by TEM and SEM. Before measurement the concentrations of latex samples were adjusted to about 1.5 wt % solids. The diameters of at least 50 nonaggregated particles were achieved from electron microscopic negatives using a microscope equipped with a micrometer scale. The number average diameters D_n and weight average diameters D_w were calculated from the following equations:

$$D_n = (\Sigma D_i^3 / \Sigma n)^{1/3}$$

$$D_w = (\Sigma D_i^6 / \Sigma D_i^3)^{1/3}$$

6-Nitrobenzisoxazole-3-carboxylic Acid[14]

Into a 50 mL flask were added 0.29 g of recrytallized methyl 6-nitrobenzisoxazole-3-carboxylate, 12.5 mL of 95.5 wt % sulfuric acid and 2.5 mL of DI water. The mixture was heated in a boiling water bath for 20 min and then quickly poured into ice-water contained in a 100 mL beaker. After cooling overnight, the white crystals were washed by water, and then dried in a vacuum desiccator at 40 °C. The overall yield was 78 %. The final light yellow needles had mp 168-169 °C [lit.[14] mp 167-169 °C (monohydrate)]. A ^{1}H NMR spectrum showed less than 3 mol % of methyl ester remaining. The final light yellow needles were used for kinetic studies without further purification.

Kinetic Analysis

A 0.0106 M substrate solution was prepared by adding 0.022 g of 6-nitrobenzisoxazole-3-carboxylic acid into 10 mL of ethanol containing 2 mM HCl on the day of use. The latex kinetic media were prepared by mixing 1.67 mL of 30 mM NaOH, the appropriate amount of latex with known solid content, and nitrogen-purged water into a 25 mL volumetric flask so that a 2 mM NaOH solution (pH 11.2 ± 0.1) was obtained.

The following kinetic run is typical. A 3.0 mL sample of the latex kinetic medium was pipetted into a 1-cm polystyrene cuvette. The solution was allowed to equilibrate to 25.0 °C for 15 min. The temperature was controlled by circulating water from a thermostatted bath through the cuvette chamber of the UV spectrophotometer (HP 8452A). Then, 19.0 μL of the above substrate acid solution was added and mixed by rapidly shaking the cuvette for 2 s to start the reaction. The λ_{max} of the decarboxylation

product, 2-cyano-5-nitrophenoxide, was 398 nm in water, 424 nm in TMA quaternized latex, and 430 nm in TBA quaternized latex. For kinetic analysis the average absorbance between 400 and 430 nm was assumed to be linearly proportional to the product concentration.

The first-order rate constant (k_{obsd}) for appearance of 2-cyano-5-nitrophenoxide was obtained by fitting data to the first order increasing exponential equation, using commercial (TableCurve, Jandel Scientific) software. Rate constants were measured in duplicate and the results were reproducible to within 5 % of the mean.

RESULTS

Latex Synthesis and Characterization

The latex particles with average diameters of 20 nm, 135 nm and 1.05 μm were respectively prepared by microemulsion, emulsion and dispersion copolymerization of styrene and vinylbenzyl chloride in weight ratio of 50:50 in first two methods and 25:75 in the last method. Based on the weight of styrene and vinylbenzyl chrolide, 1.0 mol % of crosslinking monomer, divinylbenzene (DVB), was used in microemulsion and emulsion polymerization as our lab used before. For dispersion polymerization, only 0.3 mol % of DVB (based on styrene and vinylbenzyl chloride) was used because a larger amount of DVB would lead to either irregular-shaped particles or particle coagulation.[15] Treatment of these latexes with tributylamine or trimethylamine produced colloidal particles containing quaternary ammonium chloride repeat units which can function as anion-exchange sites. Figure 1 illustrates the common chemical structure of these cationic polymer particles with different sizes.

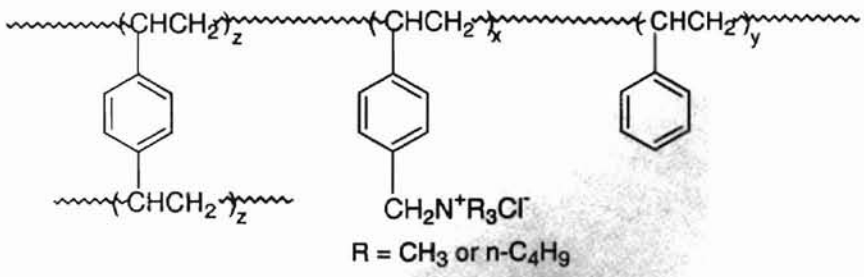

Figure 1. Chemical structure of cationic polystyrene latex

The diameters of dry original latex particles were measured by transmission electron microscopy (TEM) for microemulsion latex or emulsion latex and by scanning electron microscopy (SEM) for dispersion latex. The micrographs of microemulsion and dispersion latex are shown in Figure 2 and 3. However, the sizes measured by TEM or SEM were inaccurate for all of the quaternary ammonium latexes because of particle distortion during measurements.[8]

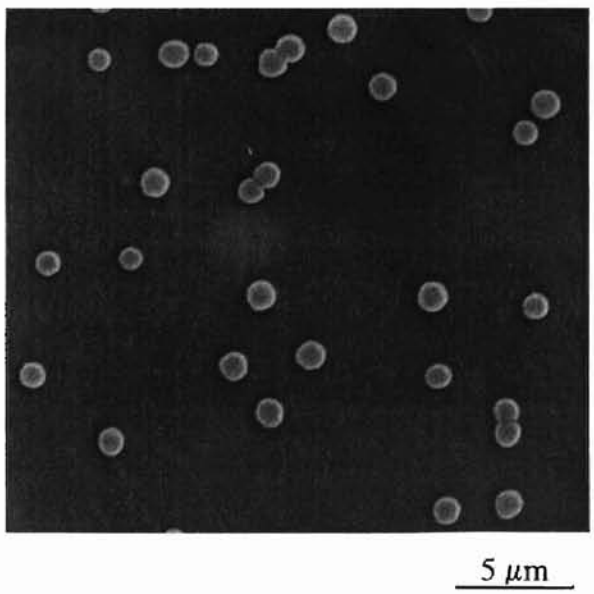

Figure 2. SEM of dispersion latex

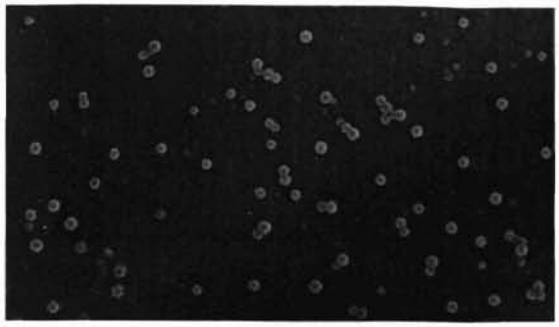

0.1 μm

Figure 3. TEM of microemulsion latex

The study of catalysis by polymer colloids requires latex particles containing carefully controlled compositions and structures and also latex solutions containing negligibly small amounts of polyelectrolytes and other organic impurities introduced during polymerization. Thus the purification of cationic polymer particles is very important. The purities can be verified by IR and ^{1}H NMR spectroscopy. For VBC-TBA and VBC-TMA latex IR spectra, the disappearance of the 1265 cm^{-1} peak proves the loss of CH_2Cl in quaternized latex particles. Furthermore, the assigned peaks in ^{1}H NMR spectra for TBA (Figure 4 in Appendix) or TMA (Figure 5 in Appendix) groups in polymer structures show the evidence of N^+ formation. Starting material $ArCH_2Cl$ or by-product $ArCH_2OH$ as well as product $ArCH_2N^+$ could have peaks at about 4.4 ppm in ^{1}H NMR spectra, but the size of the peak in this region did not suggest any large amount of any such groups. The CH backbone peak of polymer structure of TBA quaternized latex merged with tri-*n*-butyl ammonium ion peaks. The absence of sharp peaks brought by long chain H (around 1 ppm) of STAC surfactant or by 5-ring H (around 2 ppm) of PVP stabilizer (Figure 4) in ^{1}H NMR spectra confirmed the results of purification.

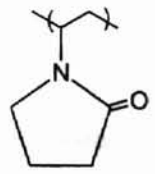

$[CH_3(CH_2)_{17}N(CH_3)_3]Cl$
stearyltrimethylammonium chloride
(STAC)

poly(N-vinylpyrrolidone)
(PVP)

Figure 4. Chemical structures of STAC surfactant and PVP stabilizer

The chloride ion contents in latex were determined by potentiometric titration using a chloride ion selective electrode. The quaternary ammonium ion concentration is assumed to be equal to the chloride ion concentration. The profiles of these pure cationic cross-linked polystyrene particles with different sizes are reported in Table 2 and Table 3.

Table 2. Sizes of Latexes

Latex sample	D_w[a]	D_n[a]	D_w/D_n
microemulsion[b]	19.6 nm	19.2 nm	1.02
emulsion[b]	135 nm	134 nm	1.01
dispersion[b]	1.05 μm	1.00 μm	1.05

[a] At least fifty particles were measured on micrograph negatives. [b] The standard deviations of measurements of microemulsion, emulsion and dispersion latex particles are 0.5 nm, 3 nm, and 0.06 μm respectively.

Table 3. Compositions of Cationic Latexes

Sample[a,b]	N^+/g[c]	Quaternization Yield[d] (%)	N^+ (mol%)	other[e] (mol%)	Styrene (mol%)	DVB (mol%)	D_h[f]
mTMAQ38	2.60	94	37.8	2.2	59.0	1.0	24.6 nm
mTBAQ37	1.86	92	37.0	3.0	59.0	1.0	27.1 nm
eTMAQ36	2.48	90	36.2	3.8	59.0	1.0	
eTBAQ36	1.81	89	35.8	4.2	59.0	1.0	
dTMAQ43	2.42	64	42.8	24.1	32.8	0.3	1.45 μm
dTBAQ55	2.08	82	54.9	12.0	32.8	0.3	1.60 μm

[a] m-, e-, d- represent respectively microemulsion, emulsion and dispersion. [b] The numbers mean mole percentage of N^+ sites in repeat units of latex particles. [c] Experimental values of N^+ sites in unit of mequiv per gram of dry latex. [d] The quaternization percent yield was calculated from the theoretical value and experimental data of N^+ contents in unit of mequiv per gram of dry latex. [e] Mole percentage calculated by difference for unquaternized VBC units. However IR and NMR spectra did not show residual VBC. [f] Hydrodynamic diameter from dynamic light scattering in 2 mM NaOH at pH 11.2.

First-order Rate Constants

The above latexes were tested for the ability to promote the decarboxylation of 6-nitrobenzisoxazole-3-carboxylate (Scheme 1). The results are reported in Table 4. The decarboxylation of **1** in aqueous solution accelerated upon addition of cationic latexes as evidenced by rapid appearance of yellow product, 2-cyano-5-nitrophenoxide (**2**). The λ_{max} of the decarboxylation product was 398 nm in water, 424 nm in TMA quaternized latex and 430 nm in TBA quaternized latex. Such a red shift for the absorption maximum of this compound was also reported in laurylated quaternized polyethylenimine by Klotz[16] and in poly(vinylbenzo-18-crown-6) by Smid.[17]

The first-order rate constants (k_{obsd}) for appearance of 2-cyano-5-nitrophenoxide were calculated from the first-order rate equation (2), where A_t, A_0, and A_{inf} refer to the

$$\ln(A_{inf} - A_t) = \ln(A_{inf} - A_0) - kt \qquad (2)$$

absorbances at times t, 0, and infinity.[18] Fitting the data obtained from the UV spectrophotometry to equation (1) gave the rate constant k_{obsd} listed in Table 4. All correlation coefficient values (R^2) were greater than 0.995.

Table 4. First-order Rate Constants of Decarboxylation[a]

	latex (mg/mL)	$10^4[N^+]$[b] (M)	$10^3 k_{obsd}$[c] (s^{-1})	k_{obsd}/k_w[d]
mTMAQ38	0.500	13.0	0.785	310
eTMAQ36	0.500	12.4	0.794	314
dTMAQ43	0.500	12.1	0.495	196
mTBAQ37	0.463	8.61	16.1	6360
eTBAQ36	0.467	8.45	23.1	9130
dTBAQ55	0.463	9.63	12.4	4900

[a] In 2 mM NaOH, pH = 11.2 ± 0.1, at 25.0 ± 0.1 °C, substrate concentration [S] = 8.74×10^{-5} M. [b] Concentration of quaternary ammonium unit in kinetic reaction. [c] Data are average of 2-3 experiments that deviated over a range of ≤ 5 % of the reported k_{obsd}. [d] The first-order rate constant in water was $k_w = 2.53 \times 10^{-6}$ s^{-1}.

In Table 4, the [N^+] was a factor of about ten greater than the substrate concentration. For microemulsion and emulsion latexes, with excess N^+ amount there were no deviations from first-order kinetics, and stable values of A_{inf} were obtained. At this particle concentration for dispersion latex, the kinetic data were somewhat noisy due to very small amount of light reaching the detector, but the data still followed pseudo-first-order kinetics. On the other hand, it is very important to keep the particles of dispersion latex stable during the kinetic process. In a control experiment for dispersion latex, there was no increase of UV absorbance versus wavelength after 2 hr, which is the typical data collection period, by use of a blank sample of the latex in the reference beam of spectrophotometer. Experimentally the highest latex concentration was 0.5 mg mL^{-1}.

Difference of Catalytic Activity between Higher and Lower Latex Concentration

In the above decarboxylation experiments, we found TBA quaternized latex showed much higher catalytic activity than TMA quaternized latex. In order to get shorter reaction periods in actual experiments and avoid other unwanted effects, we focused our further kinetic investigation on TBA quaternized latexes.

When the concentration of N^+ is much greater than the substrate concentration, the experimental data in microemulsion, emulsion and dispersion latex all obeyed the first-order kinetics. These experimental curves and corresponding calculated curves (smooth line) fitted by equation 2 are presented in Figures 5-7. At such high latex concentration (about 5 times larger than substrate concentration) the excess of latexes provide so many anion-exchange sites that at least half of substrates bind to latexes, and the mass transfer of substrate from water to latex is not a factor in the rates of reaction.

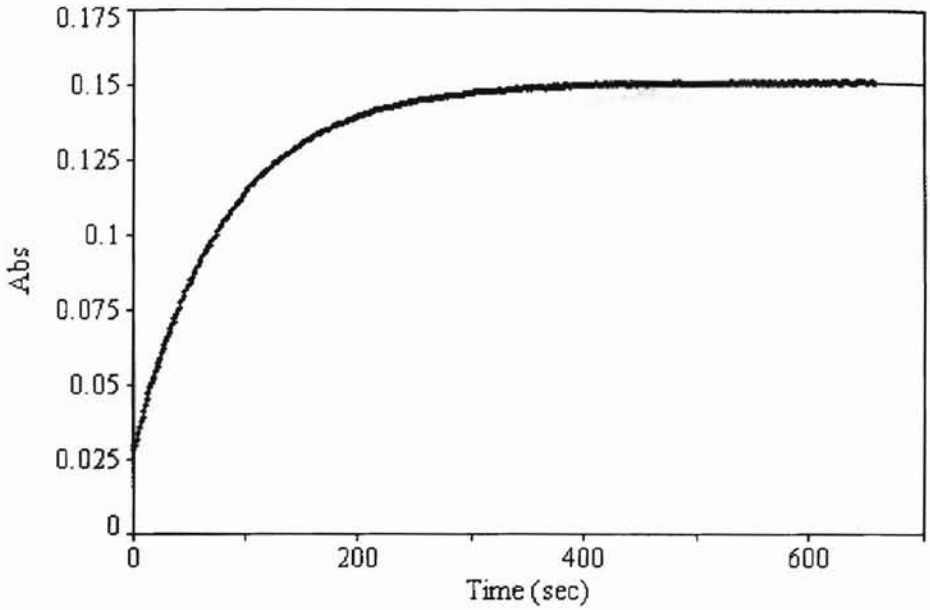

Figure 5. Plot of decarboxylation of **1** measured by absorbance of **2** at 400-430 nm in the microemulsion TBA latex at $[N^+] = 3.325 \times 10^{-4}$ M, $[S] = 0.665 \times 10^{-4}$ M. $R^2 = 0.9999$.

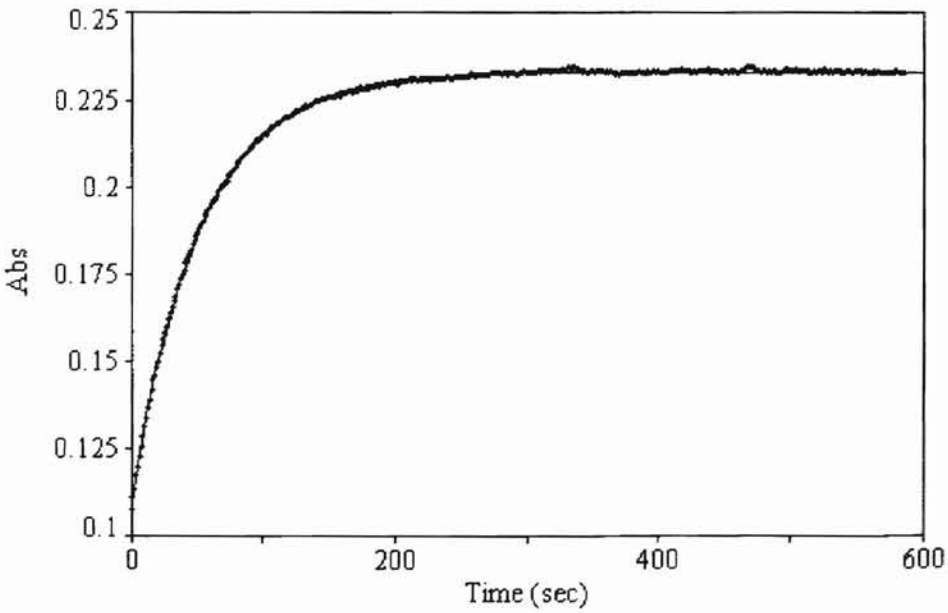

Figure 6. Plot of decarboxylation of **1** measured by absorbance of **2** at 400-430 nm in the emulsion TBA latex at $[N^+] = 3.325 \times 10^{-4}$ M, $[S] = 0.665 \times 10^{-4}$ M. $R^2 = 0.9996$.

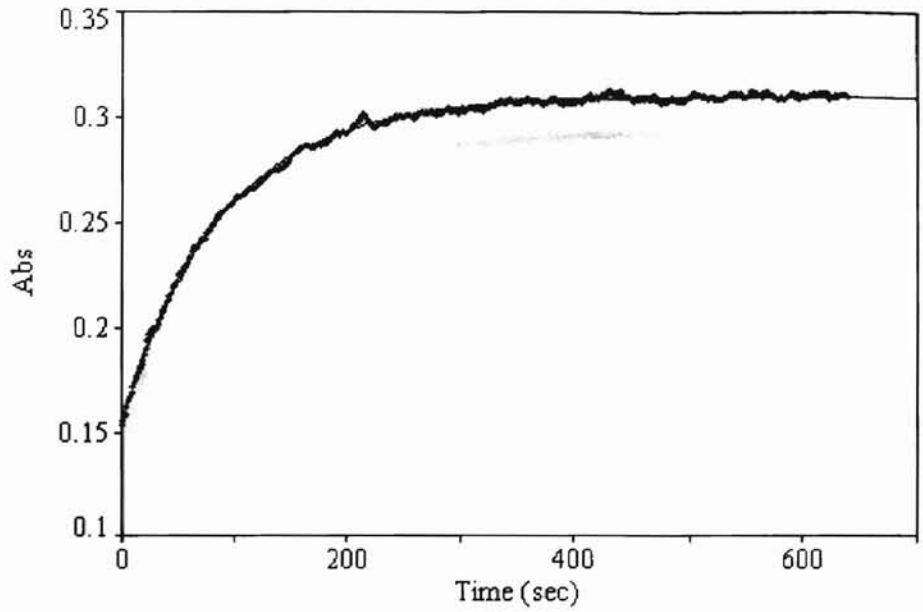

Figure 7. Plot of decarboxylation of **1** measured by absorbance of **2** at 400-430 nm in the dispersion TBA latex at $[N^+] = 3.325 \times 10^{-4}$ M, $[S] = 0.665 \times 10^{-4}$ M. $R^2 = 0.9983$.

To find out what happens when latex concentration is far below the substrate concentration, we carried out a group of kinetic experiments in which the concentration of substrate is about 10 times larger than the concentration of quaternary ammonium units. The experimental curves and fitted curves are shown in Figures 8-10. The data from microemulsion and emulsion latex are still compliant to the first-order kinetic process. However the data from the dispersion latex do not fit first-order kinetics. As we can see in Figure 10, there are three different deviation periods of experimental curves from calculated curves. At starting and longer time the deviation periods of experimental curve are below fitted curve. However, the middle deviation period of experimental curve is above the fitted curve.

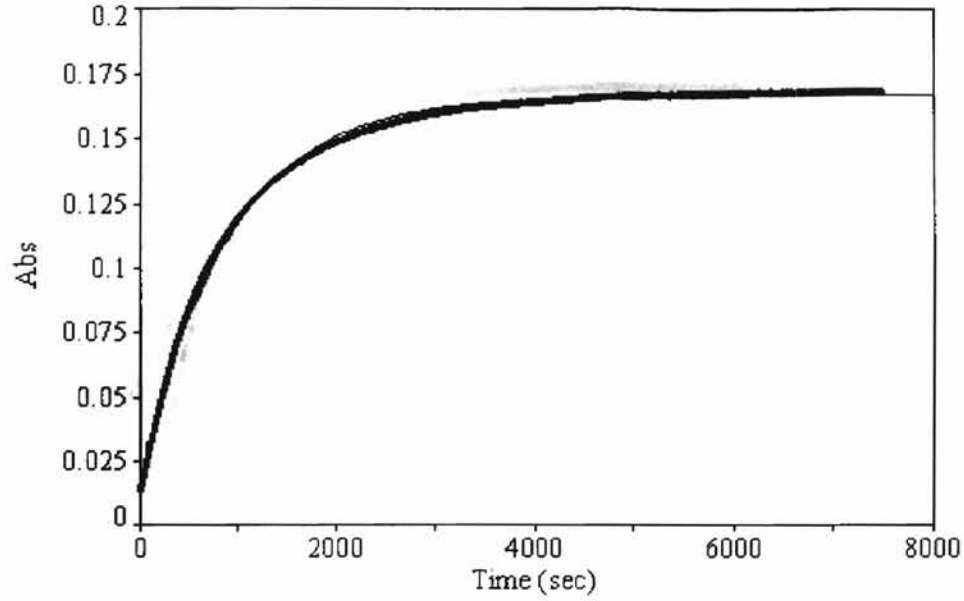

Figure 8. Plot of decarboxylation of **1** measured by absorbance of **2** at 400-430 nm in the microemulsion TBA latex at $[N^+] = 0.065 \times 10^{-4}$ M, $[S] = 0.665 \times 10^{-4}$ M. $R^2 = 0.9975$. The best fit to a first-order rate equation gave $k_{obsd} = 1.11 \times 10^{-3}$ s^{-1}.

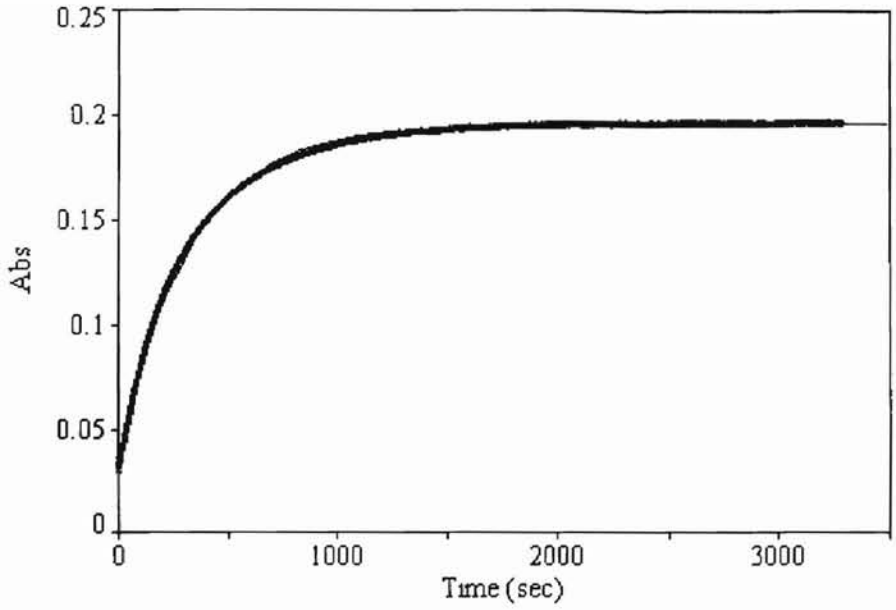

Figure 9. Plot of decarboxylation of **1** measured by absorbance of **2** at 400-430 nm in the emulsion TBA latex at $[N^+] = 0.065 \times 10^{-4}$ M, $[S] = 0.665 \times 10^{-4}$ M. $R^2 = 0.9978$. The best fit to a first-order rate equation gave $k_{obsd} = 3.05 \times 10^{-3}$ s^{-1}.

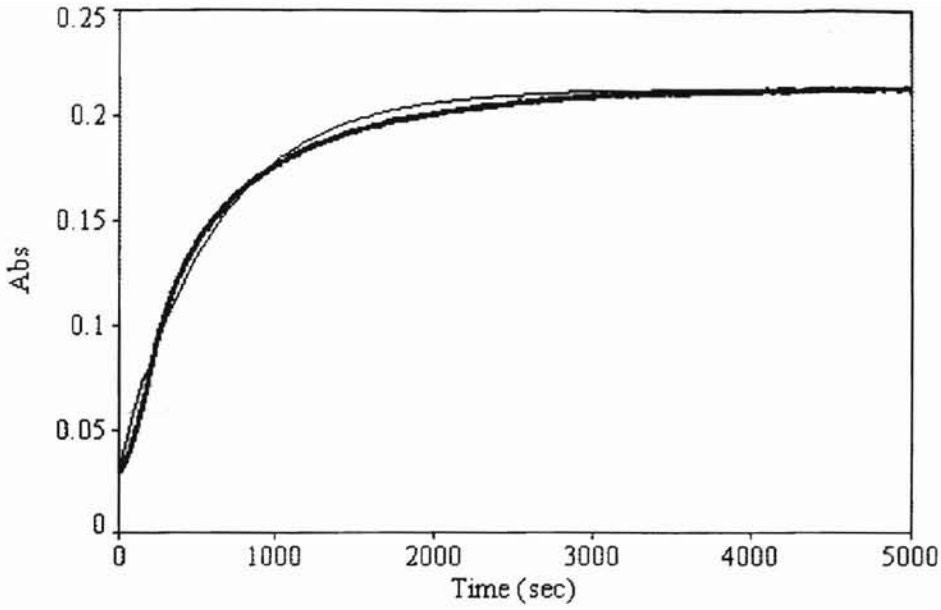

Figure 10. Plot of decarboxylation of **1** measured by absorbance of **2** at 400-430 nm in the dispersion TBA latex at $[N^+] = 0.065 \times 10^{-4}$ M, $[S] = 0.665 \times 10^{-4}$ M. $R^2 = 0.9858$. The best fit to a first-order rate equation gave $k_{obsd} = 1.65 \times 10^{-3}$ s^{-1}.

To make clear what happens to k_{obsd} when the first deviation period (retardation period) is left out, we truncated Figure 10 at t = 150 s and 300 s and replotted these experimental and fitted curves at a newly defined t = 0. These truncated curves are depicted in Figures 11,12. These truncated curves still don't fit well to the first-order equation.

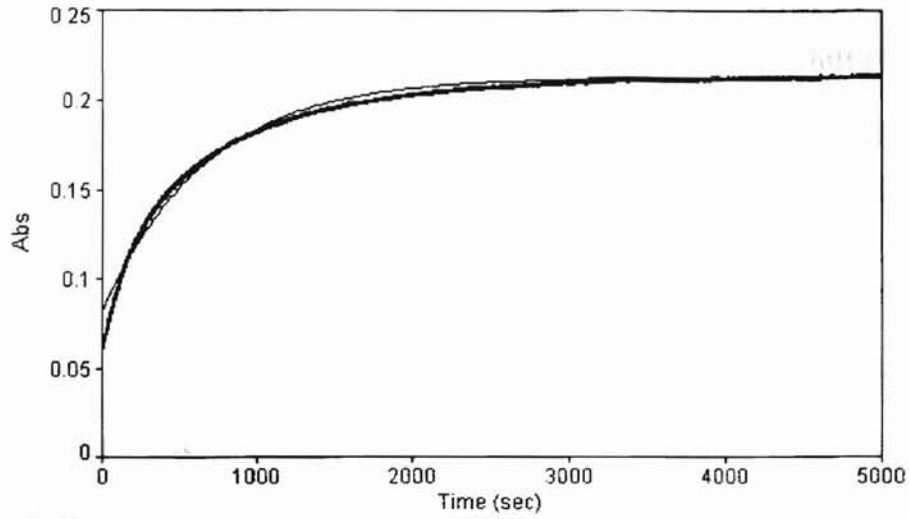

Figure 11. Truncated curve of Figure 10 at t = 150 s. $R^2 = 0.9905$. The best fit to a first-order rate equation gave $k_{obsd} = 1.49 \times 10^{-3}\ s^{-1}$.

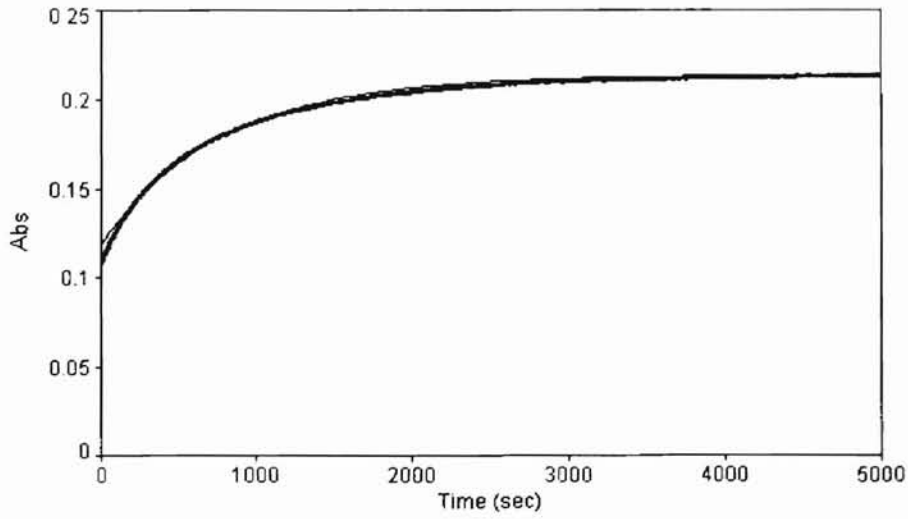

Figure 12. Truncated curve of Figure 10 at t = 300 s. $R^2 = 0.9958$. The best fit to a first-order rate equation gave $k_{obsd} = 1.29 \times 10^{-3}\ s^{-1}$.

Effects of Red Shift Change on Calculation of k_{obsd}

In the previous section it has been pointed out that there is a change of λ_{max} dependent on the types of latex systems, which is the so-called red shift phenomenon. The λ_{max} of the decarboxylation product was 398 nm in water, 424 nm in TMA quaternized latex and 430 nm in TBA quaternized latex. However these values were based on the measurements of the final kinetic plots of UV absorbance versus wavelength at much higher latex concentrations. When we did the kinetic experiments at lower latex concentrations, we found the phenomenon of red shift was also concentration dependent. These phenomena can be seen in Figure 13. The λ_{max} of the decarboxylation product in TBA quaternized microemulsion latex at $[N^+] = 0.065 \times 10^{-4}$ M was 398 nm. However, the λ_{max} values of the decarboxylation product at $[N^+] = 0.465 \times 10^{-4}$ M and $[N^+] = 1.330 \times 10^{-4}$ M were 416 nm and 428 nm respectively.

In the first case the latex concentration was so dilute that negligible amount of **2** could be bound to the N^+ sites of the latex, and the λ_{max} of the decarboxylation product in this solution had the same value as in water alone. When the latex concentration increased, the λ_{max} shifted to higher region and finally went up to 430 nm at $[N^+] > 3.325 \times 10^{-4}$ M.

In our kinetic study k_{obsd} was calculated from UV absorbance versus the reaction time. The wavelength of absorbance was the average between 400 nm and 430 nm. Because the λ_{max} shifted at various latex concentration, we were concerned about the possible change of k_{obsd} using absorbance at exact λ_{max} versus average wavelength. For comparison, we used TBA quaternized dispersion latex as an example and chose two latex concentrations $[N^+] = 0.065 \times 10^{-4}$ M and $[N^+] = 1.330 \times 10^{-4}$ M.

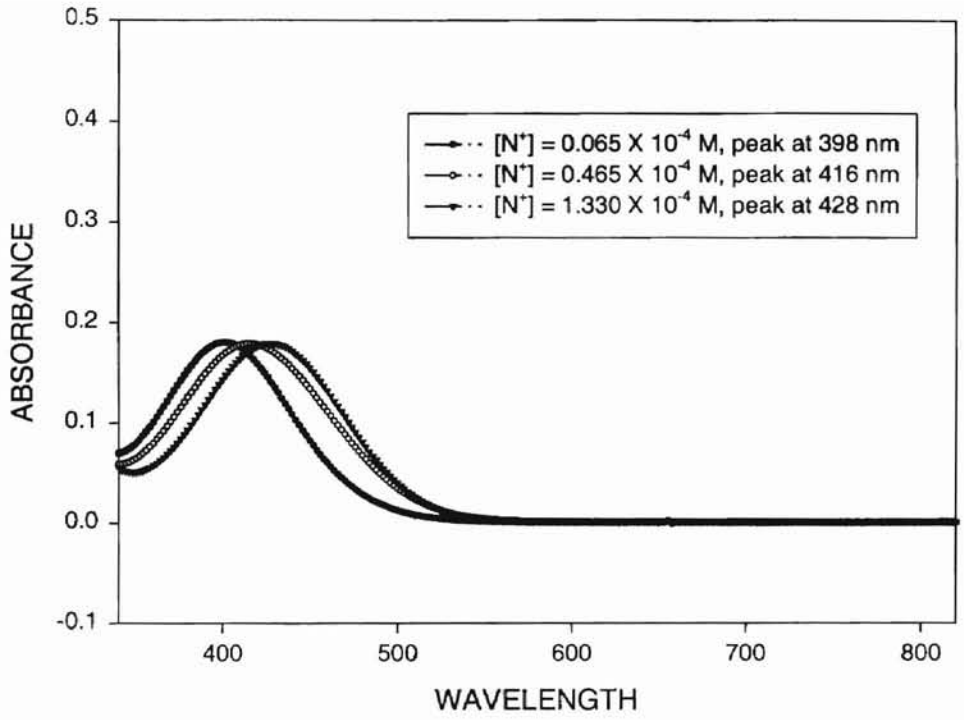

Figure 13. Red shift of λ_{max} dependent on the concentration of microemulsion TBA latex; [S] = 0.665×10^{-4} M

The substrate concentration was [S] = 0.665×10^{-4} M. Unlike the measurement at UV average wavelength, to get the profile of UV absorbance versus reaction time we measured the absorbance of the peak every one or two minutes once the experiment was started. These kinetic curves at exact λ_{max} and average wavelength between 400 nm and 430 nm are depicted in Figure 14 and 15.

Fitting these data into the first-order equation 2 gave us the values of k_{obsd}. For $[N^+] = 0.065 \times 10^{-4}$ M the value of k_{obsd} was 0.106 min^{-1} using λ_{max} = 398 nm and 0.109 min^{-1} using average wavelength. For $[N^+] = 1.330 \times 10^{-4}$ M the value of k_{obsd} was 0.436 min^{-1} using λ_{max} = 428 nm and 0.443 min^{-1} using average wavelength.

Finally we conclude that the values of k_{obsd} calculated by two different methods are very similar, so the results determined from the plots of UV absorbance at average wavelength versus the reaction time are acceptable.

Light Scattering Problem at Lower Concentrations of Dispersion Latex

To clearly observe the induction periods we also carried out two other kinetic experiments at latex concentration lower than substrate concentration and put the three kinetic curves in one graph which is shown in Figure 16. As seen in this picture the retardation period became shorter with increase of latex concentration. Once the latex concentration was higher than substrate concentration the retardation period disappeared, as shown in Figure 7.

We also find a strange phenomenon in Figure 16. These three kinetic curves at different low latex concentrations have different final absorbances despite starting with

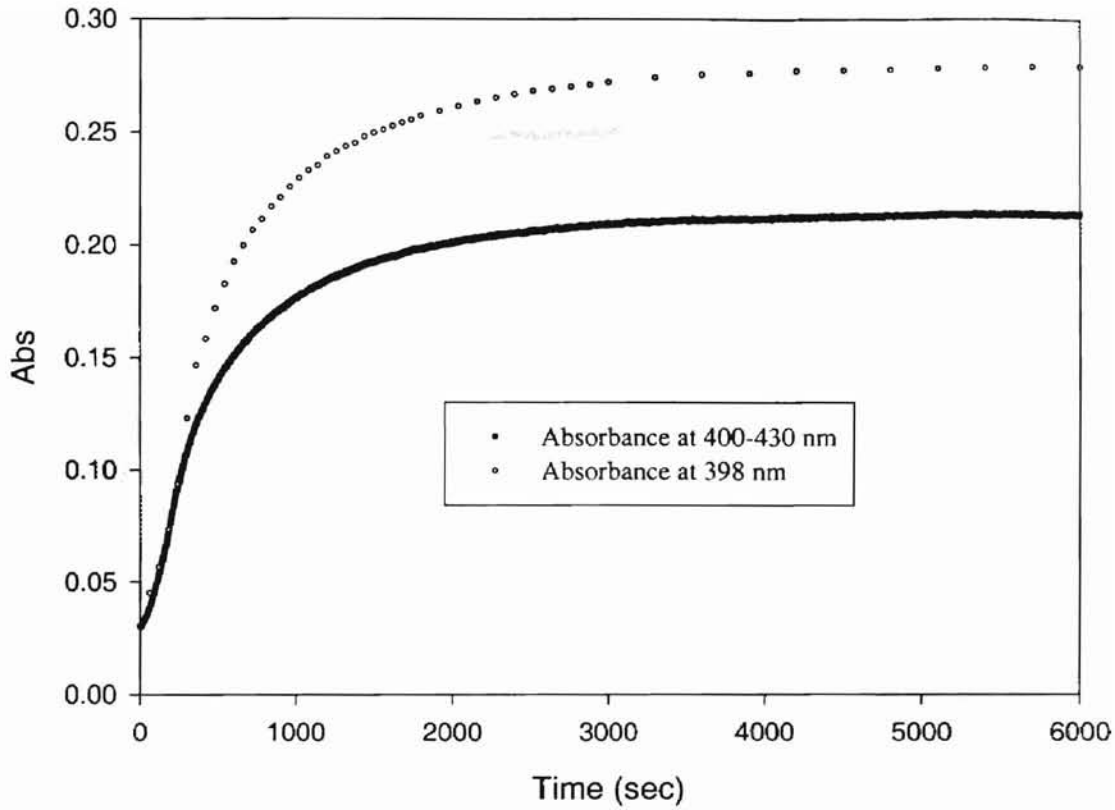

Figure 14. Formation of **2** measured by averaged absorbance at 400-430 nm and 398 nm using $[N^+] = 0.065 \times 10^{-4}$ M in dispersion TBA latex, $[S] = 0.665 \times 10^{-4}$ M. The fitted curve of the black line is shown in Figure 9.

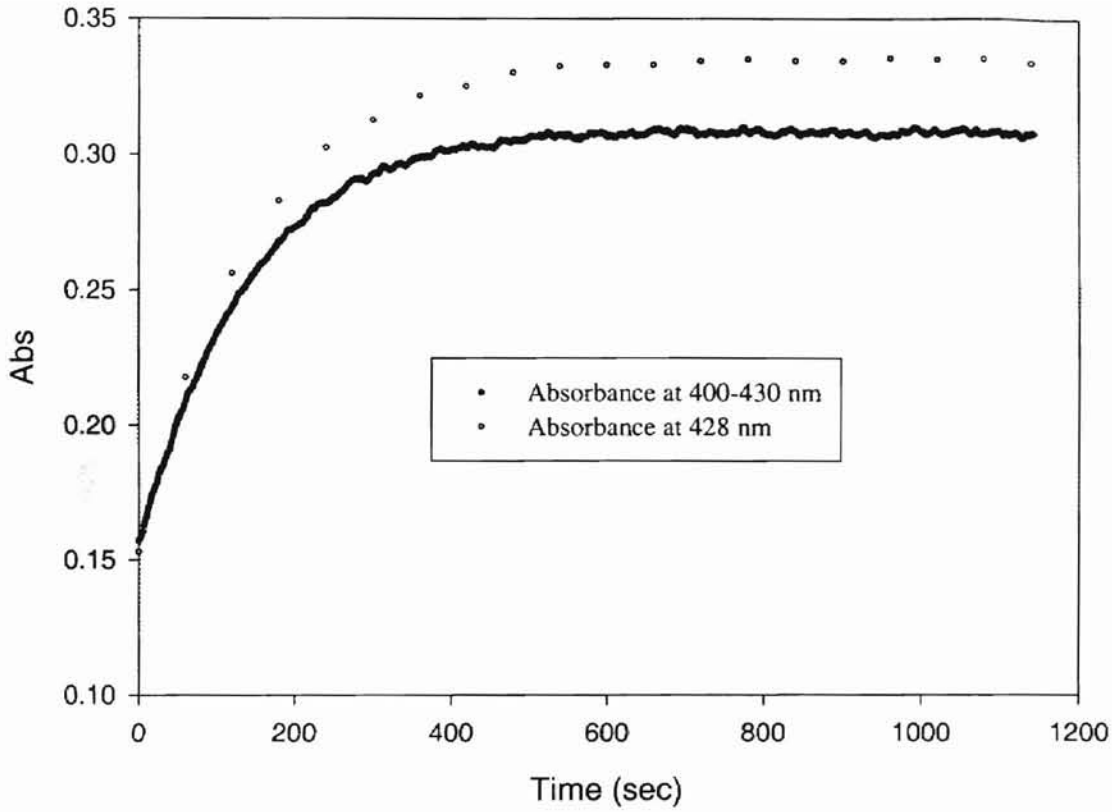

Figure 15. Formation of **2** measured by averaged absorbance at 400-430 nm and 398 nm using $[N^+] = 1.330 \times 10^{-4}$ M in dispersion TBA latex, $[S] = 0.665 \times 10^{-4}$ M. The fitted curve of the black line is shown in Figure 9 of Appendix.

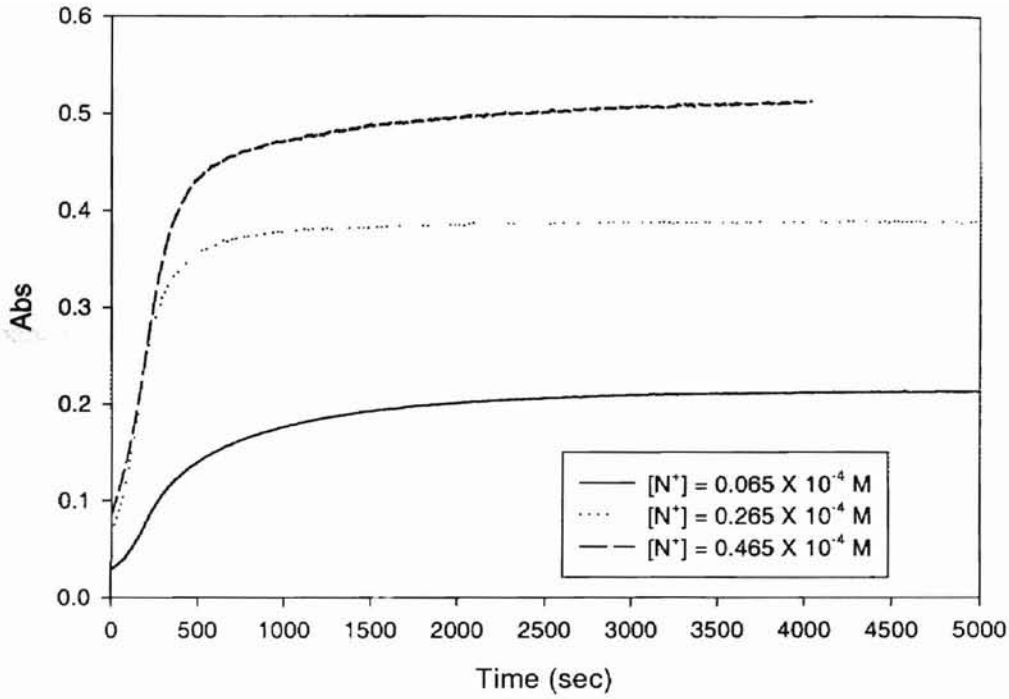

Figure 16. Plot of decarboxylation of **1** measured by absorbance of **2** at 400-430 nm at three lower concentrations of the dispersion TBA latex, [S] = 0.665 $\times 10^{-4}$ M

the same substrate concentration. Experimentally the final absorbance in dispersion TBA latex was 0.32 at much higher latex concentration where λ_{max} = 428 nm (Figure 14) and 0.22 at $[N^+] \approx 0$ where λ_{max} = 398 nm (Figure 13). The A_∞ value of the middle curve in Figure 16 went constant and landed within the usual region of final absorbance. The extremely low value of final absorbance of the lowest curve in Figure 16 can be explained by the fact that the scarcity of anion exchange sites at much lower latex concentration leaded to much slower reaction and hence the experimental time scale was not enough to reach the complete reaction.

When the latex concentration approached substrate concentration, the final absorbance of the top curve in Figure 16 was unusually high. To clarify this puzzle we checked the UV spectra after kinetic experiments were done. The results are shown in Figure 17. The final UV spectra at much lower latex concentration showed clear absorbance peaks in Figure 17(b) and (c). However the final UV spectrum of the top curve in Figure 16 showed strong absorbance in Figure 16(a), which extended to 800 nm and had no maximum at $\lambda > 360$ nm and a shoulder at $\lambda \approx 480$ nm.

However, Figure 17(b) still showed absorbance extending to 800 nm. In order to see how the shoulder develops with the changes of the latex concentration and product concentration, we used different amounts of product ions according to different latex concentrations to trace this phenomenon. To make product ion solution we first heated **1** in ethanol at 45 °C for 2 days. Then we mixed product ion **2** solution instead of substrate solution with latex and checked their UV spectra. The results at $[N^+] = 0.465 \times 10^{-4}$ M and $[N^+] = 1.330 \times 10^{-4}$ are shown in Figure 18 and 19.

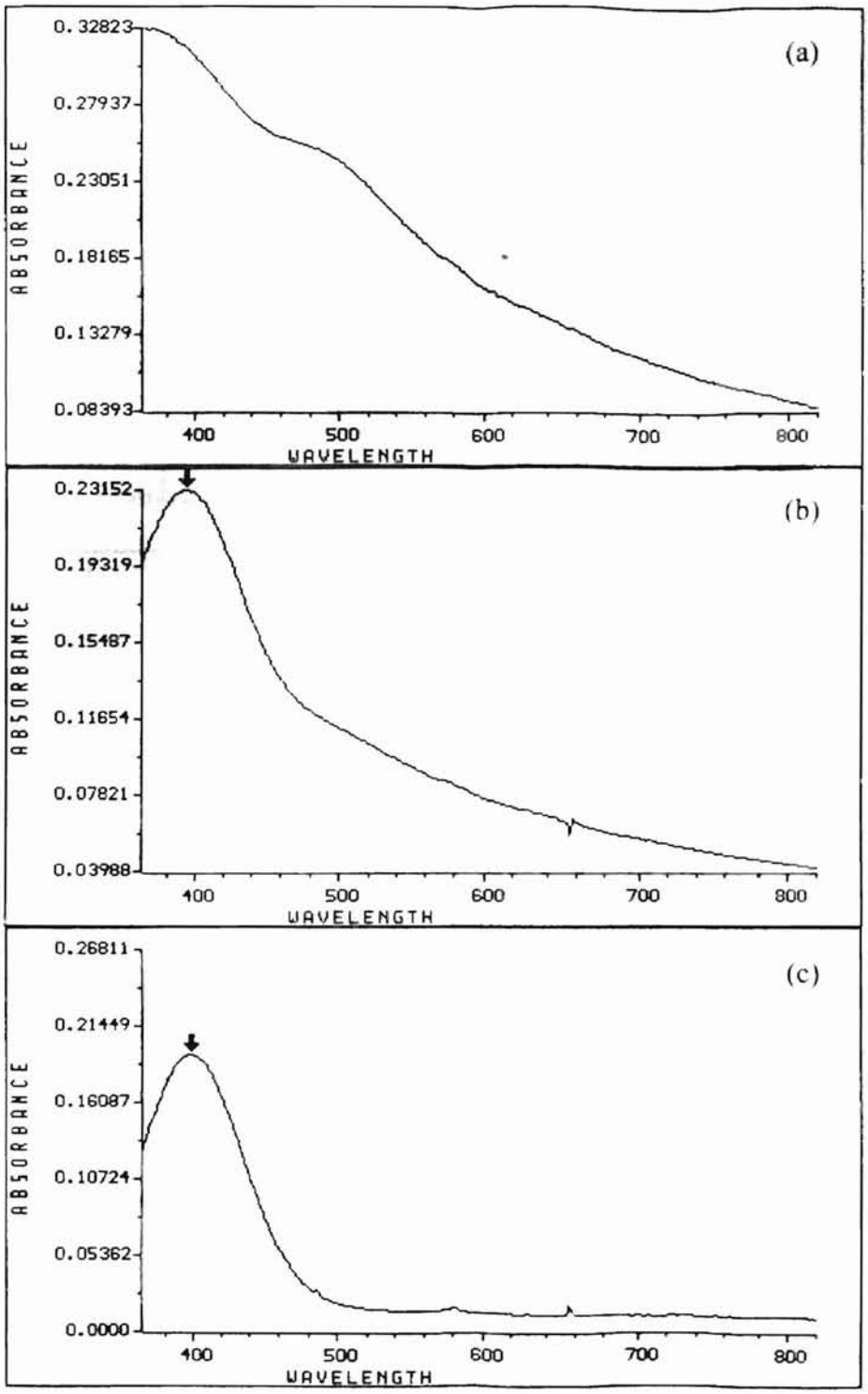

Figure 17. Final UV spectra of **2** at three low concentrations of the dispersion TBA latex: (a) $[N^+] = 0.465 \times 10^{-4}$ M, (b) $[N^+] = 0.265 \times 10^{-4}$ M, (c) $[N^+] = 0.065 \times 10^{-4}$ M. $[S] = 0.665 \times 10^{-4}$ M. The spectra correspond with the three samples in Figure 16.

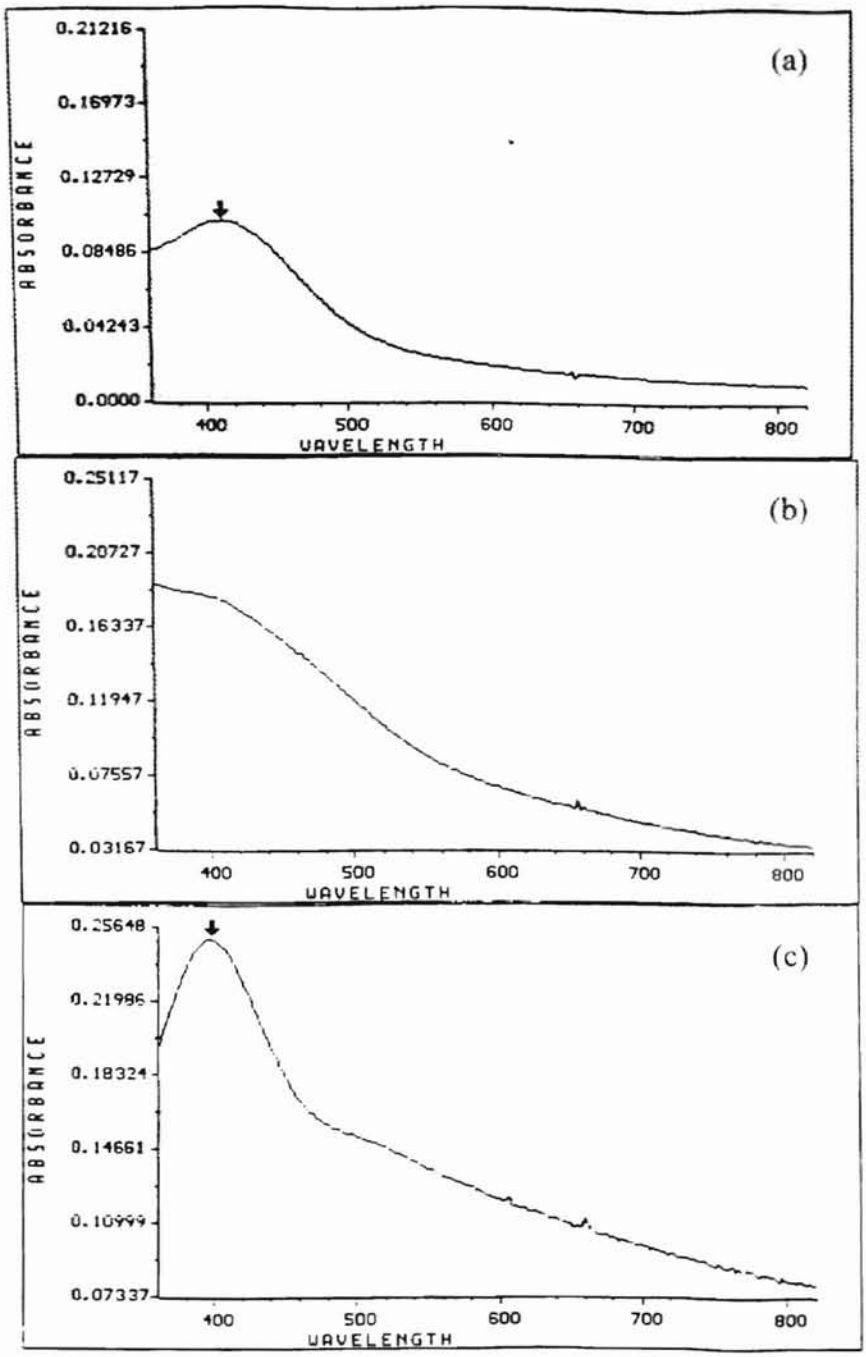

Figure 18. UV spectra of **2** at dispersion TBA latex $[N^+] = 0.465 \times 10^{-4}$ M: (a) **[2]** = 0.18×10^{-4} M in reaction mixture, (b) **[2]** = 0.36×10^{-4} M in reaction mixture, (c) **[2]** = 0.70×10^{-4} M in reaction mixture.

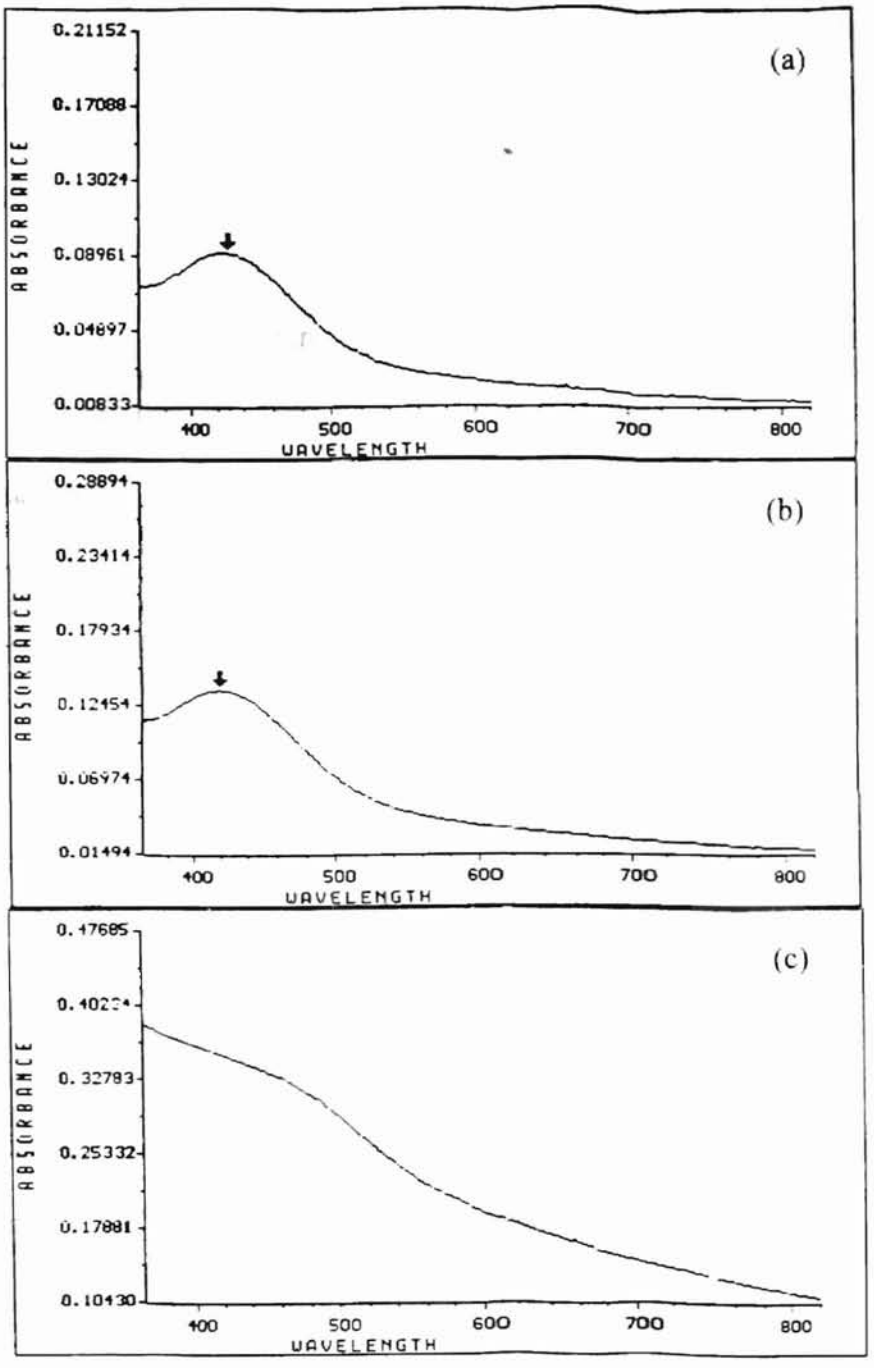

Figure 19. UV spectra of **2** at dispersion TBA latex $[N^+] = 1.330 \times 10^{-4}$ M: (a) [**2**] = 0.18 $\times 10^{-4}$ M in reaction mixture, (b) [**2**] = 0.36 $\times 10^{-4}$ M in reaction mixture, (c) [**2**] = 0.70 $\times 10^{-4}$ M in reaction mixture.

In Figure 18(b) and Figure 19(c) we can find the same big shoulders as that in Figure 17(a). These three spectra also showed strong absorbances extending to 800 nm. Since we can reproduce these big shoulders at different latex concentrations and product ion concentrations, they are not due to impurities or new compounds formed from the latexes during the kinetic process. Otherwise these impurities and byproducts would affect the UV spectra in all cases, and we would not have the clear peaks shown in Figure 18(a) and Figure 19(a). The noise in UV spectra is due to the very small amount of light reaching the detector. Particle aggregation can increase light scattering. The excess absorbance can occur at all $[N^+] > 0.265 \times 10^{-4}$ M if only we can choose suitable amounts of product ion in reaction mixture, such as $[N^+]/[2] \approx 1.9$ in Figure 19(c). So we conclude that increased light scattering is due to particle aggregation caused by product ions at concentration somewhat lower than the latex N^+ concentration.

Intraparticle First-order Rate Constants and Equilibrium Constants

In order to investigate the effect of polymer particle size on rates of reactions, we have used cationic polystyrene particles having average diameter of 20 nm, 135 nm and 1.05 μm to catalyze decarboxylation of 6-nitrobenzisoxazole-3-carboxylate. To further determine what factors are responsible for the different first-order rate constants using different particle sizes, we performed a more in-depth kinetic analysis. Only the latex concentrations higher than substrate concentrations were used because we wanted to compare the kinetic data of these three particle systems and to avoid the problems involved in the lower dispersion latex concentrations such as the retardation period and light scattering.

Analysis of the first-order rate constants versus different latex concentrations was based on the pseudophase model proposed by Menger and Portnoy,[19] which is shown in Scheme 3.

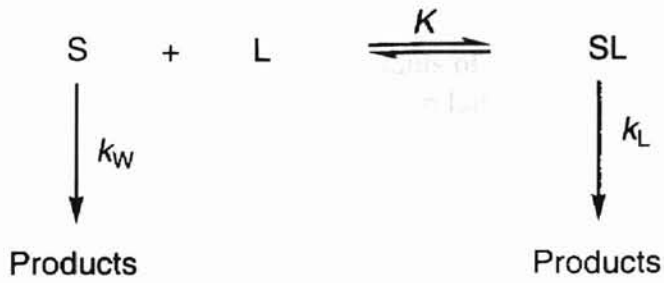

Scheme 3. Menger-Portnoy model for pseudophase catalysis in molecular aggregates

This scheme shows the products can be produced in water phase and in particle phase. The fundamental equation of this model is a rate equation (3):

$$k_{obsd} = k_w[S]_w/[S]_t + k_L[S]_L/[S]_t \quad (3)$$

where k_{obsd} is the overall first-order rate constant, k_w is the first-order rate constant in water alone, and k_L is the intraparticle first-order rate constant in the latex phase. All concentrations are based on total volume of dispersion. $[S]_t$ is the analytical concentration of substrate in the dispersion. $[S]_w$ and $[S]_L$ are the concentrations of substrate free in the aqueous phase and bound in the particles.

By combining the first-order equations in both aqueous phase and latex phase we can derive a nonlinear equation (4),[20]

$$k_{obsd} = (k_w/K + k_L[N^+]) / (1/K + [N^+]) \quad (4)$$

where K is the binding constant of substrate to ion exchange sites in the latex, shown in Scheme 3.

The first-order rate constants obtained at high concentrations of microemulsion, emulsion and dispersion latex are presented in Tables 5-7. The corresponding nonlinear plots fitted by equation (4) are depicted in Figures 20-22.

Table 5. First-order Rate Constants of Decarboxylation in Microemulsion Latex[a]

latex (mg/mL)	$10^4[N^+]$ (M)	$10^3 k_{obsd}$ (s^{-1})
0.1074	1.995	9.438
0.1789	3.325	12.02
0.2864	5.325	13.75
0.3938	7.325	15.22
0.5017	9.325	16.15

[a] In 2 mM NaOH, pH = 11.2 ± 0.1, at 25.0 ± 0.1 °C, [S] = 0.665×10^{-4} M.

Table 6. First-order Rate Constants of Decarboxylation in Emulsion Latex[a]

latex (mg/mL)	$10^4[N^+]$ (M)	$10^3 k_{obsd}$ (s^{-1})
0.0734	1.330	12.06
0.1100	1.995	15.03
0.1467	2.660	17.23
0.1834	3.325	19.17

[a] In 2 mM NaOH, pH = 11.2 ± 0.1, at 25.0 ± 0.1 °C, [S] = 0.665×10^{-4} M

Table 7. First-order Rate Constants of Decarboxylation in Dispersion Latex[a]

latex (mg/mL)	$10^4[N^+]$ (M)	$10^3 k_{obsd}$ (s^{-1})
0.0443	0.997	6.103
0.0639	1.330	7.392
0.0958	1.995	8.973
0.1596	3.325	11.21
0.2556	5.325	12.74

[a] In 2 mM NaOH, pH = 11.2 ± 0.1, at 25.0 ± 0.1 °C, [S] = 0.665×10^{-4} M

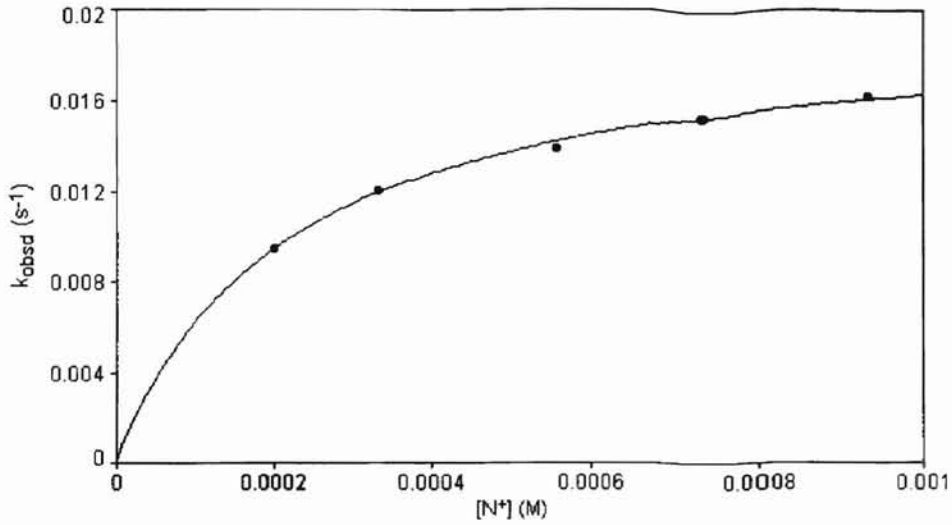

Figure 20. Dependence of rate constant on concentration of mTBAQ37 latex. R^2 = 0.9966

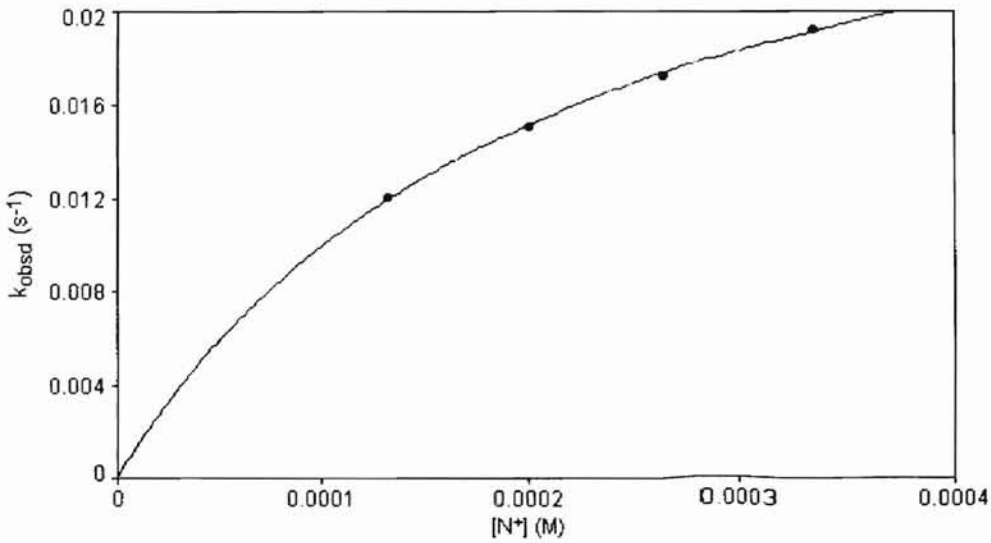

Figure 21. Dependence of rate constant on concentration of eTBAQ36 latex. R^2 = 0.9987

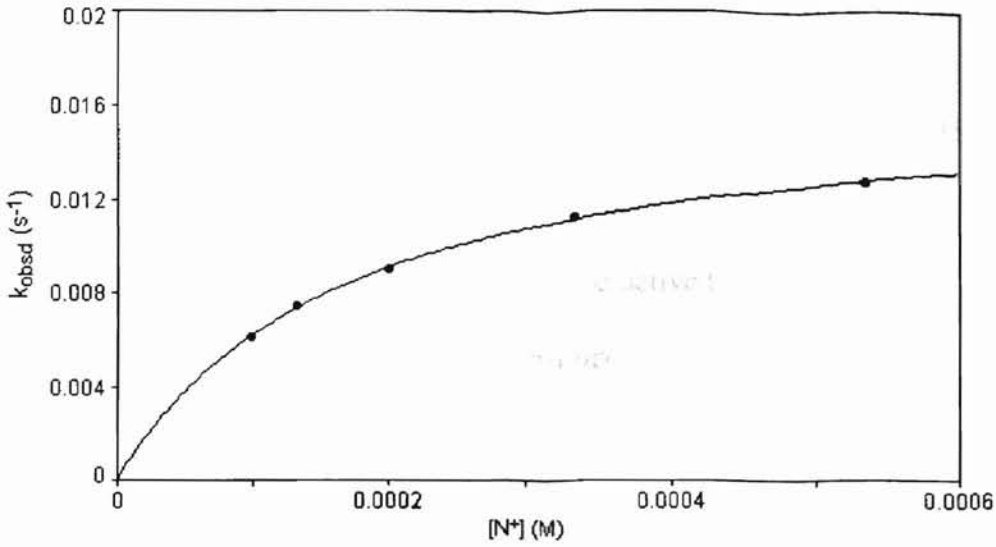

Figure 22. Dependence of rate constant on concentration of dTBAQ55 latex. R^2 = 0.9993.

From the nonlinear curve shapes we can see that the first-order rate constant (k_{obsd}) increases with the increase of latex concentration. In principle k_{obsd} should become constant when the substrate is fully bound at still higher latex concentrations. Nonlinear regression analysis of the kinetic data in Tables 5-7 using equation (4) gives the values of parameters shown in Table 8, which are the intraparticle first-order rate constant (k_L) and the equilibrium distribution constant (K) for decarboxylation of 6-nitrobenzisoxazole-3-carboxylate in microemulsion, emulsion, and dispersion latex.

Table 8. Intraparticle Rate Constants and Binding Constants for Decarboxylation of **1** in Different Particle Size Latexes[a]

latex sample	$10^3 k_L$ (s^{-1})	K (M^{-1})
mTBAQ37	19.8	4500
eTBAQ36	31.5	4600
dTBAQ55	17.0	5700
TBAQ24×1[b]	65	1200

[a] $k_w = 2.53 \times 10^{-6}$ s^{-1}. [b] Reference 4.

DISCUSSION

Latex particles used for kinetic studies were 20 nm, 135 nm and 1.05 μm in diameter respectively. The data in Table 4 show that no matter what the particle sizes are, the tributylamine quaternized latexes are more active than their trimethylamine quaternized analogues. Tributylammonium ion provides organic substrates more lipophilic environment inside the latex particle and can extract more substrate molecules into the latex phase. The data in Table 1 have the same results as above although they were the work in our lab five years ago. Because the work in this paper is totally independent from the previous work, we did not produce exactly same latex as before. For instance, the emulsion latex sample TBAQ24 in Table 1 contains 24 mol % of N^+ sites in repeat units of latex particles. However, in Table 4 the emulsion latex sample eTBAQ36 contains 36 mol % of N^+ sites in particles. This difference is simply due to the different quaternization yield. The values of k_{obsd}/k_w, which are 9000 in Table 4 for eTBAQ36 and 10000 in Table 1 for TBAQ24, agree well. Since usually $k_w/K \ll k_L[N^+]$, equation 4 suggests an inverse relationship between k_L and K. This can be verified by comparison of data in Table 8. As we pointed out before, basically the emulsion latex samples of eTBAQ36 and TBAQ24 have the almost same observed rates. So in Table 8 the sample eTBAQ36 has smaller k_L than TBAQ24 but larger K than TBAQ24.

In Table 4 with both TMA and TBA quaternized groups, the decarboxylation rates are smallest in dispersion latexes, which give us the hint that there is a factor which strongly affects the reaction rate in the latex having particles > 1 μm.

At latex concentrations both higher and lower than the substrate concentration the good fits to first-order kinetics shown in Figures 5, 6, 8, and 9 imply the same mechanism of decarboxylation in the microemulsion latex as in the emulsion latex. The particles of these two kinds of latexes are small enough and can provide higher surface area and shorter diffusional path of organic anion into ion-exchange sites. So the reaction doesn't suffer diffusional limitation in either latex system. The substrate ions can freely enter latex phase and accumulate to enough amount so that the reaction in the latex phase always follows first-order kinetics.

On the other hand, the difference of catalytic activity between higher and lower concentration of dispersion latex shows different mechanisms of reaction. When the dispersion latex concentration is much greater than the substrate concentration, anion exchange sites on the particle surface bind the substrate molecules quickly, and the decarboxylation proceeds by normal first-order kinetics. However, when the dispersion latex concentration is much less than the substrate concentration, diffusion of reactants through water can be the slow mass transport process. After initial shaking the reaction mixture is still quiet and mass transfer in water phase is a diffusional process. So few substrate ions can be bound to N^+ sites on the particle surface at the beginning of the reaction. This mass transfer process is gradual and the reaction doesn't proceed by "burst kinetics": Substrate initially bound to particles reacts fast, and substrate initially outside of the particles reacts extremely slowly.[21,22]

Tomoi et al. proved that slow mass transfer of reactants from the liquid phase to the particle phase limited the rates of polymer-supported phase transfer catalyzed reactions using polymer beads with 20-200 μm in diameter if the reaction half-life is

reasonably short, such as < 1 $h.^{-1}$. The method and speed of mixing affect observed rates. With no agitation the mass transfer of reactants to the catalyst surface would occur by diffusion through the liquid. In this case both mass transfer and intraparticle diffusion affect reaction rates. The basic principle behind use of submicroscopic polymer latexes rather than macroscopic polymer beads as catalysts is that the mass transfer and intraparticle diffusional limitation to rates of reactions that occur on time scale of seconds to minutes with large beads are completely overcome in well mixed colloidal dispersions. According to theoretical calculation at $[N^+] = 0.065 \times 10^{-4}$ M for dispersion latex, the average distance between particles is about 100 μm and the average diffusion time in this distance is about 10 s. However the calculated intraparticle diffusion time is only the order of 10^{-4} s. These results suggest that the intraparticle diffusion can not limit reaction rates and the mass transfer is the major factor for slow reaction rates in dispersion latex particles.

The kinetic curve shown in Figure 10 clearly identifies the mechanism of this slow mass transfer process. Compared with the best fit first-order kinetic curve there are retardation periods over the first 10-15 % conversion and around 90 % conversion. We attribute the early retardation period to slow mass transport of reactant anions from the aqueous phase to the particle surfaces and the late retardation period to a high occupancy of the product anion **2** to the N^+ sites.

In Table 8 the highest value of k_L in emulsion latex accounts for the highest value of k_{obsd} of sample eTBAQ36 in Table 4, because basically there is not much difference between the values of K in microemulsion, emulsion and dispersion latex. On the other hand, since intraparticle diffusional limitation won't affect either emulsion latex particle

or microemulsion latex particle, the lower value of k_L in microemulsion latex than in emulsion latex is only caused by the more hydrated binding sites. Due to the extremely high surface area of microemulsion latex particles there are more N^+ sites on the particle surface.

Thus, these values in Table 8 strongly verify our previous assumption that when the cationic colloidal polymer particles < 1 μm in diameter are used as catalyst support, their high surface areas and the short diffusion paths to the particle interiors result in little or no diffusional limitation to reaction rates.

CONCLUSION

This research project demonstrated the effects of cationic polymer colloidal particle size on the reactivity of organic anions by using decarboxylation of 6-nitrobenzisoxazole-3-carboxylate as model reaction and cationic polystyrene particles having average diameter of 20 nm, 135 nm, and 1 μm as catalytic media. The good fits to first-order kinetics at all $[N^+]$ for both emulsion latex and microemulsion latex shows no diffusional limitation in either of these two latex systems. The larger value of intraparticle rate constant (k_L) of the decarboxylation in emulsion latex suggests that emulsion latex particles have the less hydrated binding sites. Moreover, we find that there is a retardation period in kinetic plot of UV absorbance versus reaction time at latex concentration lower than substrate concentration in dispersion latex, which clearly shows the mass diffusional limitations to reactions in polymer particles > 1 μm.

RESEARCH PROSPECT

To further understand the catalytic reactivity of different particle size with different mass diffusion process between water and particle we also intended to test the catalytic reactivity using chloromethylated biobeads which had an average diameter of 70 μm. However this kind of experiment was not successful. Because such large particles settled down quickly we could not track the kinetics directly in a UV spectrometer.

Since catalytic activity of different size particles depends on mass transfer process and on substrate concentration in water and particle phases, the solubility of substrate would affect the distribution of substrate throughout the reaction system and hence affect the mass transport. So the comparison experiments between a highly soluble substrate and a lowly soluble substrate in the water phase would tell us how the substrate distribution in particle phase and in water phase affect the kinetics. More research is needed to cover the binding abilities of substrate ions and product ions to active sites, which can be studied in terms of partition coefficient. The promising substrate of high solubility could be paraoxon, an insecticide. The promising substrate of low solubility could be *p*-nitrophenyl acetate.

REFERENCES

1. Ford, W. T.; Tomoi, M. *Adv. Polym. Sci.* **1984**, 55, 49.
2. Helfferich, F.; *Ion Exchange*; McGraw-Hill: New York, 1962, p261-262.
3. Ford, W. T. *React. Funct. Polym.* **1997**, 33, 147.
4. Lee, J.- J.; Ford, W. T. *J. Org. Chem.* **1993**, 58, 4070.
5. Lee, J.- J.; Ford, W. T. *J. Am. Chem. Soc.* **1994**, 116, 3753.
6. Moss, R. A.; Alwis, K. W.; Bizzigotti, G. O. *J. Am. Chem. Soc.* **1983**, 105, 681.
7. Bunton, C. A.; Minch, M. J. *Tetrahedron Lett.* **1970**, 3881.
8. Ford, W. T.; Yu, H.; Lee, J.- J.; El-Hamshary, H. *Langmuir* **1993**, 9, 1698.
9. Ford, W. T.; Yu, H. *Langmuir* **1993**, 9, 1999.
10. Antonietti, M.; Lohmann, S. *Macromol. Rapid Commun.* **1995**, 16, 283.
11. Kemp, D. S.; Paul, K. G. *J. Am. Chem. Soc.* **1970**, 92, 2553.
12. Kemp, D. S.; Paul, K. G. *J. Am. Chem. Soc.* **1975**, 97, 7305.
13. Borche, W. *Chem. Ber.* **1909**, 42, 1316.
14. Lindemann, H.; Cissee, H. *Liebigs Ann. Chem.* **1929**, 469, 44.
15. Tseng, C. M.; Lu, Y. Y.; El-Aasser, M. S.; Vanderhoff, J. W. *J. Polym. Sci., Polym. Chem. Ed.* **1986**, 24, 2995.
16. Suh, J.; Scarpa, I. S.; Klotz, I. M. *J. Am. Chem. Soc.* **1976**, 98, 7060.
17. Shah, S. C.; Smid, J. *J. Am. Chem. Soc.* **1978**, 100, 1426.
18. Bunnett, J. F. In *Techniques of Chemistry VI;* Bernasconi, C. F., Ed.; Wiley-Interscience: New York, 1986; p176-183.
19. Menger, F. M.; Portnoy, C.E. *J. Am. Chem. Soc.* **1967**, 89, 4698.

20. Tee, O. S.; Federtchenko, A. A. *Can. J. Chem.* **1997**, 75, 1434.

21. Fersht, A. *Enzyme Structure and Mechanism*, W. H. Freeman: New York, 1985, chapter 4.

22. Moss, R. A.; Chung, Y.- C. *Langmuir* **1990**, 6, 1614.

Appendix

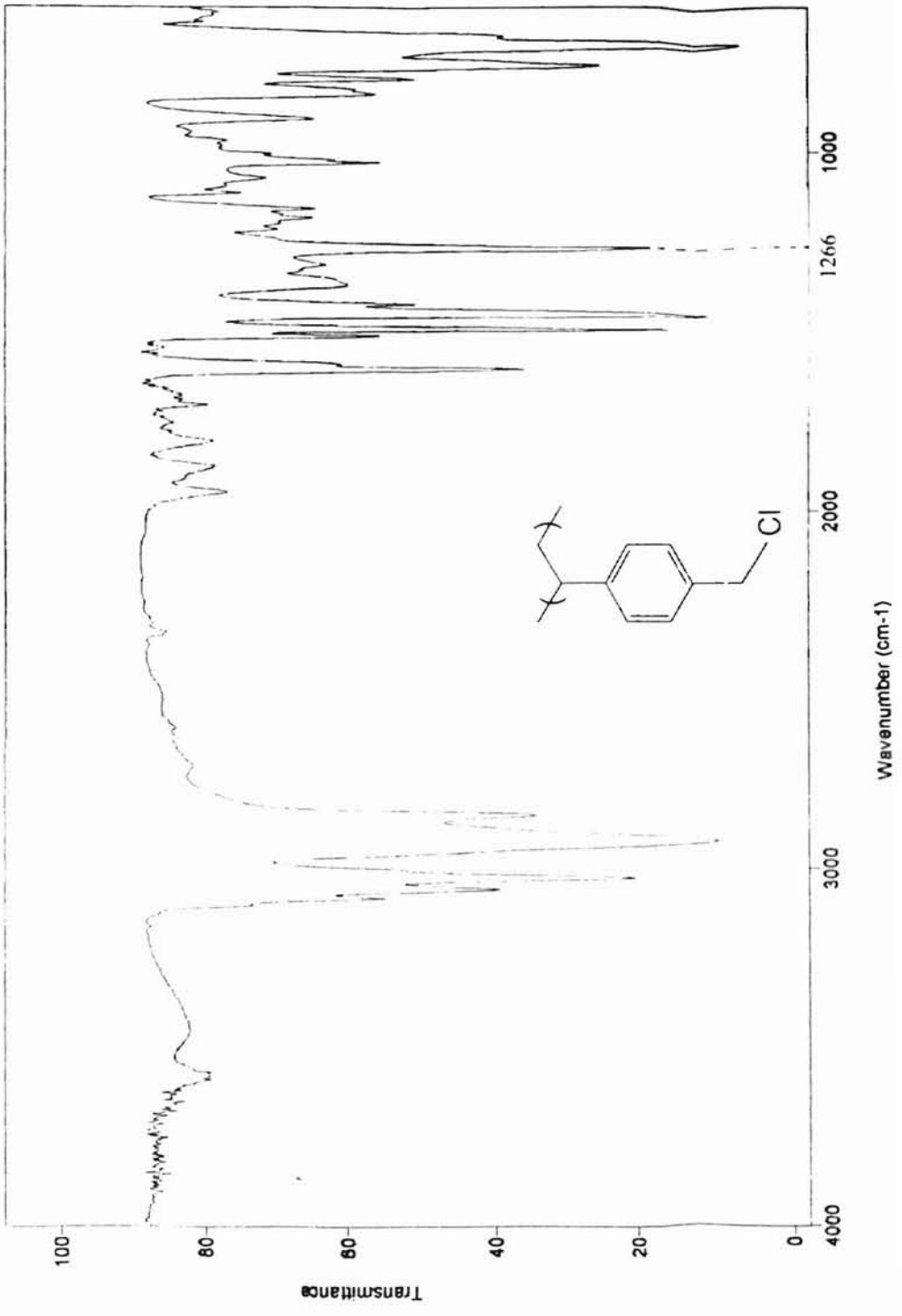

Figure 1. FTIR Spectrum of Microemulsion Latex

Figure 2. FTIR Spectrum of Microemulsion TBA Latex

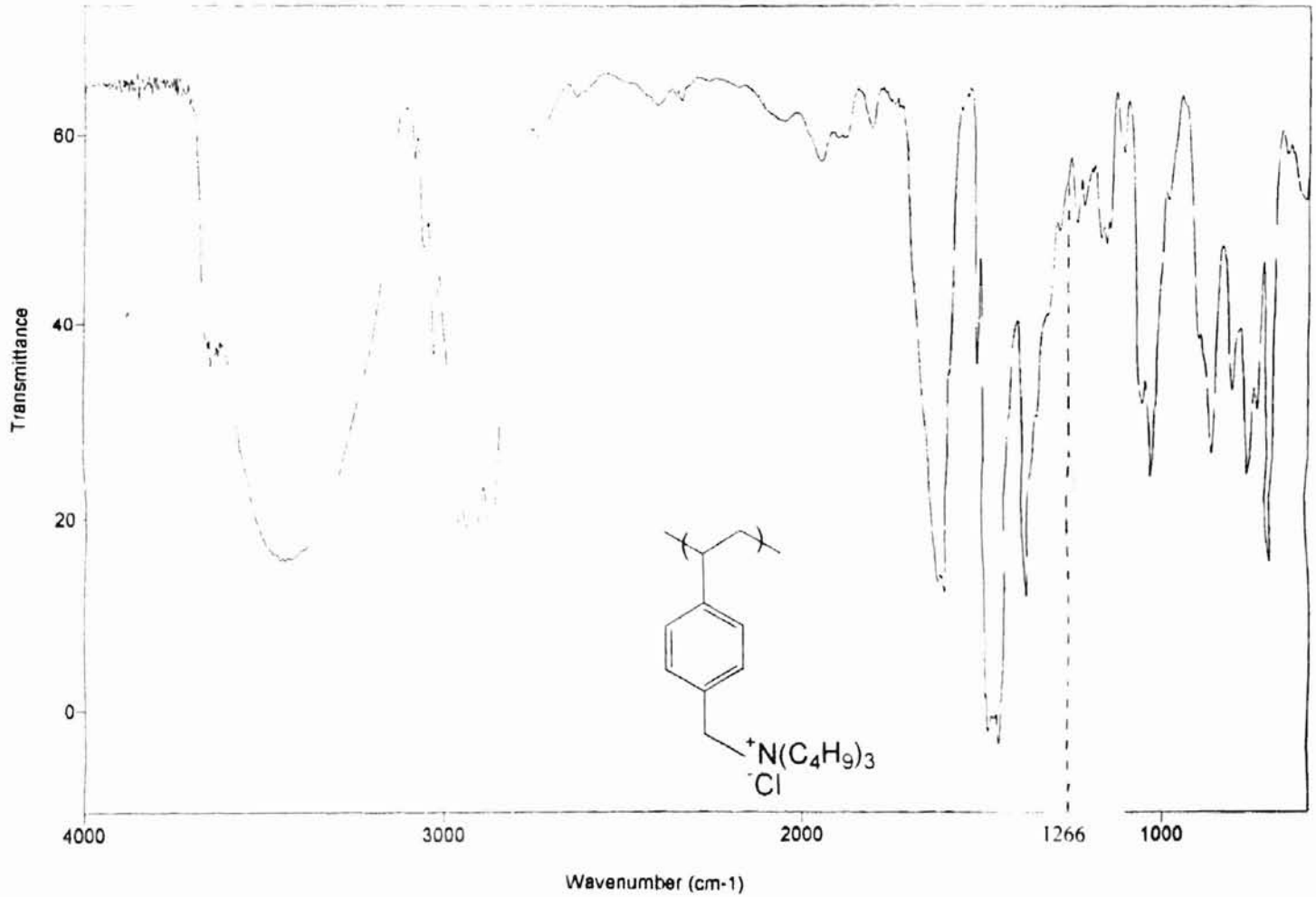

Figure 3. FTIR Spectrum of Microemulsion TMA Latex

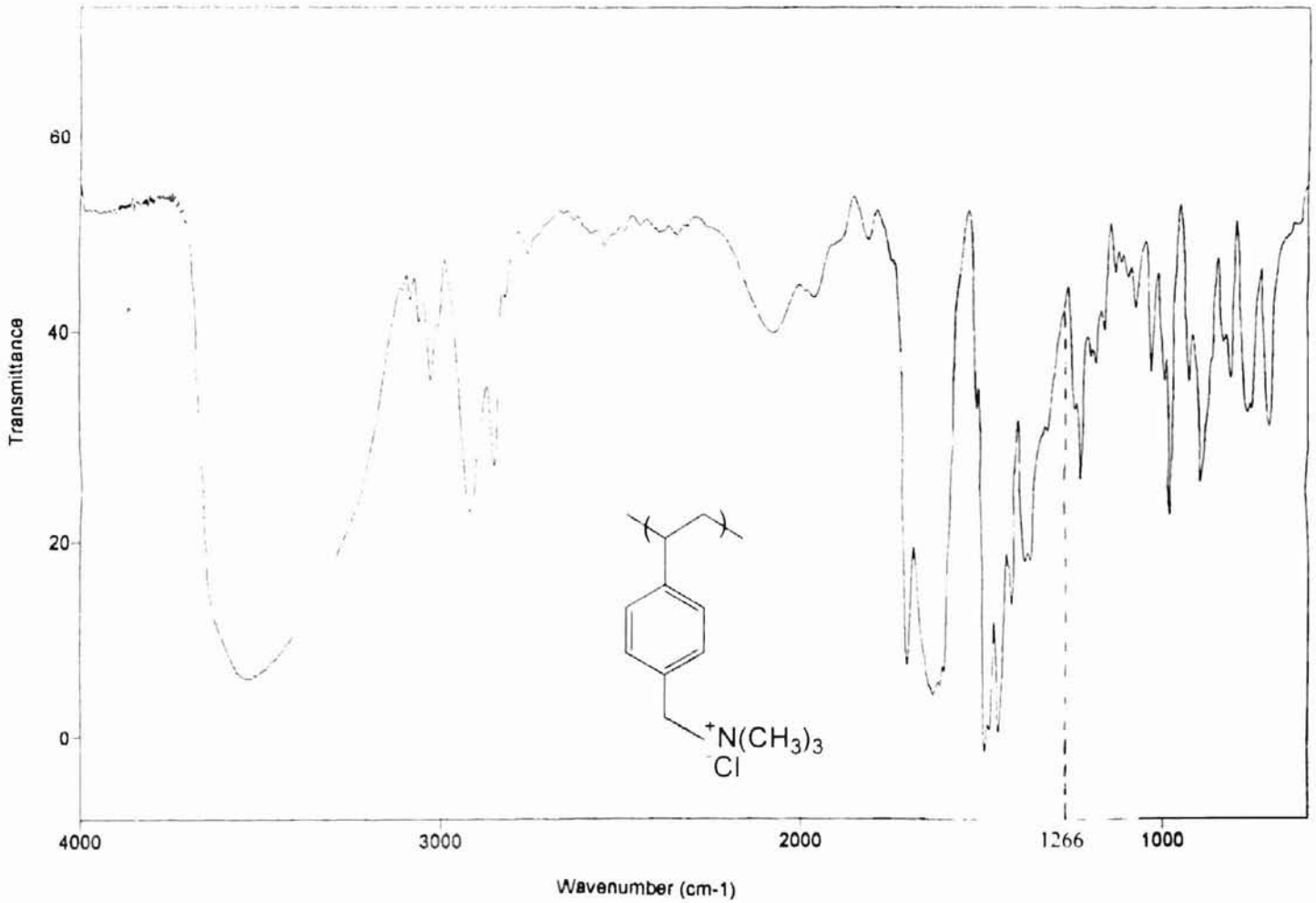

Figure 4. ^{1}H NMR Spectrum of Dispersion TBA Latex

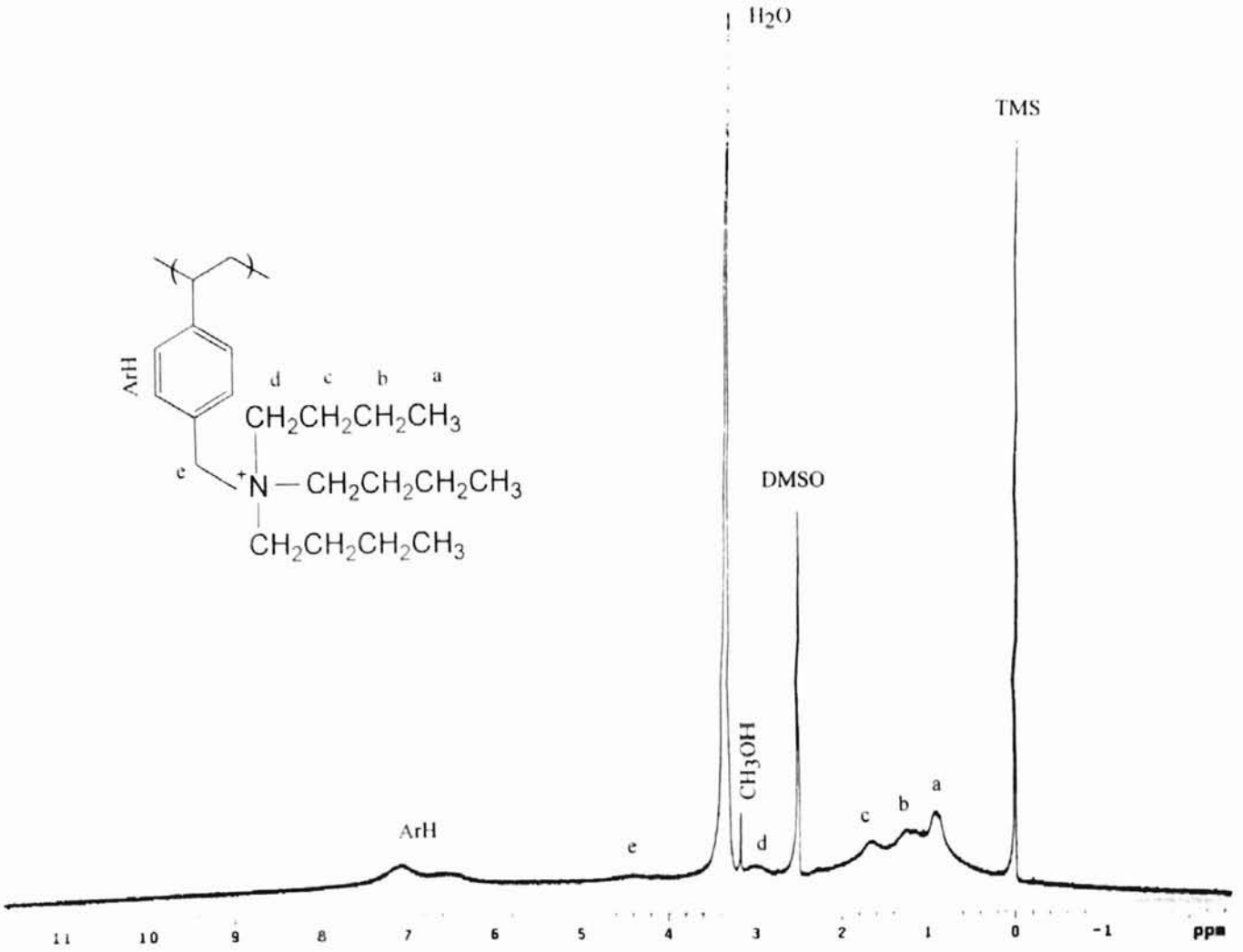

Figure 5. ^{1}H NMR Spectrum of Dispersion TMA Latex

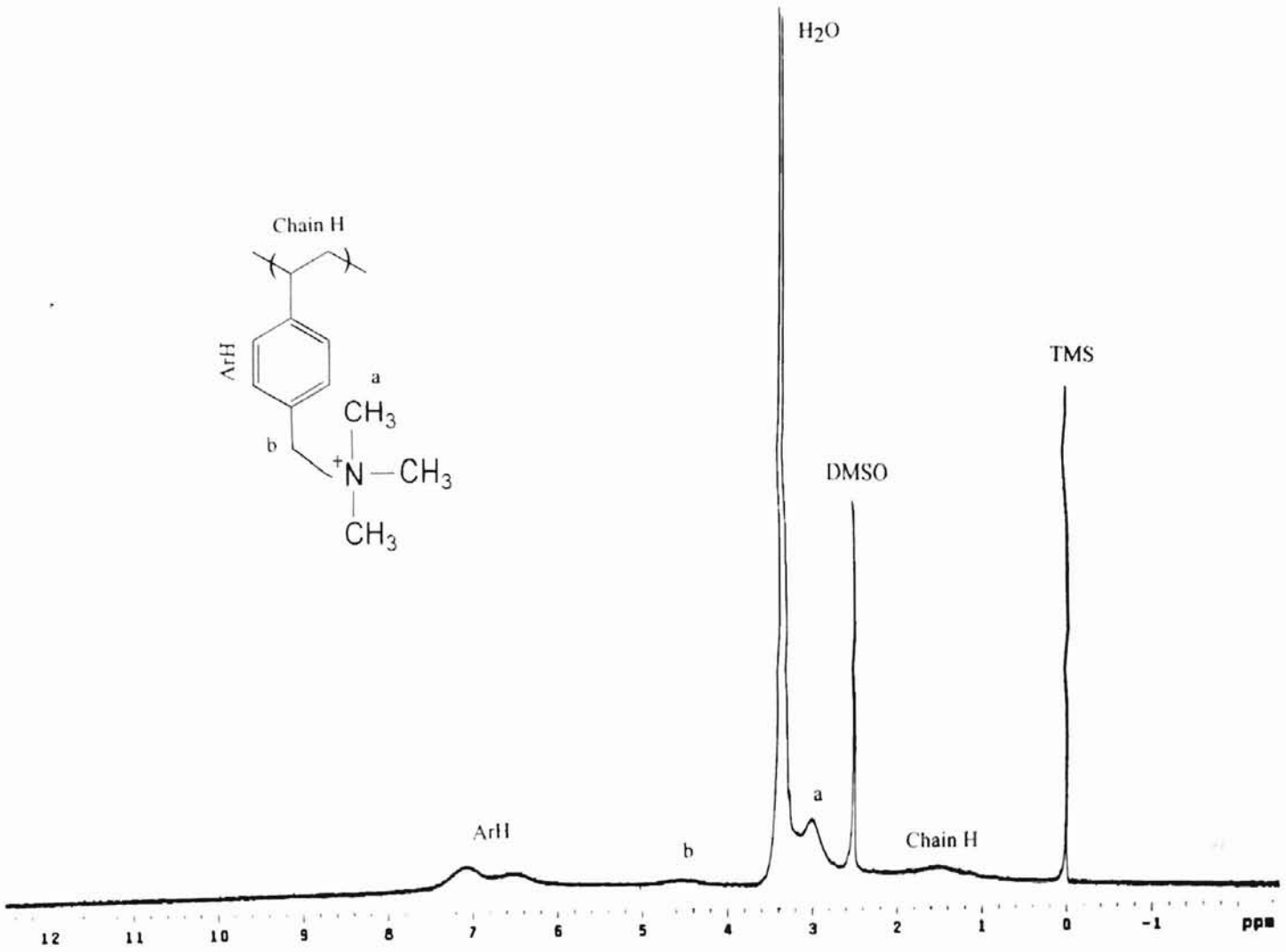

Figure 6. ^{1}H NMR Spectrum of Methyl 6-nitrobenzisoxazole-3-carboxylate

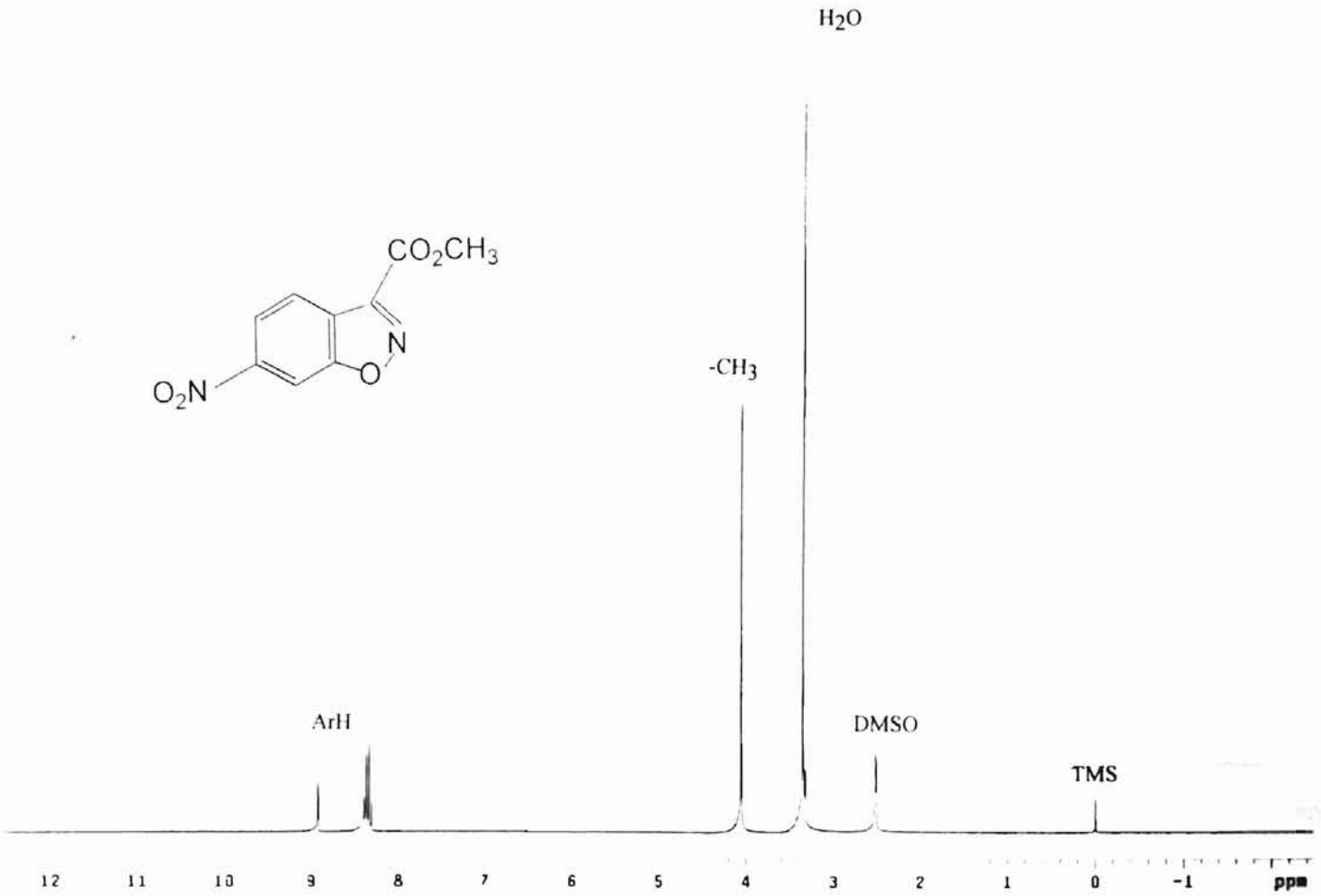

Figure 7. ^{1}H NMR Spectrum of 6-Nitrobenzisoxazole-3-carboxylic Acid

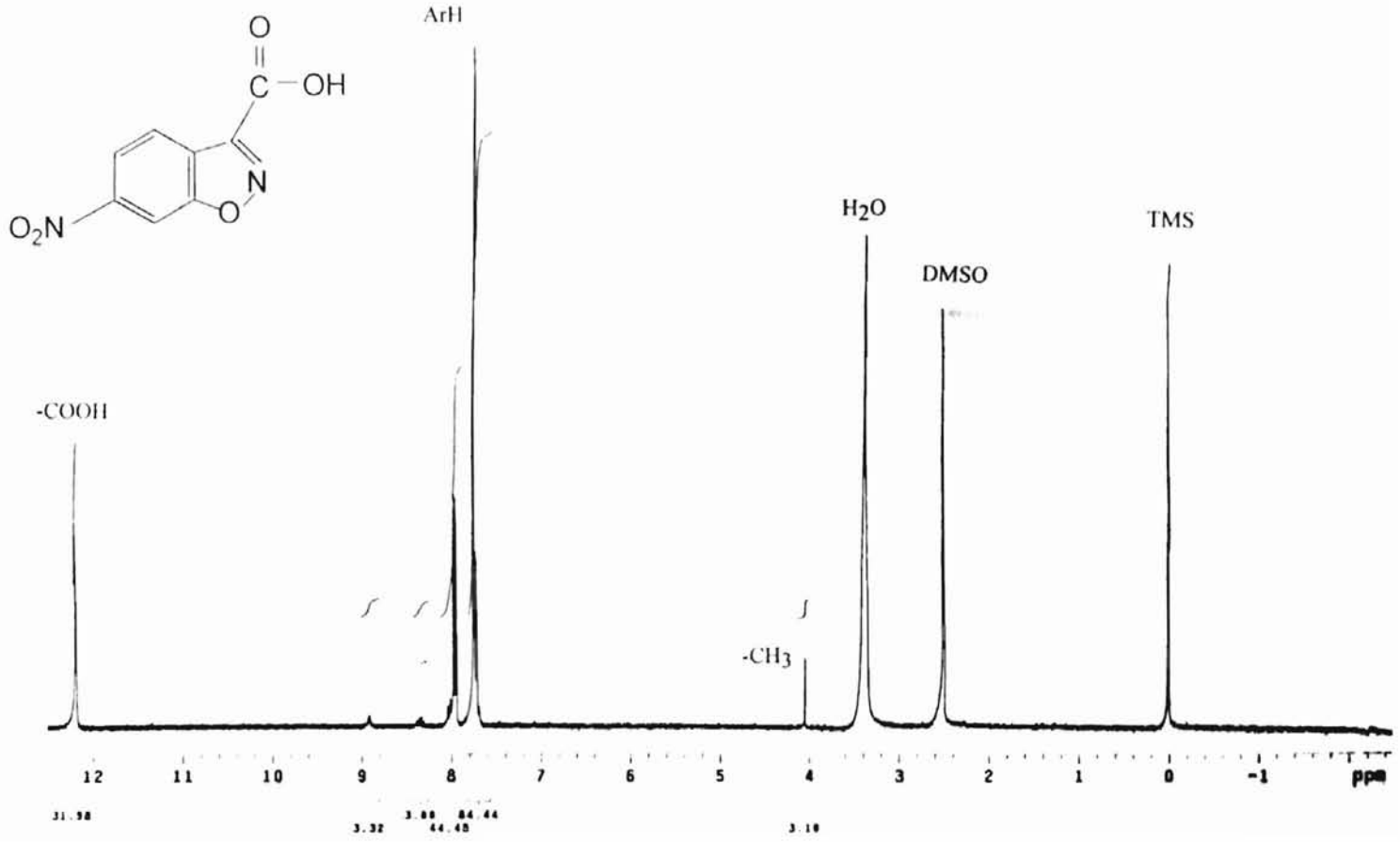

Figure 8. Kinetic Curve of Dispersion Latex at $[N^+] = 0.997 \times 10^{-4}$ M

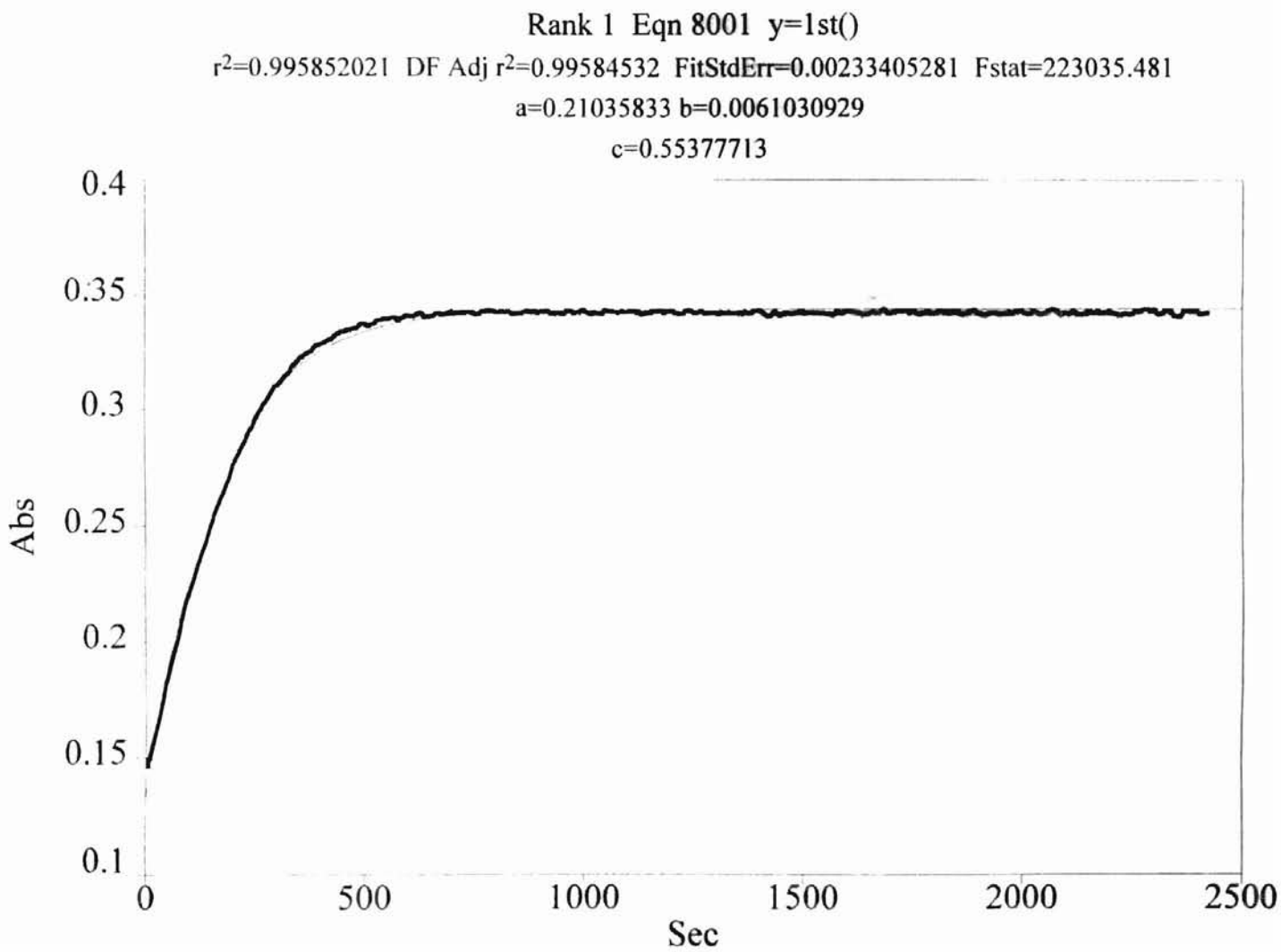

Figure 9. Kinetic Curve of Dispersion Latex at $[N^+] = 1.330 \times 10^{-4}$ M

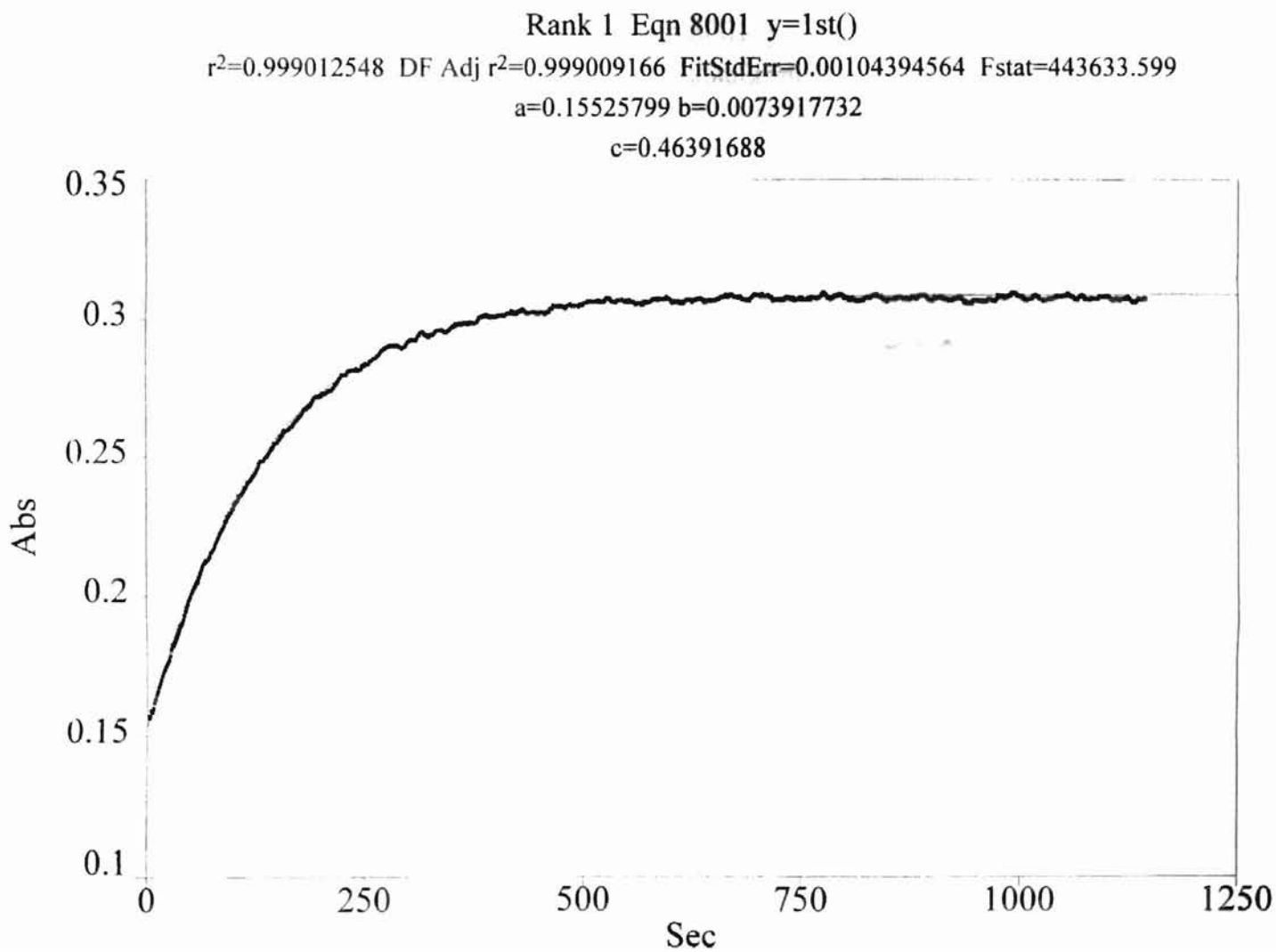

Figure 10. Kinetic Curve of Dispersion Latex at $[N^+] = 1.995 \times 10^{-4}$ M

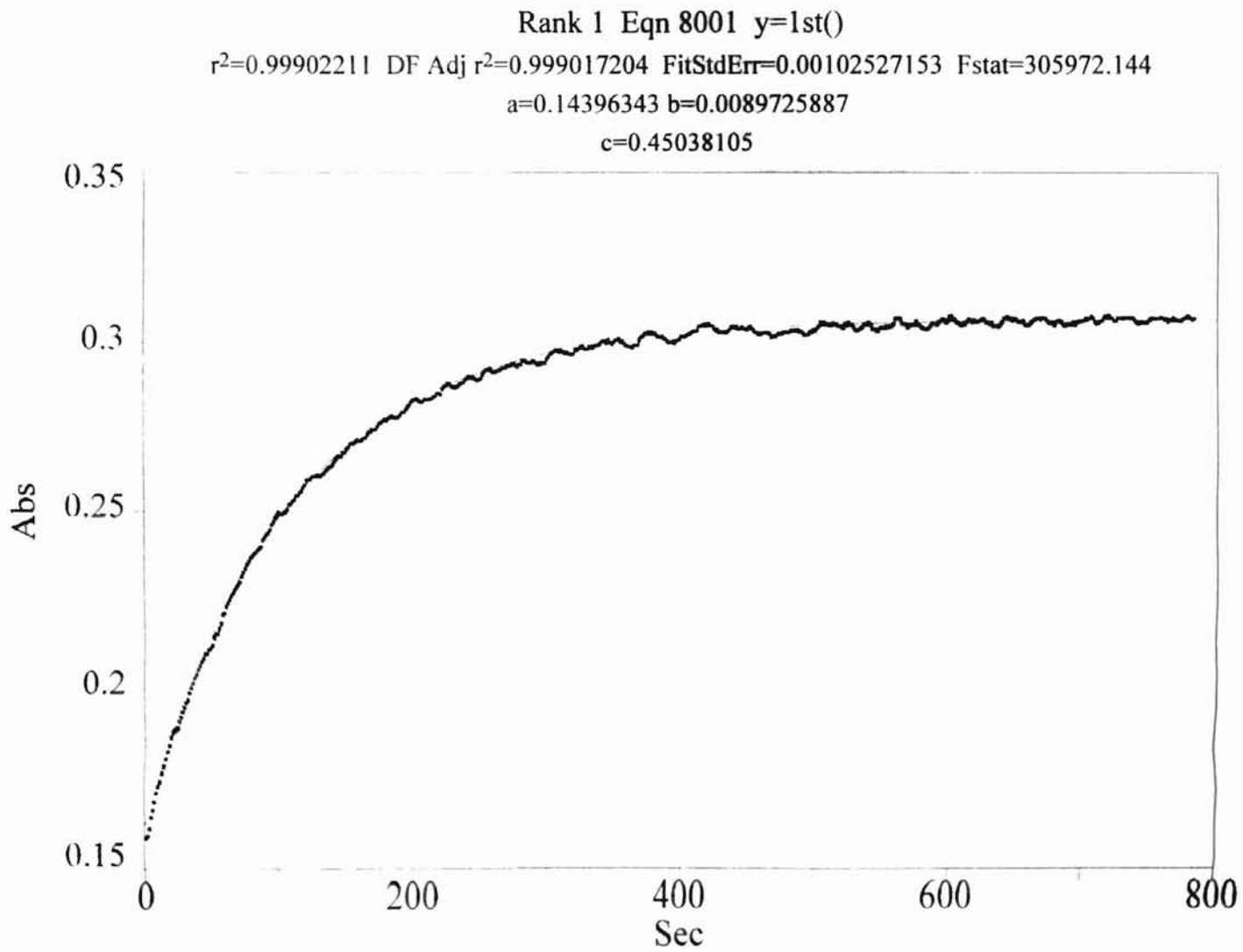

Figure 11. Kinetic Curve of Dispersion Latex at $[N^+] = 3.325 \times 10^{-4}$ M

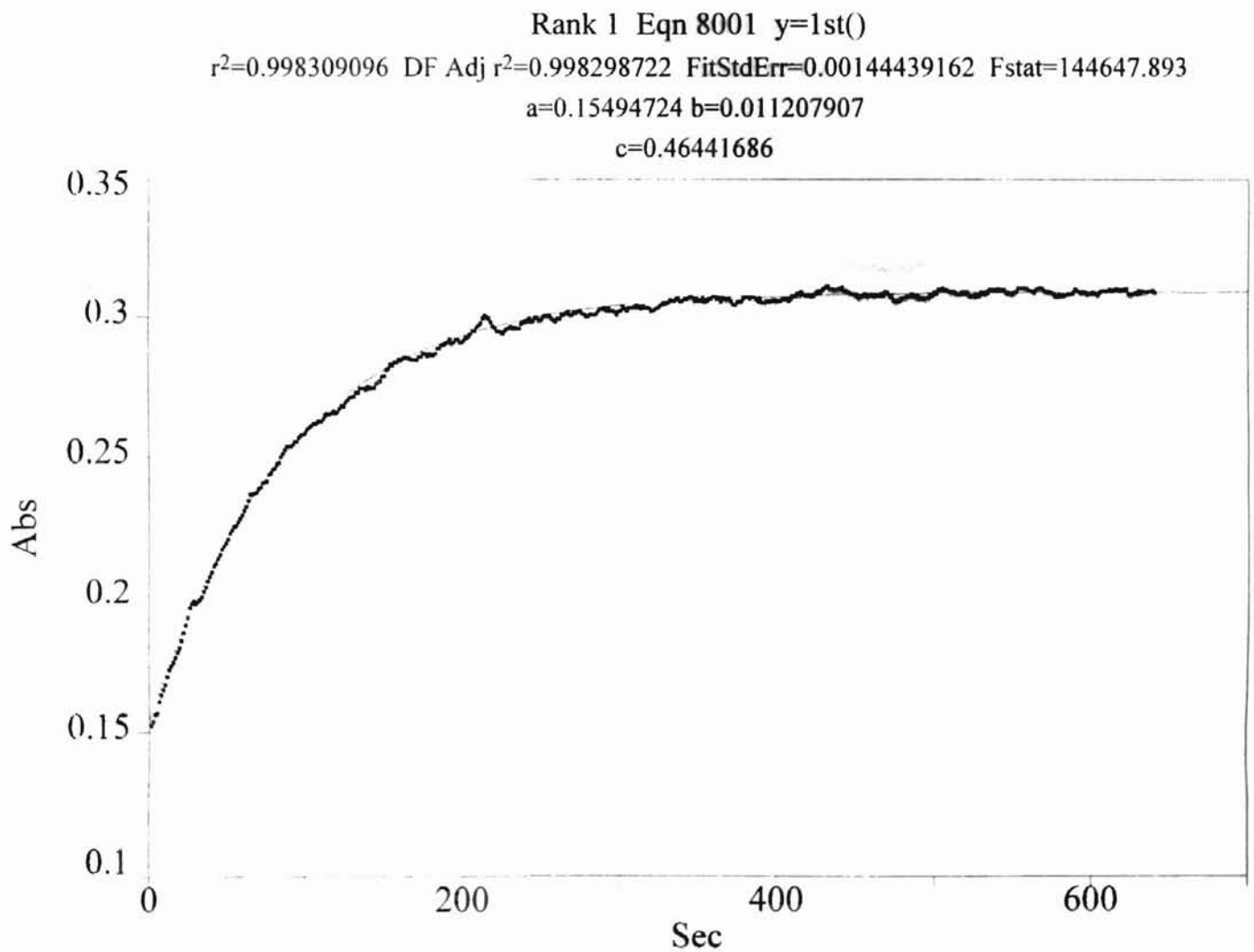

Figure 12. Kinetic Curve of Dispersion Latex at $[N^+] = 5.325 \times 10^{-4}$ M

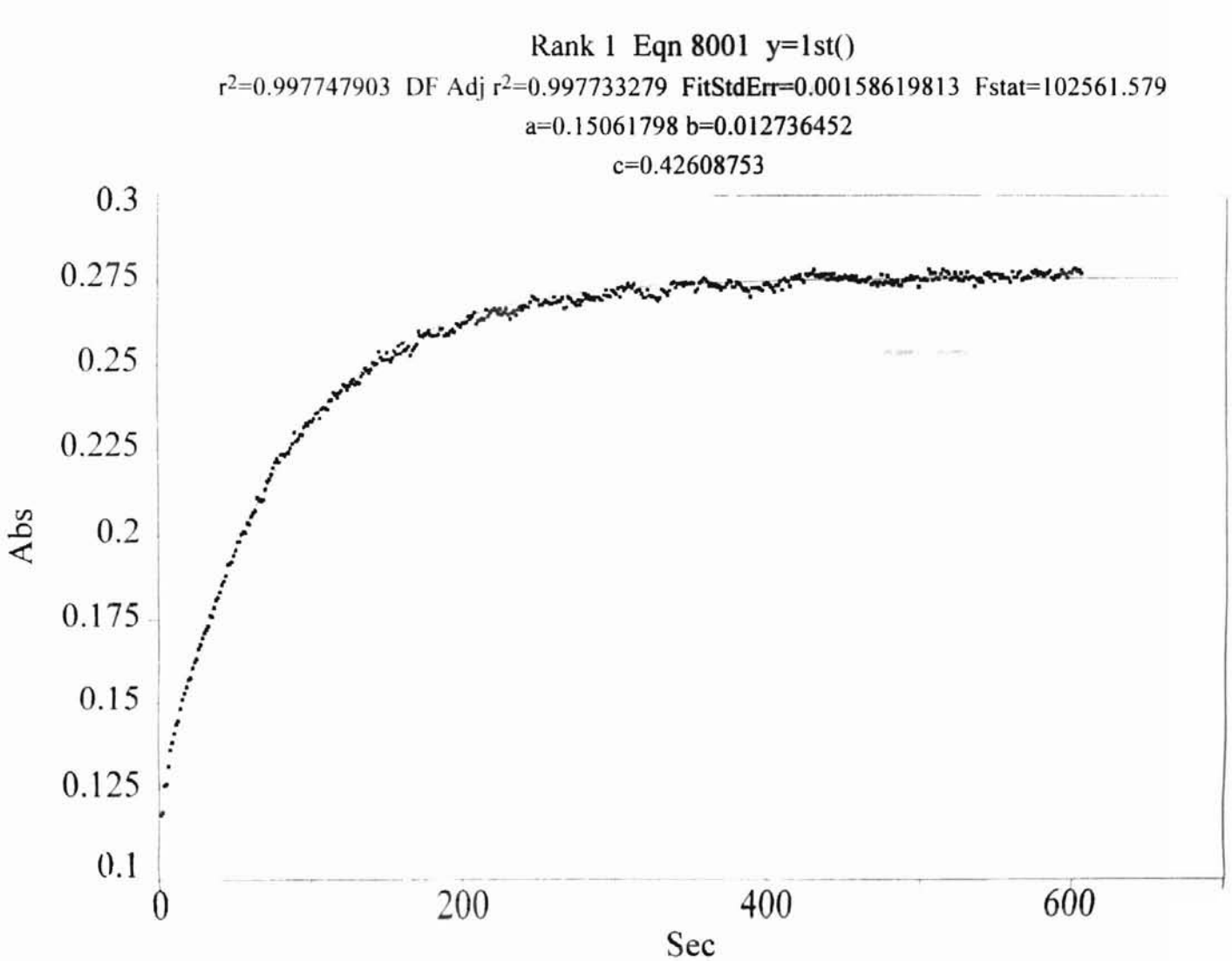

Figure 13. Kinetic Curve of Emulsion Latex at $[N^+] = 1.330 \times 10^{-4}$ M

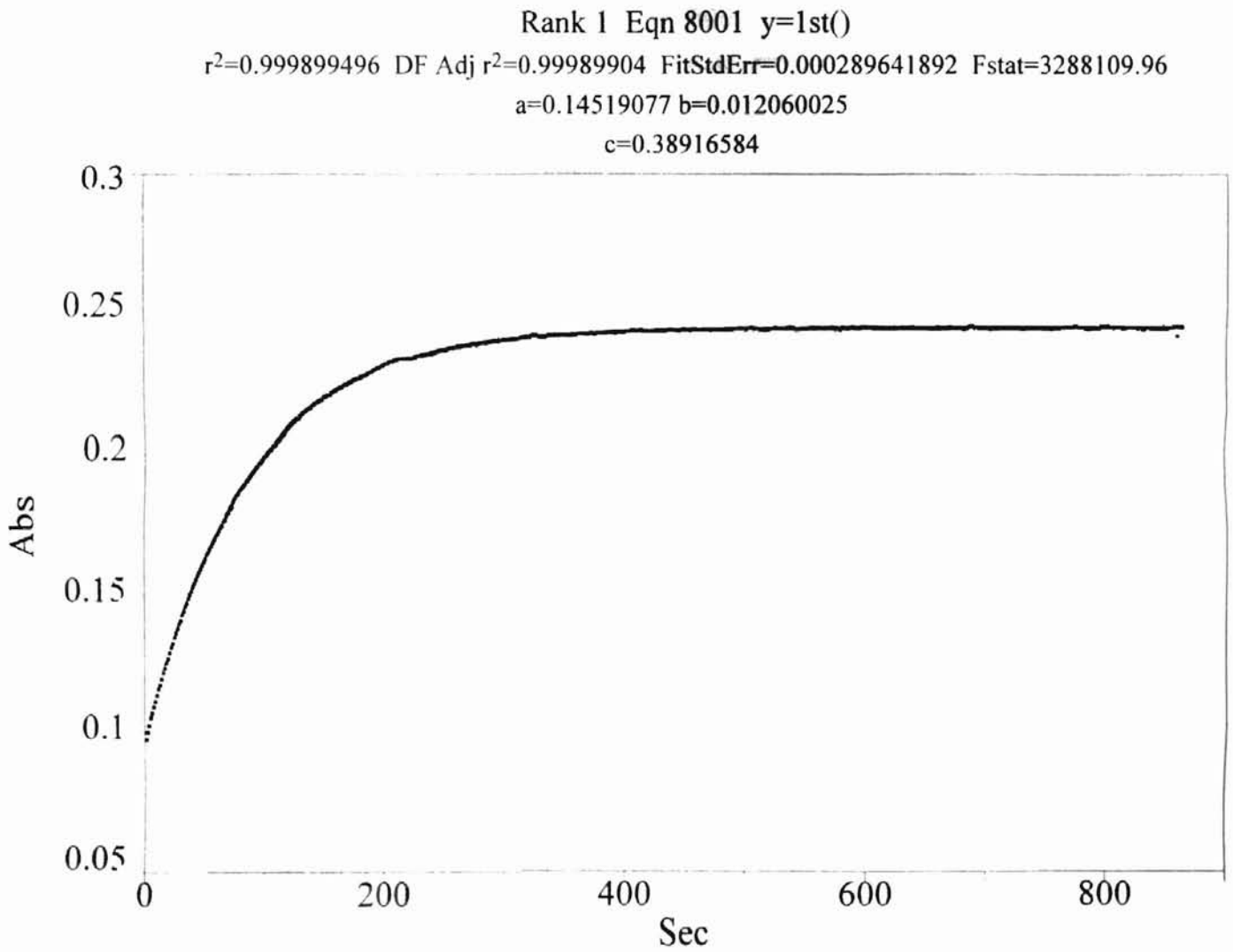

Figure 14. Kinetic Curve of Emulsion Latex at $[N^+] = 1.995 \times 10^{-4}$ M

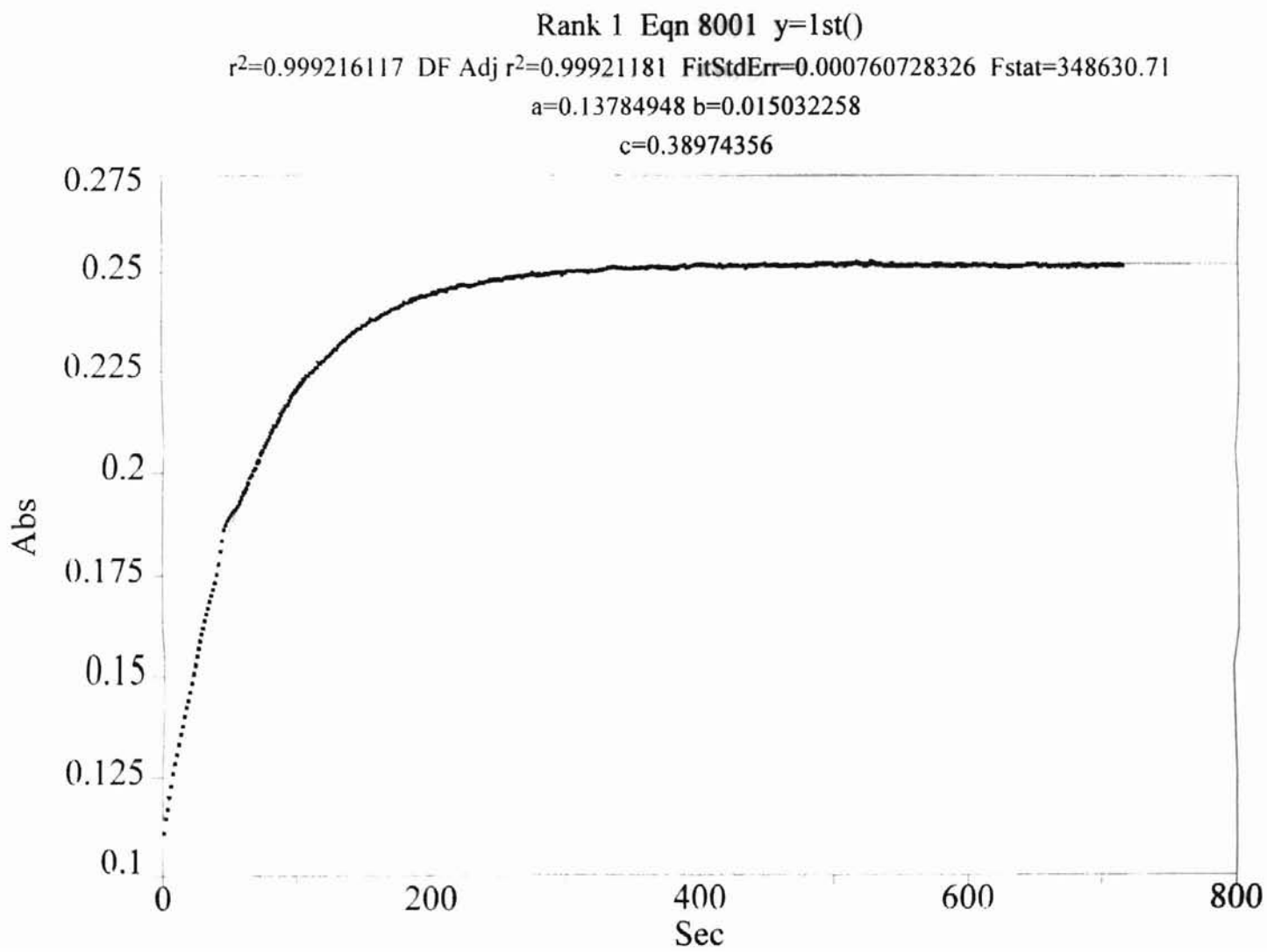

Figure 15. Kinetic Curve of Emulsion Latex at $[N^+] = 2.660 \times 10^{-4}$ M

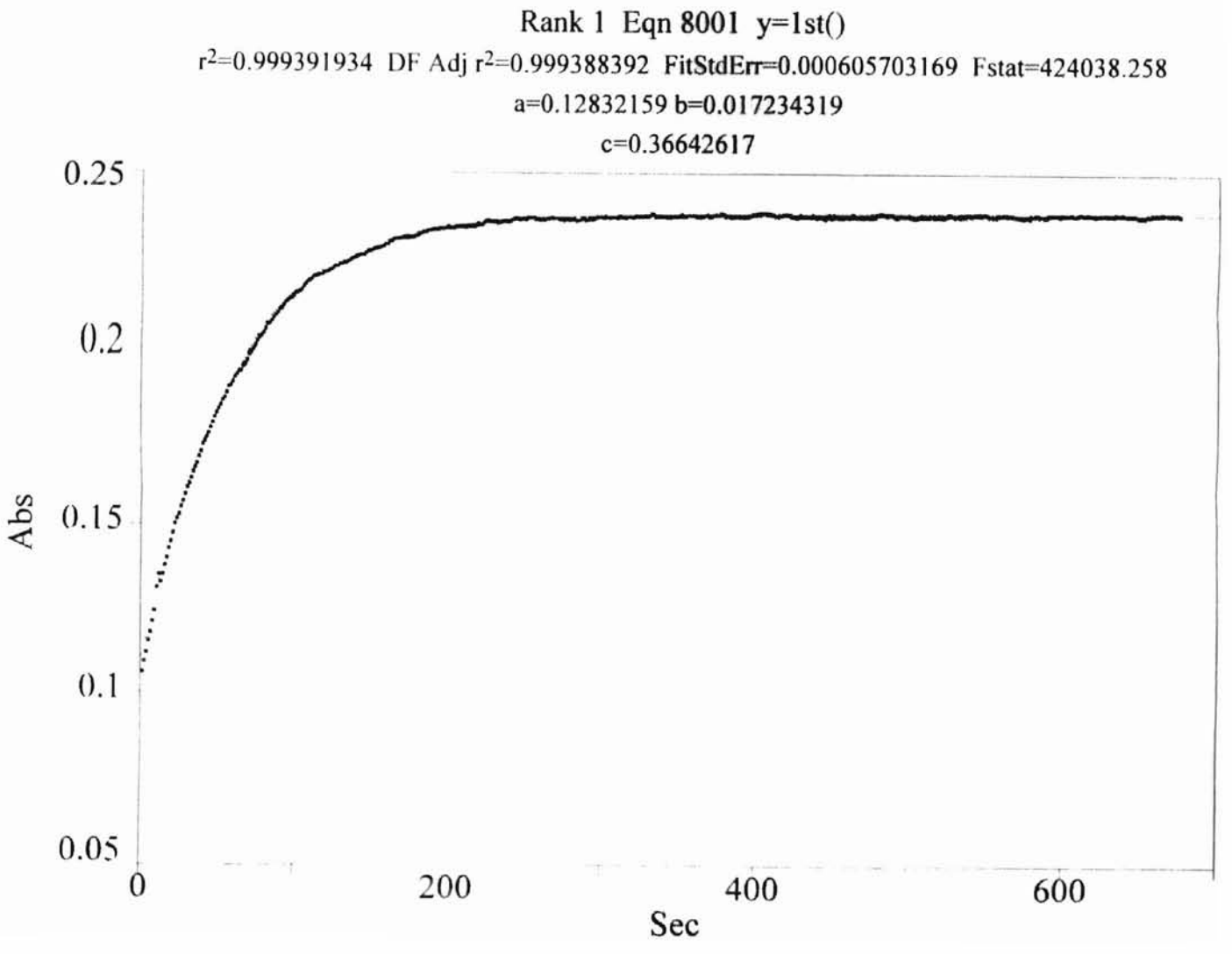

Figure 16. Kinetic Curve of Emulsion Latex at $[N^+] = 3.325 \times 10^{-4}$ M

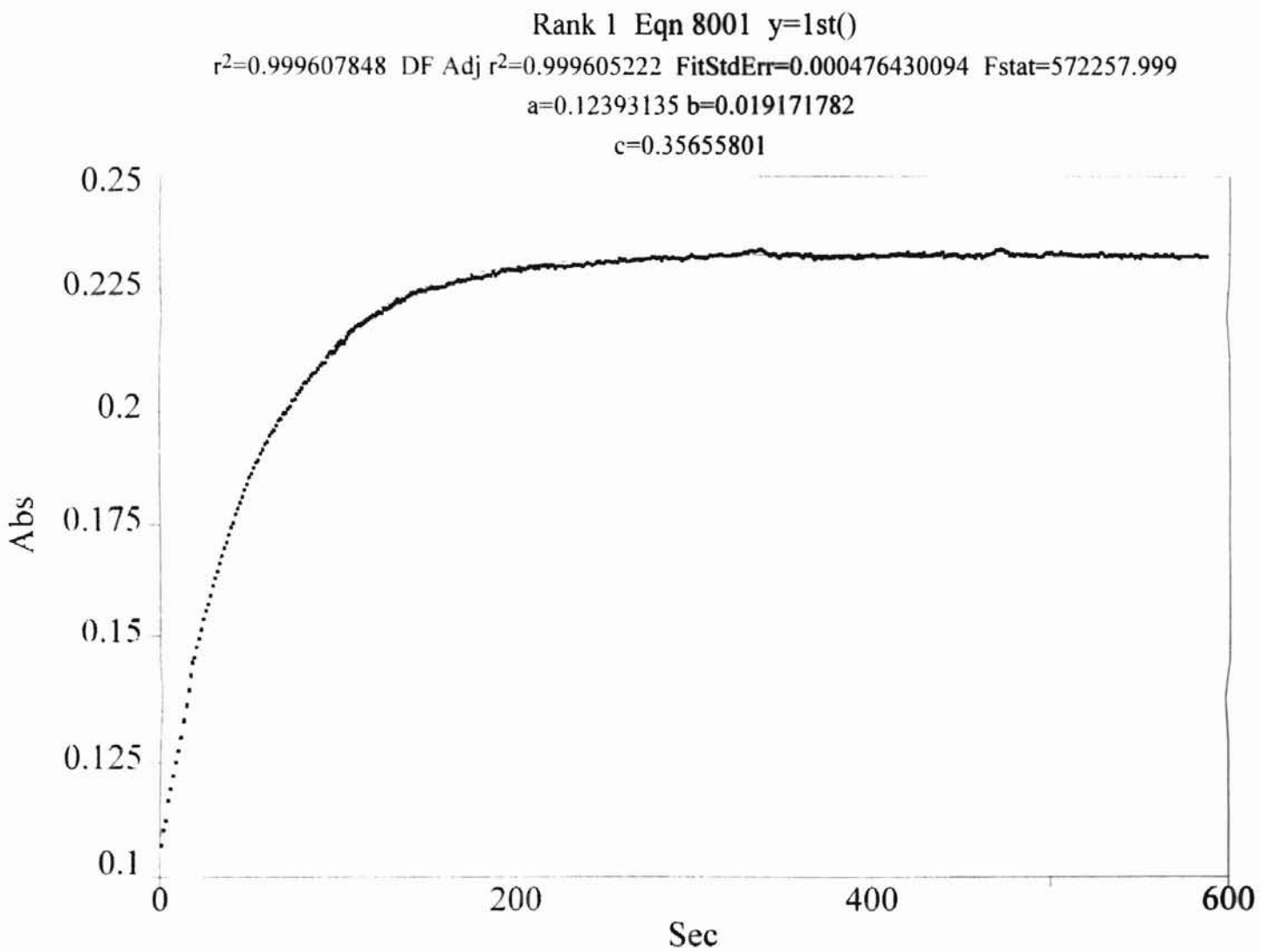

Figure 17. Kinetic Curve of Microemulsion Latex at $[N^+] = 1.995 \times 10^{-4}$ M

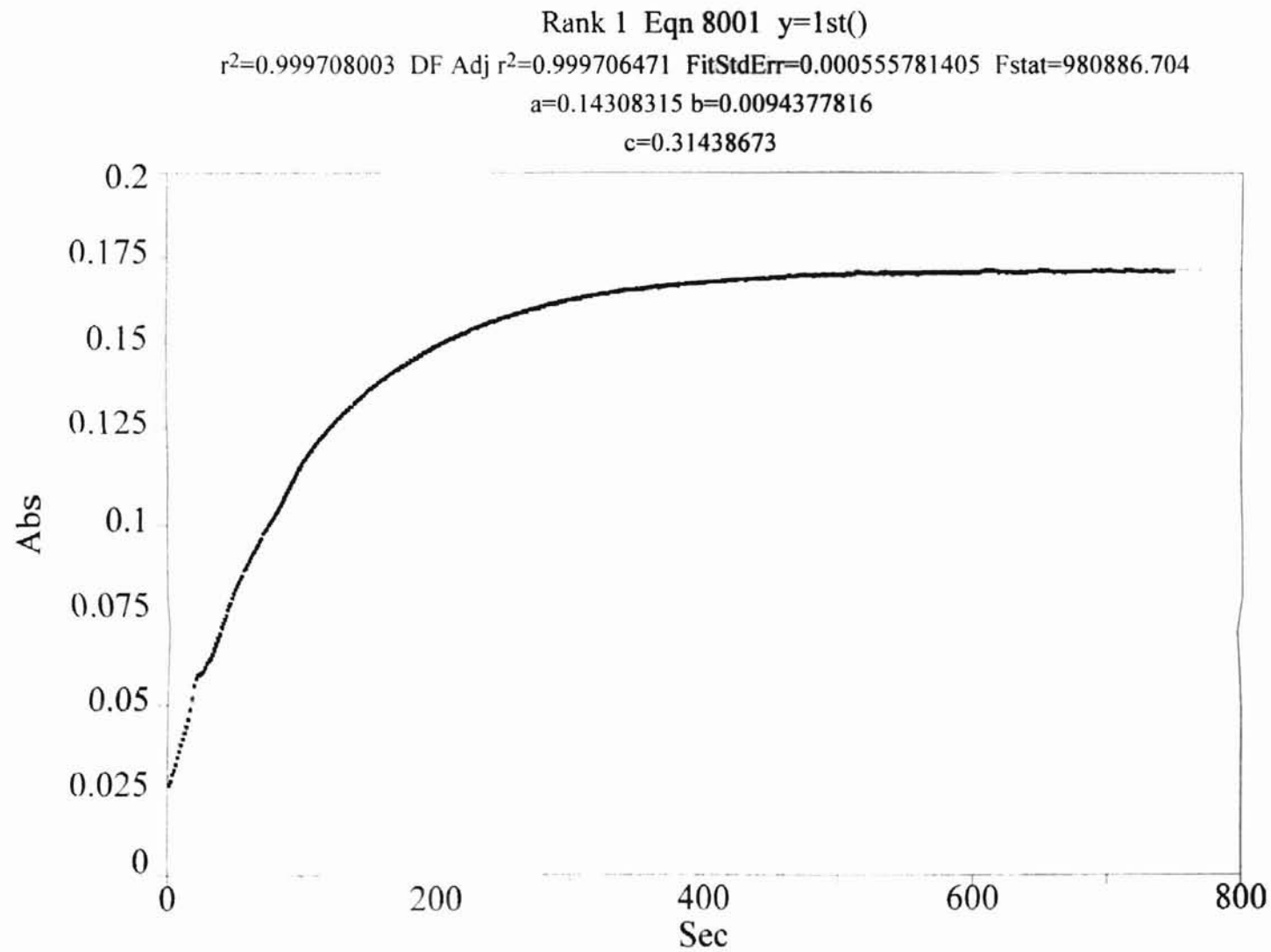

Figure 18. Kinetic Curve of Microemulsion Latex at $[N^+] = 3.325 \times 10^{-4}$ M

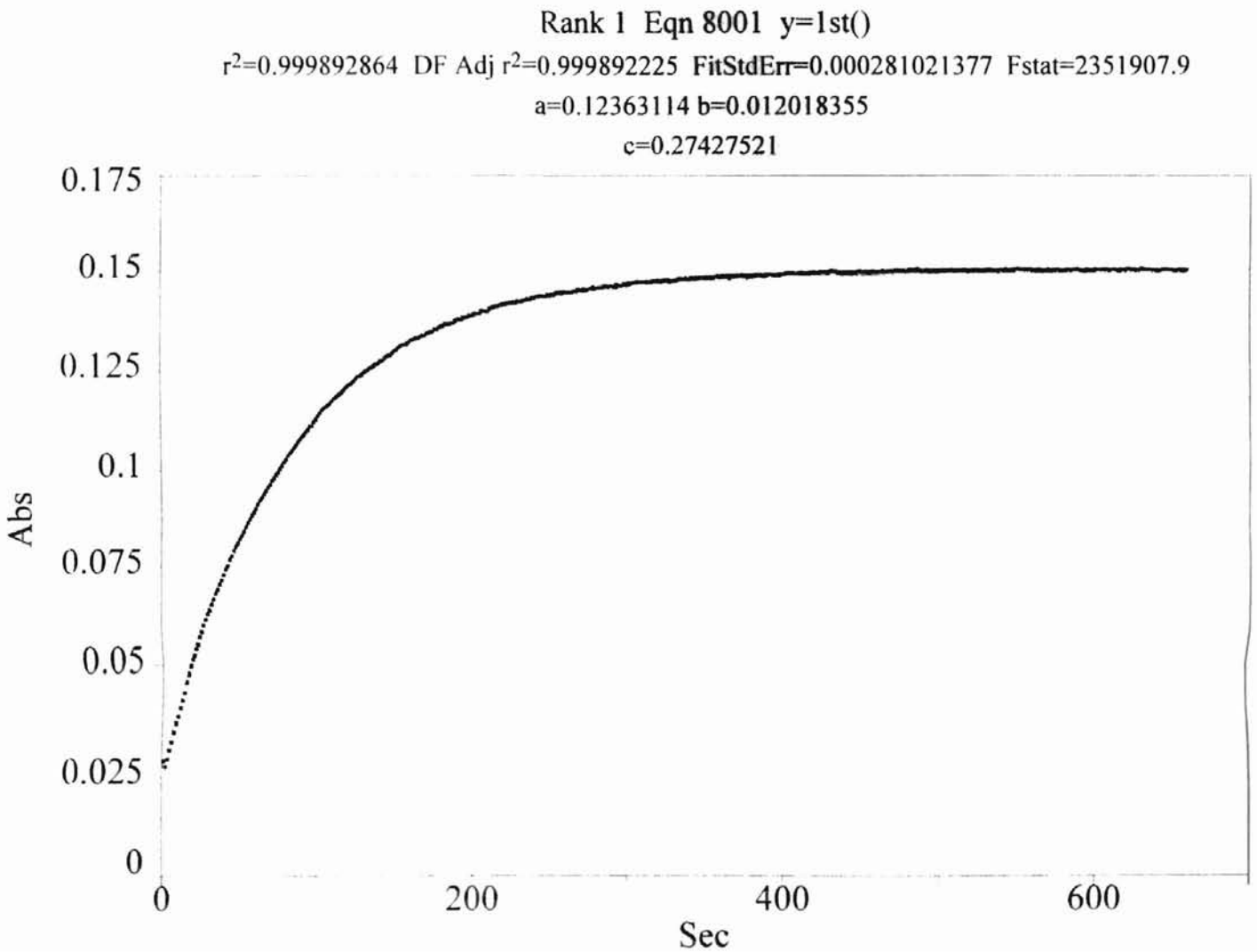

Figure 19. Kinetic Curve of Microemulsion Latex at $[N^+] = 5.325 \times 10^{-4}$ M

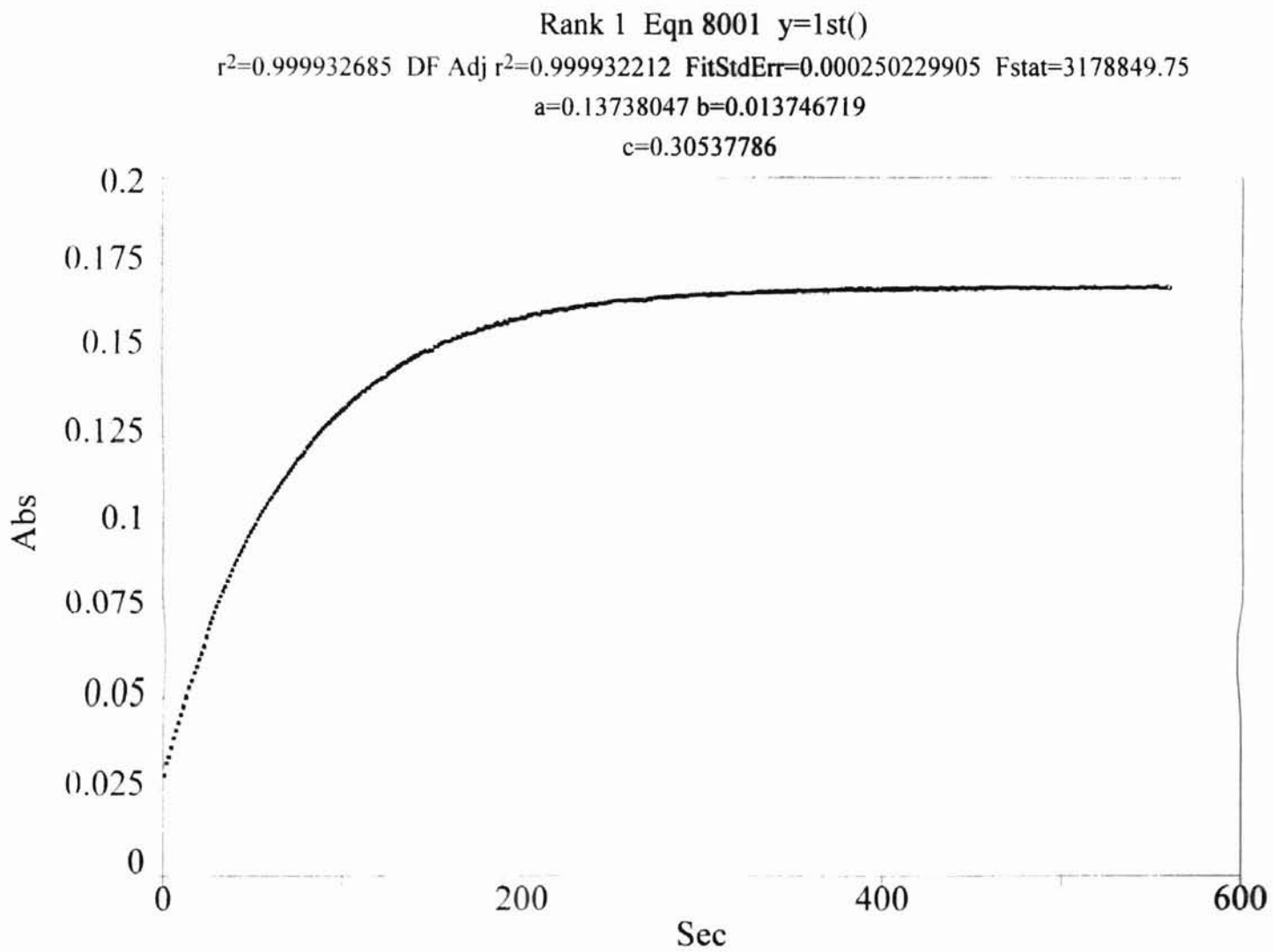

Figure 20. Kinetic Curve of Microemulsion Latex at $[N^+] = 7.325 \times 10^{-4}$ M

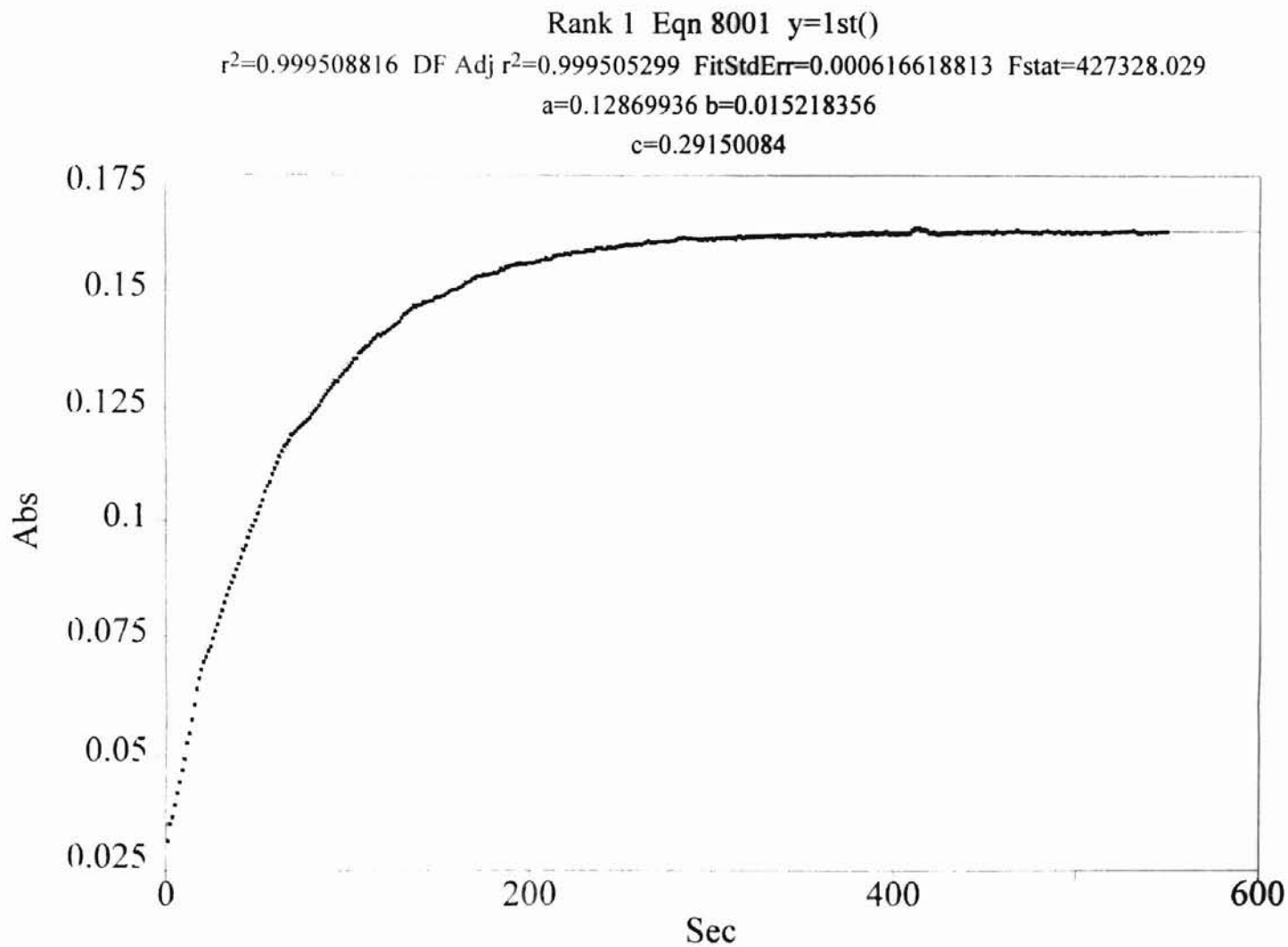

Figure 21. Kinetic Curve of Microemulsion Latex at $[N^+] = 9.325 \times 10^{-4}$ M

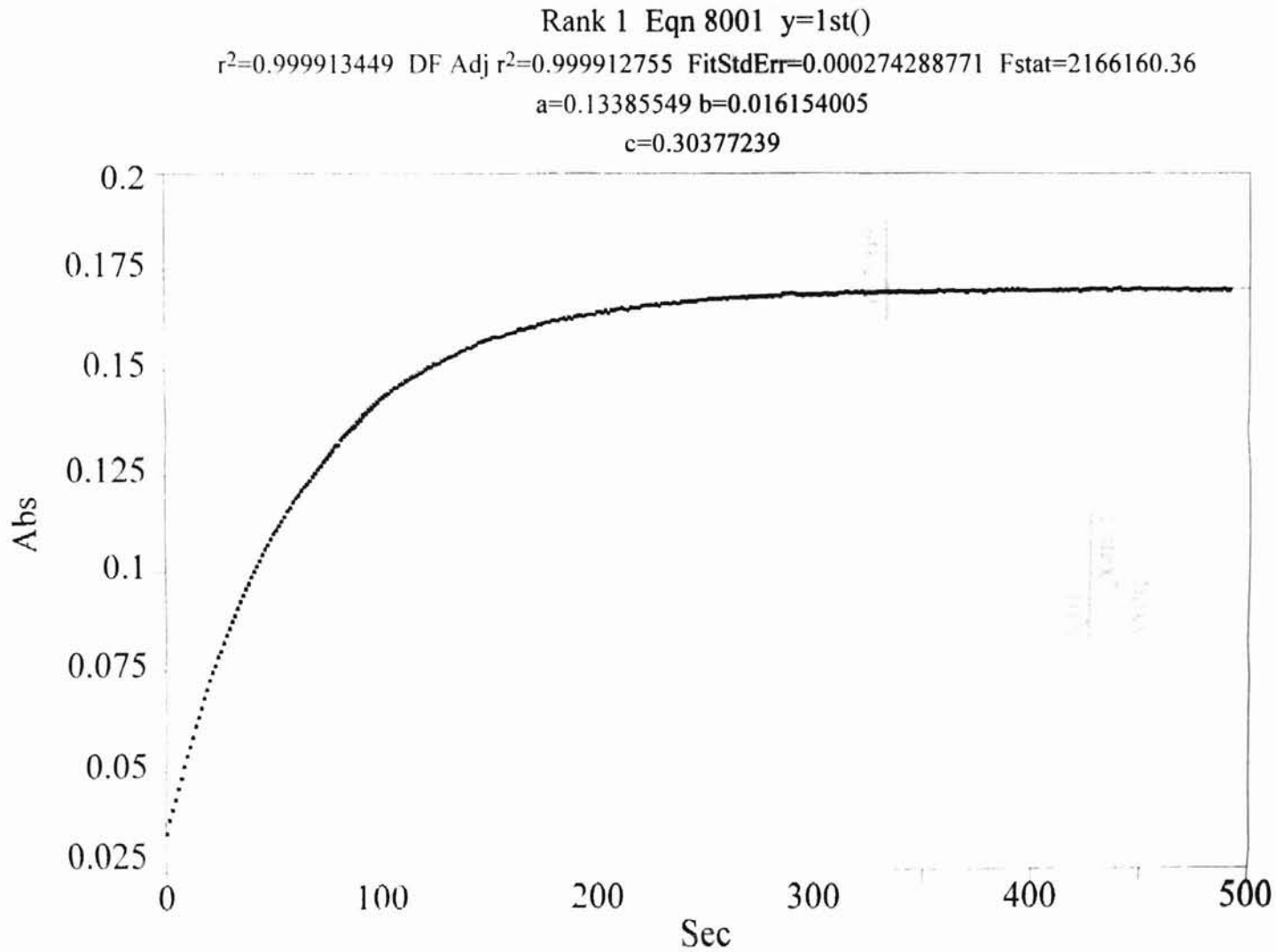

Table 1. First-order Rate Constants of Decarboxylation at Low Concentration of Microemulsion Latex[a]

latex (mg/mL)	$10^4[N^+]$ (M)	$10^3 k_{obsd}$ (s^{-1})
0.0035	0.065	1.11
0.0143	0.265	3.66
0.0250	0.465	5.67
0.0358	0.665	6.91

[a] In 2 mM NaOH, pH = 11.2 ± 0.1, at 25.0 ± 0.1 °C, [S] = 0.665×10^{-4} M.

Table 2. First-order Rate Constants of Decarboxylation at Low Concentration of Emulsion Latex[a]

latex (mg/mL)	$10^4[N^+]$ (M)	$10^3 k_{obsd}$ (s^{-1})
0.0036	0.065	3.05
0.0146	0.265	7.05
0.0257	0.465	8.59
0.0367	0.665	9.53

[a] In 2 mM NaOH, pH = 11.2 ± 0.1, at 25.0 ± 0.1 °C, [S] = 0.665×10^{-4} M

VITA

Guang Liu

Candidate for the Degree of

Master of Science

Thesis: EFFECTS OF CATIONIC POLYMER COLLOIDAL PARTICLE SIZE ON THE REACTIVITY OF ORGANIC ANIONS

Major Field: Chemistry

Biographical:

Personal Data: Born in Hengyang , Hunan Province, China, June 27, 1967, son of Yueqiu Liu and Chunlian Liao.

Education: Received Bachelor of Science Degree in Polymer Science and Engineering from Tsinghua University , Beijing, China, in July 1990. Completed requirements for Master of Science Degree with a major in Chemistry at Oklahoma State University in May, 2000.

Professional Experience: Assistant Engineer and Engineer, Beijing Research Institute of Materials and Technology, Beijing, China, from August, 1990 to June, 1996; Teaching and Research Assistant, Department of Chemistry, Oklahoma State University, from August, 1996 to May, 2000.